The secreted lipase FGL1 of the phytopathogenic fungus *Fusarium graminearum* (teleomorph *Gibberella zeae* (Schwein.) Petch) is a novel virulence factor and suppresses plant defense in *Triticum aestivum* (L.)

Dissertation zur Erlangung

des akademischen Grades

Dr. rer. nat.

des Departments Biologie

der Fakultät für Mathematik, Informatik

und Naturwissenschaften

an der Universität Hamburg

vorgelegt von

Christian Axel Voigt

aus Erlangen

Hamburg 2005

Genehmigt vom Department Biologie
der Fakultät für Mathematik, Informatik und Naturwissenschaften
an der Universität Hamburg
auf Antrag von Herrn Professor Dr. W. SCHÄFER
Weiterer Gutachter der Dissertation:
Herr Professor Dr. H. LÖRZ
Tag der Disputation: 18. November 2005

Hamburg, den 04. November 2005

Professor Dr. Arno Frühwald
Dekan

für Susanne

für die Familie

für die Freunde

Without speculation there is no good and original observation.

Charles Darwin (1809-1882)

Contents

I. Introduction 1

I.1. The phytopathogenic fungus *Fusarium graminearum* 1

I.2. Role of plant callose synthesis during fungal penetration 4

I.3. Aims of this study 9

II. Experimental Procedures 11

II.1. Materials 11

II.2. Microbial strains and culture conditions 11

II.3. Primers 12

II.4. Cloning of the lipase cDNA and lipase gene 13

II.5. Expression analysis by RT-PCR 14

II.6. Expression analysis by quantitative real-time PCR 15

II.7. Detection of extracellular lipolytic activity 16

II.8. Heterologous expression of the *FGL1* gene in *Pichia pastoris* 17

II.9. Transformation-mediated gene disruption 18

II.10. Southern blot analysis 19

II.11. Plant infection and pathogenicity tests on wheat 19

II.12. Plant infection and pathogenicity tests on maize 21

II.13. Membrane preparation 21

II.14. (1,3)-*β*-glucan synthase assay 22

II.15. Callose extraction 23

II.16. Callose determination 23

II.17. NADH oxidase activity assay 24

II.18. Microscopic analyses 24

II.19. Accession numbers 25

III. Results.....26

III.1. Cloning and sequence analysis of the lipase gene *FGL1* from *F. graminearum*.....26

III.2. Expression of *FGL1* in culture and *in planta*.....28

III.3. Inhibition of FGL1 produced in a heterologous host.....29

III.4. FGL1 inhibition *in planta*.....30

III.5. *F. graminearum* transformation and characterization of secreted lipase activity of *Δfgl1* strains.....31

III.6. Plant infection with *Δfgl1* strains.....34

III.7. Phylogenetic analysis of (1,3)-*β*-glucan synthases.....41

III.8. Organ specific expression analysis of *TaGSL* genes.....44

III.9. Organ-specific callose concentration, callose synthase activity and callose deposition.....47

III.10. Callose deposition, concentration and synthase activity in wheat spikes during infection.....49

III.11. Glucan synthase-like gene expression in wheat spikes during infection.....52

III.12. Differences in type II resistance against *F. graminearum* infection and in inhibition of callose synthase due to free fatty acid application of the wheat cultivars Nandu and Batis.....55

III.13. Differences in infection progress and restoration of virulence of a lipase-deficient *F. graminearum* mutant due to FFA application *in planta*.....58

IV. Discussion 66

IV.1. Characterization of the secreted lipase FGL1 66

IV.2. Importance of the secreted lipase FGL1 to virulence 67

IV.3. General importance of extracellular lipases 70

IV.4. Papilla-like barrier formation associated with *Δfgl1* infection 71

IV.5. Organ-specific *GSL* gene expression in wheat during normal growth 72

IV.6. Organ-specific callose synthesis in wheat during normal growth 75

IV.7. Organ-specific callose deposition in wheat during normal growth 77

IV.8. Suppression of wheat callose synthesis during infection 78

IV.9. Putative regulation of callose synthesis during infection 80

IV.10. Suppression of wheat callose synthesis caused by the secretion of FGL1 81

IV.11. Model of type II resistance to fungal infection in wheat 83

V. Summary 86

VI. Zusammenfassung 88

VII. References 91

Figures

Figure 1. Symptoms of *F. graminearum* infection on cereals. 1
Figure 2. Catalytic action of lipases. 3
Figure 3. Chemical structure of callose. 4
Figure 4. Hypothetical model of the callose synthase complex. 7
Figure 5. Induction of extracellular lipolytic activity of *F. graminearum* cultures using different vegetable oils. 26
Figure 6. Phylogenetic tree of secreted fungal lipases. 27
Figure 7. Expression analysis of FGL1 and lipolytic activity of *F. graminearum* supernatants under different culture conditions. 28
Figure 8. Expression analysis of *FGL1* during infection of wheat. 29
Figure 9. Inhibition of *F. graminearum* lipase FGL1 by ebelactone B. 29
Figure 10. Effect of ebelactone B on *F. graminearum* infection of wheat (cv. Nandu). 31
Figure 11. Analysis of *F. graminearum* wild-type and mutant strains via Southern blot and *FGL1* gene expression. 33
Figure 12. Extracellular lipolytic activity of *F. graminearum* wild-type (wt), *Δfgl1* strains (1-5), and ectopic strains (ect1/2) after induction by wheat germ oil. 34
Figure 13. Infection of wheat spikes (cv. Nandu) with *F. graminearum* wild-type, *Δfgl1* strains, and ectopic strains. 35
Figure 14. Spike stem appearance and kernel quality after infection of wheat spikes (cv. Nandu) with *F. graminearum* wild-type and *Δfgl1* strain 3. 37
Figure 15. External view and longitudinal section of wheat spikelets (cv. Nandu) and adjacent rachis region of *F. graminearum* wild-type and *Δfgl1* strain 3 infection. 38
Figure 16. Infection of maize ears with *F. graminearum* wild-type, Δfgl1 strains 1, 2, and 3, and ectopic strain ect1. 39
Figure 17. Phylogenetic tree of putative (1,3)-β-glucan synthases from *Triticum aestivum* (TaGSL), *Hordeum vulgare* (HvGSL), *Zea mays* (ZmGSL), *Oryza sativa* (OsGSL) and *Arabidopsis thaliana* (AtGSL). 43

Figure 18. Expression of *TaGSL* genes in wheat spike, leaf blade and stem tissue (cv. Nandu). 45
Figure 19. Determination of callose concentration and callose synthase activity in wheat tissue and detection of callose depositions in wheat tissue sections (cv. Nandu). 49
Figure 20. Callose deposition, concentration and synthase activity in the wheat spike (cv. Nandu) after infection. 52
Figure 21. Expression analysis of glucan synthase-like genes (*TaGSL*) in wheat spikes (cv. Nandu). 53
Figure 22. Susceptibility against *F. graminearum* infection and callose synthase activity of the wheat cultivars Nandu and Batis after addition of free fatty acids (FFA). 58
Figure 23. Schematic overview of possible cross-over events during transformation and characterization of resulting GFP-tagged *F. graminearum* strains. 60
Figure 24. Infection progress in wheat spikes (cv. Nandu) inoculated with GFP-tagged *F. graminearum* strains. 64
Figure 25. Model of type II resistance to fungal infection in wheat. 85

Tables

Table 1. Primers used in PCR reactions. (F) Forward primer; (R) Reverse primer. 12
Table 2. Virulence of *F. graminearum* strains to wheat (cv. Nandu) and maize.. 40
Table 3. Differences in virulence of GFP-tagged *F. graminearum* strains to wheat (cv. Nandu) due to addition of free fatty acids (FFA). 62

Abbreviations

bp	base pair(s)
cAMP	adenosine 3',5'-cyclic monophosphate
cDNA	complementary DNA
cGMP	guanosine 3',5'-cyclic monophosphate
CM	complete medium
cv.	cultivated variety; cultivar
DNA	deoxyribonucleic acid
DON	deoxynivalenol
dpi	days post inoculation
et al.	*et alii* → and others
FFA	free fatty acid(s)
x g	multiple of gravity (g = 9.81 m/s^2)
GSL	glucan synthase-like (gene)
hph	hygromycin B phosphotransferase
kb	kilo base pairs
kD	kiloDalton
mRNA	messenger RNA
NADH	nicotinamide adenine dinucleotide
ORF	open reading frame
PCR	polymerase chain reaction
pNPP	para-nitrophenyl palmitate
qPCR	quantitative real-time PCR
RNA	ribonucleic acid
RT-PCR	reverse transcriptase PCR
SNA	synthetic nutrient-poor medium
Tris	tris-(hydroxymethyl) aminomethane
UDP-glucose	uridine 5'-diphosphoglucose
v	volume
w	weight
wt	wild type
YPD	yeast extract/peptone/dextrose medium
ZEA	zearalenone

Units of measurements were used according to the International System of Units SI (Système International d'Unités). Chemical formulas and molecules are named after IUPAC (International Union of Pure and Applied Chemistry).

I. Introduction

I.1. The phytopathogenic fungus *Fusarium graminearum*

The phytopathogenic fungus *Fusarium graminearum* Schwabe (teleomorph *Gibberella zeae* (Schwein.) Petch) is a necrotrophic, filamentous ascomycete, which causes Fusarium head blight (FHB), one of the most destructive crop diseases (Figure 1 A). *F. graminearum* is a broad host range pathogen that infects many crop plants, especially wheat (*Triticum aestivum* L.), barley (*Hordeum vulgare* L.), and maize (*Zea mays* L.) (Desjardins *et al*., 1996; McMullen *et al*., 1997), on which it causes cob rot (Figure 1 B).

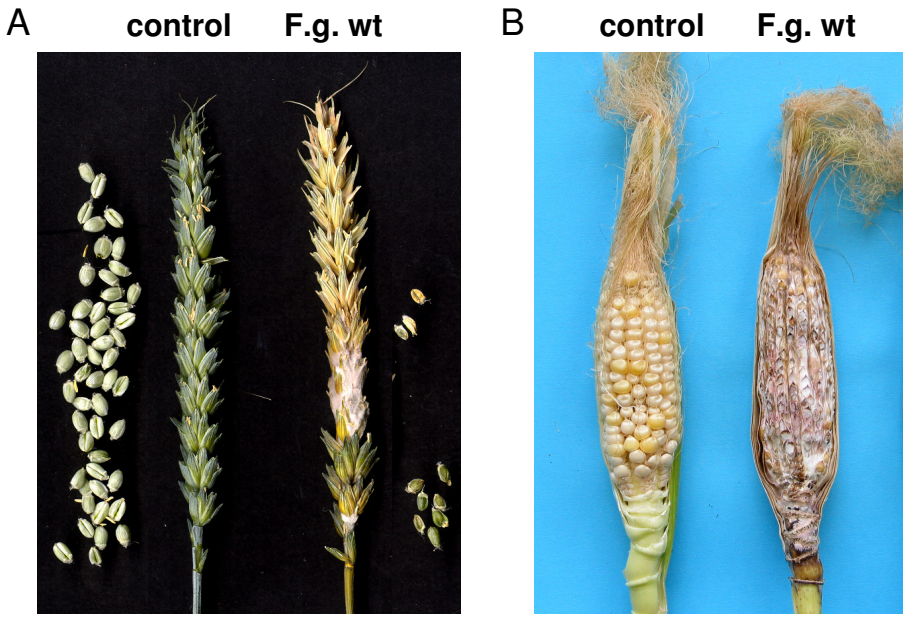

Figure 1. Symptoms of *F. graminearum* infection on cereals.

A. Inoculation of two central spikelets with *F .graminearum* wild-type conidia (F.g. wt) causes typical symptoms of FHB. Kernels represent the yield of an infected and control spike 3 weeks post infection.

B. Inoculation of maize ears was performed by injecting a *F. graminearum* wild-type (F.g. wt) conidial suspension into the silk channel. Figure shows the typical symptoms of cob rot 5 weeks post infection.

Assessments in nine US states showed losses of about 870 million US-dollars to FHB on wheat and barley from 1998 to 2000 (Nganje *et al*., 2001). Additionally, this crop disease is a growing threat to the world-wide food supply due to outbreaks in Asia, Canada, Europe, and South America (Dubin *et al*., 1997). The fungus causes direct yield losses because of sterility of the florets and shriveled, light test-weight kernels (Figure 1A). Furthermore, infected grain is often contaminated by trichothecenes and estrogenic mycotoxins (McMullen *et al*., 1997) that are hazardous to animals and humans and provoke indirect health damages (Marasas *et al*., 1984). Therefore, several countries have adopted or intend to legislate advisory limits to ensure minimum levels for the most important mycotoxins deoxynivalenol (DON) and zearalanone (ZEA) (Ishii, 1983; D'Mello and MacDonald, 1997) in retail products for human consumption and in animal feeds (van Egmond, 1989; Pricket *et al*., 2000). In the USA, an economically important part of the crop is rejected by the industry because of DON contamination.

Despite the economic importance, little is known about the molecular basis of *F. graminearum* infections. Generally, fungal pathogens secrete various extracellular enzymes hypothesized to be involved in virulence (Wanjiru *et al*., 2002). Positive effects were shown for pectinolytic enzymes from *Aspergillus flavus* (Shieh *et al*., 1997), *Botrytis cinerea* (ten Have *et al*., 1998), and *Claviceps purpurea* (Oeser *et al*., 2002). The disruption of genes encoding these enzymes resulted in the reduction of virulence in the respective fungi. The precise role of most other extracellular enzymes is still controversial (Scott-Craig *et al*., 1990;

Stahl and Schäfer, 1992; Rogers *et al*., 1994; Stahl *et al*., 1994; Wu *et al*., 1997; Wegener *et al*., 1999). Among secreted enzymes, triacyl-glycerol lipases (EC 3.1.1.3) form an extensive family, and catalyze both the hydrolysis and the synthesis of ester bonds. The biological function of lipases is the hydrolytic decomposition of triacyl-glycerols into glycerol and free fatty acids (FFA) (Figure 2). In nature, lipases are ubiquitous (Borgström and Brockman, 1984), having been found in animals, plants, fungi, and bacteria (Mukherjee and Hills, 1994; Jaeger and Reetz, 1998). Due to their high regio- and enantiospecificity, lipases are an important group of biocatalysts in organic chemistry (Jaeger and Reetz, 1998) and have many industrial applications (Schmid and Verger, 1998).

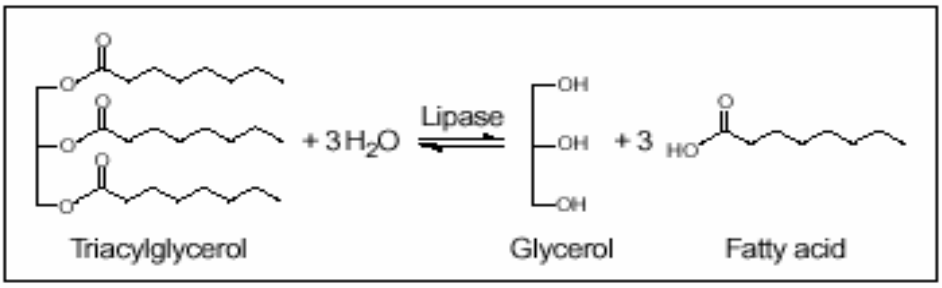

Figure 2. Catalytic action of lipases.

Triacylglycerol can be hydrolyzed into glycerol and free fatty acids (FFA). The reverse reaction esterifies glycerol and FFA into triacylglycerol (after Jaeger and Reetz, 1998).

Little is known about the influence of lipases during infection of plants by fungi. Intracellular lipases were shown to be involved in appressoria formation by *Magnaporthe grisea* (Thines *et al*., 2000). The first evidence of involvement of secreted lipases in plant infection came from Comménil *et al*. (1995, 1998, 1999). They showed that supplementation of conidial suspensions with polyclonal antibodies against an extracellular lipase of *Botrytis cinerea* suppressed lesion

formation on detached tomato leaves. Nasser Eddine *et al*. (2001) reported a secreted lipase of the pea pathogen *Nectria haematococca* MP VI, which was expressed during host infection. However, there is as yet no report of direct evidence that any secreted lipase contributes to fungal virulence.

I.2. Role of plant callose synthesis during fungal penetration

Even though many fundamental processes in plant science have been elucidated on a molecular level, some are still controversially discussed. This includes basic aspects of the involvement of callose in plant developmental processes. In this regard, particular attention has been focused on the formation of callosic papillae, the apparent cell wall thickenings of plants, as a response to microbial attack. At first glance, this seems astonishing, since papillae were discovered on plant cell walls at sites of fungal penetration by deBary over 140 years ago. Mangin reported in 1895 that callose, a (1,3)-*β*-glucan (Figure 3) with some (1,6)-branches (Aspinall and Kessler, 1957), commonly occurred in papillae.

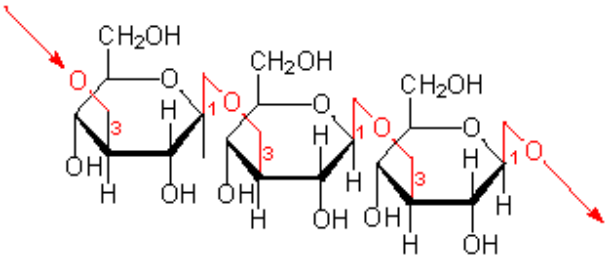

Figure 3. Chemical structure of callose.

Callose is a (1,3)-*β*-glucan composed of glucose units linked *via* (1,3)-glycosidic linkages. As a result, the polymer is arranged in a helix.

Since then, examinations (Aist and Williams, 1971; Sargent *et al.* 1973; Mercer *et al.* 1974, Sherwood and Vance, 1976; Mims *et al.* 2000) have identified callose as the most common chemical constituent in papillae. Since papillae are not regarded as a defense reaction that can completely stop the pathogen, they are thought to act as a physical barrier to slow pathogen growth (reviewed by Stone and Clarke, 1992). The host plant can gain time for initiation of defense reactions that require gene activation and expression. As a result, the plant could initiate hypersensitive reactions, synthesis of phytoalexins and pathogenesis-related (PR) proteins (Lamb and Dixon, 1997; Brown *et al.*, 1998). However, a general role of callose in the penetration process can be questioned since callosic papillae correlate with penetration failure, but not with successful fungal establishment (Aist, 1976). Thus, even though the involvement of callose in plant defense has been investigated for well over a century, its precise function during microbial attack has not been demonstrated unequivocally. Apart from microbial stress, the local deposition of callose is induced by abiotic stress and wounding. During normal growth conditions, callose is deposited at the cell plate, plasmodesmatal canals, root hair and spiral thickenings in tracheids, sieve plates of phloem elements as well as around pollen mother cells, in pollen grains and in pollen tubes (Stone and Clarke, 1992; Kauss, 1996; Ryals *et al.*, 1996; Donofrio and Delaney, 2001; Jacobs *et al.*, 2003). Due to the central importance of callose deposition in several key plant processes, many efforts have been made to purify and characterize callose synthases and their corresponding genes from plants (Meikle *et al.*, 1991; Schlupmann *et al.*, 1993; Dhugga and Ray, 1994; Bulone *et*

al., 1995; Kudlicka *et al*., 1995; Kudlicka and Brown, 1997; McCormack *et al*., 1997; Turner *et al*., 1998; Him *et al*., 2001; Jacobs *et al*., 2003). Even though purification of active callose synthase to homogeneity has not been achieved, the molecular mass and subunit composition of this enzyme could be determined. First results from partially purified callose synthase preparations have shown a composition of six to nine major polypeptides ranging in size from 25 to 92 kD (Kamat *et al*., 1992; Wasserman *et al*., 1992; Dhugga and Ray, 1994; McCormack *et al*., 1997). The presumptive catalytic subunit has been reported to have a molecular mass between 32 and 57 kD (Read and Delmer, 1987; Frost *et al*., 1990; Delmer *et al*., 1991; Li and Brown, 1993; Gibeaut and Carpita, 1994). Newer results of preparations have shown that the callose synthase activity is associated with ~200-kD polypeptides (Turner *et al*., 1998; Hong *et al*., 2001; Li *et al*., 2003).

General difficulties in preparation have arisen from the suggested structure of the enzyme. Callose synthase is likely to be a multisubunit and membrane-associated enzyme complex (Verma and Hong, 2001, Figure 4). Detergents that are normally used for extraction are regarded to dissociate the enzyme complex, resulting in a loss of activity. The purification of active callose synthase to homogeneity has not been achieved. Therefore, callose synthase activity could not be directly linked with an amino acid or nucleotide sequence. Despite these difficulties, the family of glucan synthase-like (*GSL*) genes in higher plants has been identified as presumably encoding for callose synthases (Cui *et al*., 2001; Hong *et al*., 2001; Doblin *et al*., 2001; Østergaard *et al*., 2002).

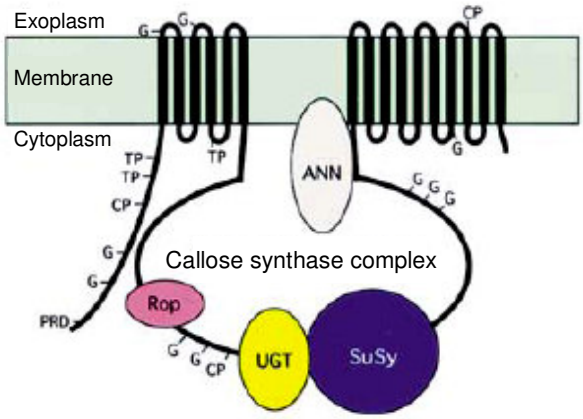

Figure 4. Hypothetical model of the callose synthase complex.
Transmembrane domains and hydrophilic loop interact with Rho-like protein of plants (Rop), annexin (ANN), UDP-glucose transferase (UGT), and sucrose synthase (SuSy). G, potential N-linked gylcosylation sites; CP, cAMP- and cGMP-dependent phosphorylation sites; TP, potential tyrosine phosphorylation sites; PRD, proline-rich domain (after Verma and Hong, 2001).

The hypothesized function of *GSL* genes is supported by homology with the yeast *FKS* genes, which are believed to be involved in callose synthesis (Douglas *et al*., 1994; Cabib *et al*., 2001; Dijkgraaf *et al*., 2002). Additionally, the size of these genes correlates with the molecular mass of ~200-kD catalytic subunit of putative callose synthases. Finally, Li *et al*. (2003) showed that the amino acid sequence predicted from a *GSL* gene in barley (*HvGSL1*) correlates with the amino acid sequence of an active (1,3)-*β*-glucan synthase fraction. *HvGSL1* is expressed at relatively high levels in early developing grain, florets, coleoptiles, and roots, but not in leaves infected with a fungal pathogen. However, most details about regulation and function of *GSL* genes in plants are known from *Arabidopsis.* Twelve *GSL* genes have been identified in *Arabidopsis* (Richmond and Somerville, 2000; Verma and Hong, 2001) and the function of

five genes has been characterized so far. *AtGSL6* (referred to as *CalS1* by Hong *et al*., 2001) encodes a callose synthase catalytic subunit with a high cell plate-specificity. Additionally, transcript levels for this gene increased slightly after inoculation of leaves with *Blumeria graminis* spores (Jacobs *et al*., 2003). Under these conditions, an increase in expression was also observed for *AtGSL5* and *AtGSL11.* Moreover, AtGSL5 as well as AtGSL1 were shown to play an essential and redundant role in plant and pollen development and in fertility (Enns *et al*., 2005). A detailed expression profile is available for *AtGSL2* (referred to as *CalS5* by Dong *et al*., 2005). It was mainly expressed in the anthers but also detected in vascular bundles of diverse tissues. The encoded glucan synthase is required for exine formation during microgametogenesis and for pollen viability.

In terms of plant defense, the *AtGSL5* encoded callose synthase is required for papillary callose formation and is involved in the regulation of the salicylic acid pathway (Jacobs *et al*., 2003; Nishimura *et al*. 2003). Interestingly, the growth of several normally virulent powdery mildew species and of *Perenospora parasitica* was ceased in *gsl5* plants, even though callose was absent in papillae or haustorial complexes. Similar results in *pmr4* plants (Nishimura *et al*. 2003) have raised the question whether the commonly model of callose contributing to resistance needs to be reevaluated.

I.3. Aims of this study

The work described here was initiated in an attempt to analyze interactions of the pathosystem *Triticum aestivum – Fusarium graminearum*. This system was chosen because Fusarium head blight (FHB) of wheat, caused by *F. graminearum*, is one of the most destructive crop diseases (McMullen *et al.*, 1997). Therefore, any new insight into this pathosystem might support the development of new strategies against FHB.

Due to the limited knowledge of a possible involvement of secreted lipases during fungal infection of plants, the first aim was to clone a lipase-encoding gene from *F. graminearum*. The subsequent characterization aimed to include the transcriptional regulation of the lipase gene in culture and *in planta*. The generation of lipase-deficient mutant strains was to be performed in an attempt to examine a putative involvement in fungal virulence. To achieve this, a vector-construct including an internal fragment of the lipase gene was to be used in a transformation-mediated gene disruption. The homologous integration of the disruption-construct via a single-crossover event should result in a dysfunction of the lipase. A role for this lipase in the virulence of *F. graminearum* to wheat and maize was to be examined in plant infection assays.

In general, the precise function of callose during microbial attack has not been demonstrated unequivocally. Therefore, the second aim of this work was to examine if callose synthesis is involved in plant defense as response to fungal penetration in the pathosystem *T. aestivum – F. graminearum.* Because almost nothing was known about the *GSL* gene regulation and callose synthase activity

in wheat, a comprehensive view on organ-specific callose synthesis in wheat was performed during normal growing conditions. These studies included quantitative real-time PCR for expression analysis since this method enables the determination of expression differences between tissues as well as the absolute expression level of individual *GSL* genes. The expression results were to be correlated with enzyme activity, amount of produced callose and callose deposition in the examined organs.

These studies were then followed by the examination of wheat heads infected by *F. graminearum* wild type, a lipase-deficient mutant, and the barley-leaf pathogen *Pyrenophora teres* to induce non-host reactions. The idea of an active role of callose in wheat defense against fungal penetration was tested by comparing *GSL* gene expression, callose synthase activity and callose deposition at different stages of wheat head infection. A putative repression mechanism of callose synthesis during successful fungal penetration was developed and tested in vitro and *in planta*, supported by the generation of GFP-tagged *F. graminearum* strains.

II. Experimental Procedures

II.1. Materials

Unless noted otherwise, restriction enzymes and other DNA-modifying enzymes were purchased from Fermentas (St. Leon Roth, Germany), with the exception of *Taq* polymerase, which was supplied by Eppendorf (Hamburg, Germany). Chemicals used in various media were obtained from Biomol (Hamburg, Germany), Merck (Darmstadt, Germany), Roth (Karlsruhe, Germany), Serva (Heidelberg, Germany), and Sigma-Aldrich (Steinheim, Germany).

II.2. Microbial strains and culture conditions

The *Escherichia coli* strain TOP10F' (Invitrogen, Carlsbad, CA, USA) was used for propagation of cDNA and genomic sequences. Heterologous gene expression was performed by using the *Pichia pastoris* strain KM71 (*arg4 his4 aox1::ARG4*) (Invitrogen) and the pGAPZα A expression vector (Invitrogen), including the *GAP* promoter for constitutive, high level expression in *P. pastoris* in the presence of glucose (Waterham *et al*., 1997). The *Fusarium graminearum* strain 8/1 was obtained from T. Miedaner (Miedaner *et al*., 2000) and maintained on SNA agar plates (Nirenberg, 1981) at 28°C. Induction of conidiation was performed by placing a mycelium plug on SNA-plates and incubating them for 2 weeks at 18°C under near-UV light (TLD 36 W-08; Philips, Eindhoven, The Netherlands) and white light (TL 40 W-33 RS; Philips) with a 12-h photoperiod. Permanent cultures were prepared as conidia suspensions in water and stored at –70°C. The *Pyrenophora teres* strain 15A was provided by B. J. Steffenson (Weiland *et al*., 1999).

II.3. Primers

Table 1. Primers used in PCR reactions. (F) Forward primer; (R) Reverse primer.

A. Conventionel PCR		
Identification	Sequence (5' → 3')	Description
GSP-lipase	TCGAATTCACYGGYCACTCYCTCGGYGGYGC	degenerated primer on lipase motif
FGL1F	ATGCGTCTCCTGTCACTCCTC	complete ORF of lipase gene *FGL1* from *F. graminearum*
FGL1R	TCATACTATGATGAGCGG	
FGL1F-int	CGGCGCCGCAGCATACT	internal fragment of *FGL1*
FGL1R-int	GGGTCCTTGGCGTTCGT	
FGL1-5'Eco	GAATTCATGCGTCTCCTGTCACTCCTC	complete *FGL1* ORF+ restriction sites
FGL1-3'Xba	TCTAGAGATACTATGATGAGCGG	
FGL1-KO5'	GGCGCCATCATCATTCCTATAACAAACATC	internal *FGL1* fragment for cloning of KO-construct
FGL1-KO3'	GGCGCCGGCACTCCTGTATCTTCTCCTA	
β-TubF	TGCTGTTCTGGTCGATCTTG	internal fragment of *β*-tubulin gene as control
β-TubR	GACGGAAGTTTGGACGTTG	
B. Quantitative real-time PCR		
Identification	Sequence (5' → 3')	Accession no.[a]
TaUbiqF	GACCCTCACCGGCAAGACCATC	X56601
TaUbiqR	GTTCACCAAAGCTGCTCCACACCA	
TaGSL2F	TATTGCGGTGTATCTGCTTTCCTG	TaGSL2+4[b]
TaGSL2R	CAACCGCGACCGACCTG	
TaGSL3F	GCGTGCTGGTTTATGGCTTCTC	TaGSL3+7+16+17+20[b]
TaGSL3R	CGGGTGGCTCGGTCCTTCT	
TaGSL8F	TTGGGCTTAATCAGATCGCACTAT	TaGSL8+11+18[b]
TaGSL8R	GCAACCTCCAGCCCTTTCACAA	
TaGSL10F	GTGGGGACAGAGCGAGAACA	TaGSL10[b]
TaGSL10R	GGTATGACATGAATCCAGCAAGTG	
TaGSL12F	TGCATGCCTTATTGGATTTACAGACT	TaGSL12+21[b]
TaGSL12R	CATCCAGCAACTCAAAACTACAAGC	
TaGSL19F	GCTGCGCCTCCTGATCTACCAAT	TaGSL19[b]
TaGSL19R	GGCCCTATCTTACGGAGCACAGC	
TaGSL22F	GATTTCTTCCGGATGCTCTCA	CA682267[b]
TaGSL22R	TCTCGGCGAATTTCTTGTGCTC	CD886203[b]
		CD886204[b]
TaGSL23F	TGGTGGGAGATAGAGCAGGAG	CA484126[b]
TaGSL23R	AAGGGGAACCATGACAGGACAGTA	CK153351[b]
		CK153351[b]

[a]Sequence data primer design is based on.

[b]Contig assembled from sequences as indicated at http://cellwall.stanford.edu/

II.4. Cloning of the lipase cDNA and lipase gene

Total RNA from fungal cultures was isolated with the Invisorb Spin Plant-RNA Mini Kit (Invitek, Berlin, Germany) and the synthesis of cDNAs was performed with the GeneRacer Kit (Invitrogen) according to manufacturer's instructions. The amplification of 3' ends of lipase cDNAs was conducted with the GeneRacer 3' Primer (Invitrogen) and the gene-specific degenerated primer GSP-lipase. In order to design the primer GSP-lipase, the conserved motif characteristics of lipases [LIV]-x-[LIVFY]-[LIVMST]-*G*-[HYWV]-S-*x*-*G*-[GSTAC] (PROSITE Consensus pattern, http://ca.expasy.org/cgi-bin/nicedoc.pl?PDOC00110) were used. A PCR with GSP and GeneRacer 3' Nested Primer was performed according to proposed cycling parameters of the GeneRacer Kit manual. This reaction produced a major 700-bp fragment, which was cloned in the pGEM-T vector (pGEM-T Vector System I, Promega, Madison, WI, USA). For identification of the 5' end of the gene, the GeneRacer 5' primer and a FGL1 specific reverse primer (FGL1R-int) were used to amplify an 800-bp fragment with an overlapping region to the previous identified 3' end fragment. Based upon the resulting sequence information, two primers were designed for amplification of the whole lipase ORF and genomic gene sequence, respectively (FGL1F, FGL1R). Genomic DNA, which was used as a template for amplification of the lipase gene, was isolated according to manufacturer's instructions of the Nucleo Spin Plant Kit (Macherey-Nagel, Düren, Germany).

II.5. Expression analysis by RT-PCR

In order to study the expression of the *FGL1* gene in culture and *in planta*, RNA was isolated with the Invisorb Spin Plant-RNA Mini Kit (Invitek). For RT-PCR SuperScript II Rnase H^- Reverse Transcriptase (Invitrogen) was used according to manufacturer's instructions. The resulting single stranded cDNA was thereafter used as a template in PCR reactions to test *FGL1* transcription in different samples. The PCR reaction was carried out with *FGL1*-specific primers FGL1R-int and FGL1F-int. The cycler program consisted of an initial denaturation step for 3 min at 94°C, followed by 30 cycles of denaturation at 94°C for 30 s, annealing at 57°C for 30 s, and extension at 72°C for 1 min. The final elongation step was performed at 72°C for 10 min. The level of constitutively expressed β-tubulin mRNA served as reference (β-TubF, β-TubR).

For expression analysis *in planta*, infected spikes of wheat were collected and frozen in liquid nitrogen for subsequent RNA isolation.

To examine *FGL1*-disruption on transcriptional level, RNA was isolated from *F. graminearum* wild type and *Δfgl1* strain 3 i) from a wheat germ oil-induced *in vitro* culture after 12 h and ii) from wheat spikes 2 weeks post infection.

FGL1 non-disruption after transformation with pWT-FGL1 and *FGL1* disruption after transformation with pKO-FGL1 was also examined at transcriptional level. RNA was isolated from *F. graminearum* wild type, GFP-tagged wild type-like strains (wt-GFP-1/-2), lipase-deficient strain Δfgl1-2 and GFP-tagged lipase-deficient strains (Δfgl1-GFP-1/-2) from wheat germ oil-induced *in vitro* culture

after 12 h. Detection of *FGL1*-transcripts was performed in an RT-PCR approach as indicated above.

II.6. Expression analysis by quantitative real-time PCR

To study the expression of *GSL* genes in wheat (*TaGSL*), RNA was isolated with the Invisorb Spin Plant-RNA Mini Kit (Invitek). Samples were collected from spike, leaf blade and stem 7 d after anthesis (Zadoks stages 7.5-7.9; Zadoks *et al*., 1974) and frozen in liquid nitrogen for subsequent RNA isolation. For RT-PCR, RevertAid M-MuLV Reverse Transcriptase (Fermentas) was used according to manufacturer's instructions. The resulting single stranded cDNA was thereafter used as a template in quantitative real-time PCR (qPCR) reactions. The single stranded cDNA was normalized, depending on the level of constitutively expressed ubiquitin gene (Trevaskis *et al*., 2003). qPCR reactions were carried out with gene specific primers (Table 1 B) using the Platinum SYBR Green qPCR SuperMix-UDG (Invitrogen) in a volume of 25 µl. Quantification of gene-expression was performed with gene specific cDNA fragments of a known concentration. qPCR reactions were carried out in a iCycler Thermal Cycler (Bio-Rad, Hercules, CA, USA). The PCR program was as follows: incubation for 2 min at 50°C, then 2 min at 95°C, followed by 60 cycles of denaturation at 94°C for 30 s, annealing at 60°C for 30 s and extension at 72°C for 40 s, followed by melting curve analysis to check specificity of fragment amplification. All measurements were repeated twice with eight replicates each. Amplified fragments were analyzed by sequencing.

To study the expression of *GSL* genes in wheat during infection, samples were collected from spikes inoculated with conidia from *F. graminearum* wild type, lipase-deficient *F. graminearum* strain Δfgl1-2 and *P. teres* wild type 1 d, 3 d, 7 d, and 14 d post inoculation (dpi). Uninoculated spikes served as a reference. For RNA isolation, only directly inoculated spikelets and intermediary rachis parts were used. All subsequent procedures for RNA isolation and qPCR were performed as described above, including the primer used in qPCR reactions.

II.7. Detection of extracellular lipolytic activity

Pre-cultures from various *F. graminearum* strains were started with 10^5 conidia in 100 ml YPD medium (1 % (w/v) yeast extract, 2 % (w/v) peptone, 2 % (w/v) D(+)-glucose) and incubated for 2 d at 28°C and 150 rpm. The mycelium was washed twice with double-distilled water and transferred into flasks with 50 ml water supplemented with 2 % (v/v) of different vegetable oils or without oil. Samples were taken every 2 hours in a period of 12 h. Lipolytic activity of the samples' supernatants was measured with a lipase assay using para-nitrophenyl palmitate (pNPP, Sigma, St. Louis, MO, USA) as substrate (Winkler and Stuckmann, 1979). 20 µl of the supernatants were mixed with 200 µl of the reaction buffer (2 mM pNPP, 0.1 % (v/v) Triton X-100, 0.1 % (w/v) gum arabicum, 50 mM bis-tris-propan HCl pH 8.0). The assay was carried out in 96-well microtiter plates at 37°C. The para-nitrophenol (pNP) amount was determined photometrically at 405 nm after 60 min. Lipolytic activity was calculated using pNP as a standard. One unit (U) is equivalent to 1 nmol of pNPP hydrolyzed per minute. Total protein

concentration of the samples was determined in a Bradford assay (Bio-Rad). All measurements were repeated twice with four replicates each.

II.8. Heterologous expression of the *FGL1* gene in *Pichia pastoris*

Heterologous gene expression was performed by using *Pichia pastoris* strain KM71 and pGAPZα A expression vector (Invitrogen). Initially, the ORF of the *FGL1* gene, including the stop codon, was amplified by PCR with oligonucleotides FGL1-5'Eco and FGL1-3'Xba, providing synthetic *Eco*RI and *Xba*I restriction sites at 5' and 3' ends, respectively. cDNA from a wheat germ oil-induced *F. graminearum* culture served as a template. The 1.1 kb PCR product was then directionally cloned into *Eco*RI/*Xba*I site of *P. pastoris* expression vector pGAPZα A. Electrocompetent cells of *P. pastoris* were transformed with 30 µg of linearized vector by using Electroporator II (Invitrogen) according to manufacturer's instructions. Positive clones were selected on YPDS plates (YPD medium + 1 M sorbitol, 2 % (w/v) agar) containing 30 µg/ml zeocin (Invitrogen) for dominant selection. Sequencing was performed to verify integration of the *FGL1*-gene into the *P. pastoris* genome. To determine extracellular lipase activity of positive *P. pastoris* clones, they were incubated at 30°C and 150 rpm in YPD medium, samples were taken after 5 d, centrifuged, and supernatants were subsequently assayed for lipase activity using the lipase assay as described above. For the analysis of inhibitory effects, lipolytic active culture supernatants were supplemented with ebelactone B (Sigma) in a concentration range of 0.075 to 0.45 mM dissolved in ethanol. Lipase activities were measured in the indicated assay with pNPP as substrate.

II.9. Transformation-mediated gene disruption

To generate a construct for disruption of the *FGL1* gene, an internal fragment of the lipase gene was amplified by PCR using FGL1-KO5‘ and FGL1-KO3‘ as primers, and genomic DNA of *F. graminearum* as a template. The resulting 939-bp fragment was cloned into the fungal transformation vector pAN7-1 containing the hygromycin-resistance gene *hph* as a selective marker (Punt *et al*., 1987). The resulting disruption construct pKO-FGL1 was linearized at the unique *BstX*I restriction site, which is located in the *FGL1* insert to enhance efficiency of integration via single crossover event (Banks and Taylor, 1988; Reichard *et al*., 2000) and to reduce occurrence of tandem repeats (Itoh and Scott, 1997). Transformation was carried out according to Royer *et al*. (1995) with 30 µg of the linearized construct and protoplasts of *F. graminearum* wild-type strain 8/1 (Jenczmionka *et al*., 2003).

To generate GFP-tagged wild type-like strains, a fragment of the *FGL1* lipase gene was amplified by PCR using FGL1-KO5‘ and FGL1-3’Xba as primers and genomic DNA of *F. graminearum* as a template. The resulting 1072-bp fragment contained a 5’-deletion but the full 3’-end and was cloned into the into fungal transformation vector pAN7-1. The resulting construct pWT-FGL1 was linearized at the unique *BstX*I restriction site, which is located in the *FGL1* insert. The generation of a GFP-tagged lipase-deficient strain was performed with the disruption construct pKO-FGL1 (described above). The GFP-harboring plasmid pIGPAPA (Horwitz *et al*., 1999) was linearized within the amp^R cassette using the restriction enzyme *Cai*I to induce homologous integration into the amp^R cassette

of pWT-FGL1 and pKO-FGL1, respectively. Co-transformation was carried out according to Maier *et al*. (2005) with 30 µg of each linearized construct (pWT-FGL1 + pIGPAPA and pWT-FGL1 + pIGPAPA, respectively).

The received mutants were cultivated on CM-plates containing 100 µg/ml hygromycin B (Duchefa, Haarlem, The Netherlands). Transformants were tested by Southern hybridization for insertion of disruption construct due to homologous recombination.

II.10. Southern blot analysis

Genomic DNA from various *F. graminearum* strains was digested with restriction enzymes, separated on a 0.8 % agarose/TBE gel and blotted onto a Hybond NX membrane (Amersham Biosciences, Little Chalfont, UK). A DIG (digoxygenin)-labeled (Roche, Mannheim, Germany) DNA probe was used for overnight-hybridization at 68°C. Hybridization and washing of the blots were performed according to the manufacturer's instructions. Integration of pWT-FGL1 and pKO-FGL1, respectively, into the *F. graminearum* genome was tested by using a *FGL1*-specific probe and integration of pIGPAPA into the backbone of the FGL1-constructs by hybridization with a *GFP*-specific probe on the same membrane.

II.11. Plant infection and pathogenicity tests on wheat

Wheat plants of cultivars Nandu (Lochow-Petkus, Bergen-Wohlde, Germany) and Batis (Strube, Söllingen, Germany) were planted in soil at 21°C, approximately 70 % humidity, and a photoperiod of 16 h (10000 lx) per day. Infection was performed at plants growing for three months until anthesis (approximately 6 to 7

weeks after germination; Zadoks stages 6.5-6.9; Zadoks *et al*., 1974). A single spike was inoculated within the palea and lemma of two basal florets of two central spikelets with a droplet of 10 µl water containing 200 conidia of *F. graminearum* and *P. teres,* respectively (modified after Pritsch *et al*., 2001). The inoculated spikes were enclosed in small plastic bags during the first 3 days to ensure a high humidity for infection and to prevent a cross contamination of different *F. graminearum* isolates. The inoculated plants were incubated in a growth chamber at 21°C with a 16 h photoperiod (10000 lx). Infection of wheat spikes was monitored up to three weeks post inoculation. To detect the involvement of FGL1 in pathogenicity, inoculations were carried out with: conidia of wild-type strain, five independent *Δfgl1* strains, and two independent ectopic strains. As negative control, spikes were inoculated with pure water.

To examine an influence of ebelactone B, inoculation of a spikelet was performed with a 10 µl-droplet of 200 wild-type strain conidia supplemented with 3.3 µl ebelactone B dissolved in ethanol (concentration: 5 mg/ml) reaching a final concentration of 2 mM.

To detect a possible impact of FFA on wheat infection, 2 µl of ethanol-dissolved FFA (concentration: 3.2 mM) and pure ethanol as control were added 3 dpi to each of the wt-GFP-1 and Δfgl1-GFP-1 inoculated florets of the wheat cultivar Nandu.

II.12. Plant infection and pathogenicity tests on maize

Seeds from the maize inbred line A188 (Green and Philips, 1975) were grown in a green house (temperature: 26°C – 30°C, humidity: 70 % - 85 %, natural daily photoperiod with additional artificial light when required), in order to detect an involvement of FGL1 during maize infection. After growth of approximately four months, plants were infected 6 d after silks emerged. Before inoculation, silks were manually pollinated to ensure optimal pollination. Individual plants were inoculated by injecting conidia suspensions into the silk channel of primary ears using a syringe and cannula (Reid *et al.*, 1995). Plant infection was performed with 4 ml of conidial suspension at a concentration of 8 x 10^5 conidia per ml of *F. graminearum* wild type, three previously confirmed *Δfgl1* strains, and an ectopic strain. As a negative control, ears were inoculated with 4 ml of water. The inoculated ears were enclosed in plastic bags during the first 3 days and inoculated plants were cultivated under the same conditions as described for growing. Infection of maize cobs was monitored five weeks post inoculation.

II.13. Membrane preparation

All isolation procedures were carried out at 4°C. 200 mg of the same grounded tissue as used for RNA isolation was homogenized with the ultrasonic processor UP 200H (Dr. Hielscher GmbH, Teltow, Germany) in 3.5 ml 50 mM Tris/HCl, pH 7.3, containing 1 mM DTT, 5 mM EDTA, 25 µM PMSF (phenylmethylsulfonyl fluoride; Sigma) (modified after Shedletzky *et al.*, 1997). The homogenate was centrifuged for 5 min at 12,000 x g. Subsequently, the supernatant was centrifuged for 1 h at 100,000 x g. The membrane pellet was resuspended in 500

µl 50 mM Tris/HCl, pH 7.3. Membranes were immediately used in the (1,3)-*β*-glucan synthase assay. Total protein concentration of the samples was determined in a Bradford assay (Bio-Rad).

Additionally, a possible impact of free fatty acids (FFA) on (1,3)-*β*-glucan synthase activity was examined for the wheat cultivars Nandu and Batis. Membranes were prepared from uninoculated spikes 7 d after anthesis (Zadoks stages 7.5-7.9; Zadoks *et al*., 1974), as described above.

II.14. (1,3)-*β*-glucan synthase assay

(1,3)-*β*-glucan synthase activity was measured in a fluorescence assay. Reactions were carried out in 96-well microtiter plates with modifications to Shedletzky *et al.* (1997). 20 µl of the resuspended membranes (protein content: 2 – 2.5 µg) were incubated with 70 µl reaction buffer (50 mM Tris/HCl, pH 7.3, 0.02 % digitonin (Sigma) , 2 mM $CaCl_2$, 20 mM cellobiose, 0.5 mM uridine 5'-diphosphoglucose (UDP-glucose; Sigma)) for 1 h at 25°C. The addition of 10 µl 10 N NaOH terminated the reactions. The (1,3)-*β*-glucan (callose) produced was solubilized by shaking the microtiter plate at 80°C for 30 min.

To examine a possible impact of free fatty acids (FFA) on (1,3)-*β*-glucan synthase activity for the wheat cultivars Nandu and Batis, reaction wells of microtiter-plates were supplemented with 2 µl of ethanol-dissolved FFA of a defined concentration (final concentrations: 0.7, 7, 17.5, 35, 70, 700 µM) and pure ethanol as control. FFA: stearic acid [18:0] (Merck), oleic acid [18:1] (Sigma), linoleic acid [18:2] (Sigma), γ-linolenic acid [18:3] (Sigma).

II.15. Callose extraction

Callose was extracted from 50 mg of the same tissue as used for RNA isolation. The tissue was soaked for 5 min in 1.2 ml ethanol by shaking at 50°C. After centrifugation (5 min, 400 x g, room temperature) the pellet was washed twice in 600 µl ethanol and centrifuged (5 min, 400 x g). To solubilize callose, the washed pellet was incubated for 15 min at 80°C in 200 µl 1 N NaOH under shaking conditions (modified after Köhle *et al.*, 1985). Aliquots of 10 µl of this solution were used for callose determination in 96-well microtiter plates.

II.16. Callose determination

Extracted callose from both glucan synthase assay and callose extraction was determined by addition of 200 µl and 120 µl, respectively, of the aniline blue mix (Shedletzky *et al.*, 1997). After incubation at 50°C for 30 min and subsequently at room temperature for 30 min under shaking conditions, fluorescence was quantified with a fluorescence plate reader Fluoroskan II (Labsystems, Helsinki, Finland) using an excitation wavelength of 355 nm and an emission wavelength of 460 nm. Standard curves were generated with (1,3)-*β*-glucan form *Euglena gracilis* (Sigma-Aldrich). Defined amounts of this glucan were dissolved by heating 30 min at 80°C in 1 N NaOH. Standard samples used in glucan synthase assay contained the same components as the reaction mixtures. All measurements were repeated twice with six replicates each. Amounts of callose were expressed as *E. gracilis* glucan-equivalents.

II.17. NADH oxidase activity assay

The NADH oxidase activity assay was carried out in 96-well microtiter plates. Reaction was initiated by addition of 130 µl NADH-containing reaction buffer (50 mM Tris/HCl, pH 7.3, 150 µM NADH, 1 mM KCN; modified from Chueh *et al.*, 1997) to 20 µl of prepared membranes (protein content: 2 – 2.5 µg). Immediately after addition, the absorbance was measured at 355 nm with a fluorescence plate reader Fluoroskan II (Labsystems, Helsinki, Finland). Decrease in the absorbance was measured after 10 min. NADH oxidase activity was calculated from changes in absorbance and indicated as percentage of oxidized NADH per 10 min and µg protein.

II.18. Microscopic analyses

Freshly cut tissue from wheat spike, leaf blade, and stem was stained for 1 min in a solution containing 1 % (w/v) aniline blue and 1 % (v/v) acetic acid. Subsequently, tissues were transferred into glycerol for 2 h for washing out excessive dye (Braune *et al.*, 1983). Tissues were examined by epifluorescent illumination (365 nm excitation filter, 395 nm chromatic beam splitter, 397 nm barrier filter) using an Axioskop microscope (Zeiss, Germany).

Localization of callose depositions was additionally carried out with a stereo microscope Leica MZ6 (Wetzlar, Germany) from freshly cut, uninoculated wheat spikes as well as spikes inoculated with *F. graminearum* wild-type, Δfgl1-2 and *P. teres* wild type 1, 3, 7, and 14 dpi. Staining procedures were performed as described above.

Freshly cut wheat spikes inoculated with GFP-tagged *F. graminearum* strains (wt-GFP-1 and Δfgl1-GFP-1) were examined with a stereo fluorescence microscope Leica MZ FLIII. The filter set was the Leica GFP2 filter set (excitations 480/40 nm, barrier filter 510 nm).

II.19. Accession numbers

Sequence data of lipase gene *FGL1* from *F. graminearum* and ubiquitin as well as *TaGSL* genes from wheat cultivar Nandu have been deposited with the EMBL/DDBJ/GenBank data libraries under the following Accession No.: AY292529 (*FGL1*), DQ086482 (*TaUbiq*), DQ086483 - DQ086490 (*TaGSL2, 3, 8, 10, 12, 19, 22, 23*).

III. Results

III.1. Cloning and sequence analysis of the lipase gene *FGL1* from *F. graminearum*

Wheat germ oil was the best inducer of extracellular lipolytic activity for *F. graminearum* in comparison to other oils tested (Figure 5).

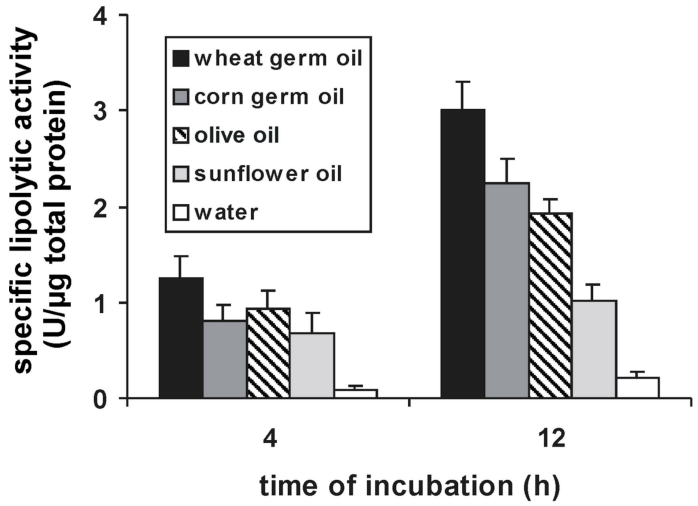

Figure 5. Induction of extracellular lipolytic activity of *F. graminearum* cultures using different vegetable oils.

Supernatant samples were taken after 4 and 12 h and lipolytic activities were measured with the pNPP lipase-assay. Error bars indicate the confidence interval with probability of error of $\alpha = 0.05$. Measurements were repeated twice with four replicates each.

cDNA derived from a wheat germ oil-induced *F. graminearum* culture served as a template for RACE-PCR. Two fragments were amplified, one from the 5' and the other from the 3'-end of a putative lipase. An ORF of 1056 bp was deduced from the sequence of both fragments. Primers designed from the ORF were used to generate the complete genomic lipase-encoding gene. The sequence of this gene, designated *FGL1,* revealed two apparent introns of 52 bp and 58 bp at

positions 91 and 257, respectively. The deduced protein consists of 352 amino acids with an N-terminal stretch of 15 hydrophobic amino acid residues corresponding to a signal peptide. Searches done using the FGL1 amino acid sequence as a query (Figure 6) showed highest similarity to lipases of *N. haematococca* (65.2 %) and *Fusarium heterosporum* (66.2 %). High-stringency Southern blot analysis of genomic DNA revealed that *FGL1* is present as a single copy in the genome (Figure 11 A).

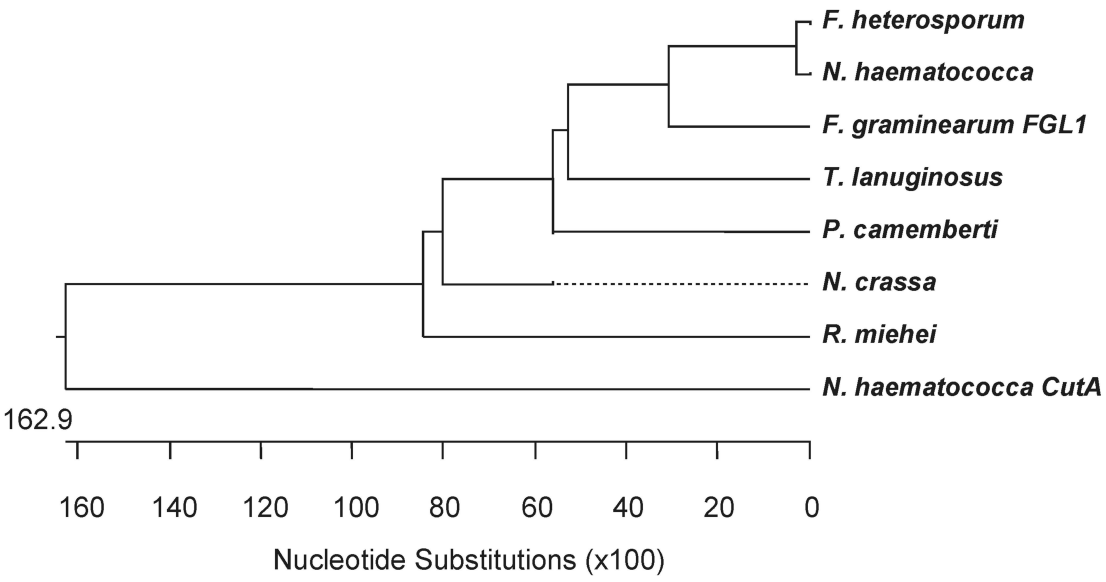

Figure 6. Phylogenetic tree of secreted fungal lipases.

F. graminearum (GeneBank Accession No. AY292529), *F. heterosporum* (S77816), *N. haematococca* (AJ271094), *Thermomyces lanuginosus* (O59952), *Penicillium camemberti* (D90315), *Neurospora crassa* (AL513444), *Rhizomucor miehei* (A02536), cutinase from *N. haematococca* (FSOCUTA M29759). The proteins were aligned using ClustalW Method (Thompson *et al*., 1994).

III.2. Expression of *FGL1* in culture and *in planta*

FGL1 transcription was detected in the presence of wheat germ oil (a putative lipase substrate) but not if glucose was present in the medium (Figure 7 A). Similarly, lipolytic activity was detected only from cultures grown in medium containing water and wheat germ oil as the sole ingredients (Figure 7 B). During host infection, *FGL1* was expressed at all time points examined (Figure 8). No *FGL1* transcripts were detected in uninoculated control plants.

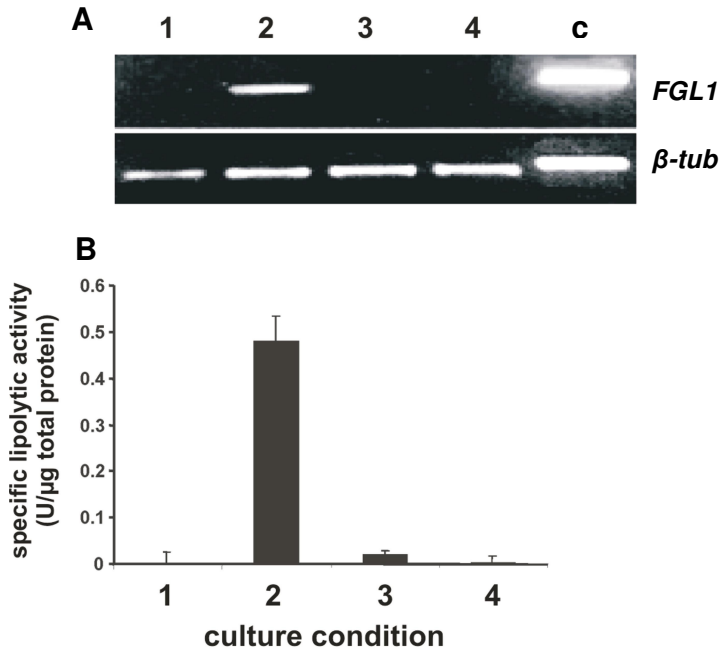

Figure 7. Expression analysis of FGL1 and lipolytic activity of *F. graminearum* supernatants under different culture conditions.

A. PCR amplification with *FGL1*-specific primers. Template cDNA was generated from isolated RNA of *F. graminearum* wild-type cultures. Cultures were incubated for 4 h at 28°C and 150 rpm in media containing H_2O (1), H_2O + 2 % wheat germ oil (2), H_2O + 1 % glucose (3), and H_2O + 1 % glucose + 2 % wheat germ oil (4). Genomic *F. graminearum* DNA was used as a control (c). β-tubulin-specific primers (*β-tub*) were used as expression control.

B. Lipolytic activity of culture supernatants was measured with the pNPP lipase-assay. Error bars indicate confidence interval with probability of error of $\alpha = 0.05$. Measurements were repeated twice with four replicates each.

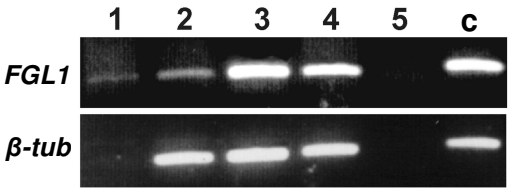

Figure 8. Expression analysis of *FGL1* during infection of wheat.

PCR amplification with *FGL1*-specific primers. cDNA generated from isolated RNA of wheat spikes infected with *F. graminearum* wild-type 1 d post inoculation (dpi) (1), 3 dpi (2), 7 dpi (3), 14 dpi. (4), and cDNA from uninfected wheat spikes (negative control) (5) served as template. Genomic *F. graminearum* DNA (including 58 bp intron DNA) used as a control (c). β-tubulin-specific primers (*β-tub*) were used as expression control.

III.3. Inhibition of FGL1 produced in a heterologous host

The identity of the *FGL1* gene product as a lipase was verified by expressing *FGL1* in *Pichia pastoris* strain KM71. The supernatant of the recombinant colony revealed high lipolytic activity as compared to colonies expressing only the vector pGAPZα A (Figure 9). The known lipase inhibitor ebelactone B reduced secreted lipase activity almost completely at a concentration of 0.45 mM (Figure 9).

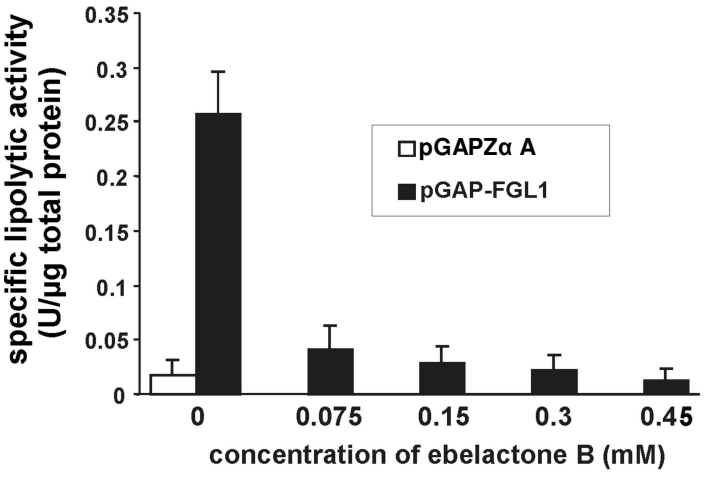

Figure 9.

III.4. FGL1 inhibition *in planta*

Inhibition of FGL1 by ebelactone B suggested that ebelactone B might influence host plant infection. To examine this, wheat spikelets were inoculated with a suspension of *F. graminearum* conidia supplemented with ebelactone B. Since ebelactone B was dissolved in ethanol, control plants were inoculated with a conidial suspension supplemented with an equivalent volume of ethanol. Additionally, the effect of 2 mM ebelactone B without conidia was also tested on control plants. Three weeks post infection, spikes inoculated with conidia only were totally bleached. Infection by conidia supplemented with ebelactone B was restricted to the inoculated spikelets (Figure 10). The remaining parts of these spikes revealed no symptoms of bleaching and were as healthy as spikes of control plants. Ethanol-supplemented wild-type conidia caused complete bleaching just like conidia alone (Figure 10). Conidial germination was not affected by 2 mM ebelactone B (data not shown).

←

Figure 9. Inhibition of *F. graminearum* lipase FGL1 by ebelactone B.

Lipolytic activity was measured in YPD-culture supernatants of *P. pastoris* strain KM71 harboring expression plasmid as a control (pGAPZα A) and of *P. pastoris* with heterologous expression of *FGL1* gene (pGAP-FGL1) using pNPP lipase assay. Cultures were incubated for 5 d at 30°C and 150 rpm. Error bars indicate confidence interval with probability of error of $\alpha = 0.05$. Measurements were repeated twice with four replicates each.

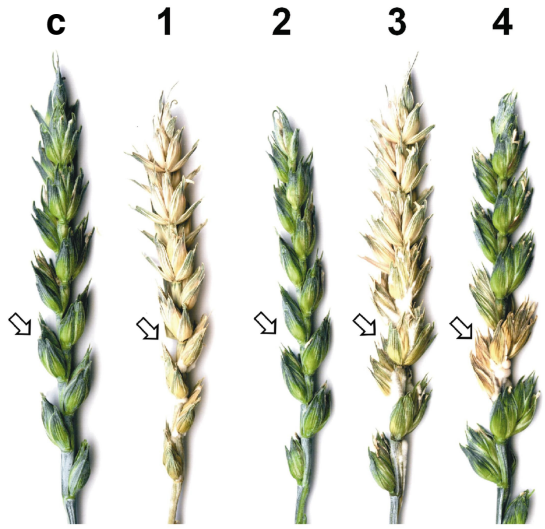

Figure 10. Effect of ebelactone B on *F. graminearum* infection of wheat (cv. Nandu).
Two central spikelets were inoculated with 20 µl of water (control; c), 400 wild-type conidia without supplementation (1), 20µl of ebelactone B dissolved in ethanol (concentration: 2 mM) without conidia (2), 400 wild-type conidia supplemented with same volume of ethanol (3) as in (4), and 400 wild-type conidia supplemented with ebelactone B dissolved in ethanol (concentration: 2 mM) (4). Arrows indicate inoculation sites. Figure shows spikes 3 weeks post infection. Pathogenicity tests were repeated nine-times.

III.5. *F. graminearum* transformation and characterization of secreted lipase activity of *Δfgl1* strains

To determine extracellular lipase activity of FGL1 in culture and during host plant infection, *FGL1* was disrupted via transformation. Fifty *F. graminearum* transformants were analyzed by PCR. The complete *FGL1* gene could not be amplified in 40 out of 50 transformants. After single conidiation, high-stringency Southern blot analysis of genomic DNA of seven randomly chosen transformants showed homologous integration of the disruption construct in five of them; vector integration in the remaining two transformants was ectopic (Figure 11 A).

FGL1-gene disruption was analyzed at the transcriptional level by isolating RNA i) from *in vitro* cultures and ii) from wheat spikes infected by *F. graminearum* wild type and strain Δfgl1-3. No *FGL1*-transcripts were amplified from cDNA of strain Δfgl1-3, whereas cDNA of the wild-type strain revealed a product of the expected size (Figure 11 B and C).

Extracellular lipase activity of the five *Δfgl1* strains and the two ectopic strains was analyzed during growth in liquid cultures supplemented with different carbon sources and was compared to that of the *F. graminearum* wild-type strain.

Lipolytic activity was not detected in supernatants of the *Δfgl1* strains, or in those of the wild-type and ectopic strains, when cultures were supplemented with glucose or glucose plus wheat germ oil. In water, slight lipolytic activity was detected, but only for the wild-type and the ectopic strains after 12 h (data not shown). In contrast, lipase activity of the wild-type and two ectopic strains was highly induced by wheat germ oil as a single carbon source, whereas the five *Δfgl1* strains had reduced extracellular lipase activity (Figure 12). The *Δfgl1* strains had increased lipolytic activity after 12 h, reaching nearly 30 % of wild-type activity. There were no significant differences in extracellular lipase activities among the five *Δfgl1* strains. Lipolytic activities of the ectopic strains were similar to those of wild-type, except for late stage cultures, which had activity reduced nearly 30 % after 10 h and 16 % after 12 h of incubation.

To confirm that no undetected mutations impaired mycelial growth of the transformants, the wild-type, *Δfgl1* strains, and ectopic strains were transferred to CM, YPD, and SNA media. No differences in growth among these strains were

observed. Additionally, neither conidial development nor germination of the *Δfgl1* and the ectopic strains deviated from wild type on SNA medium (data not shown).

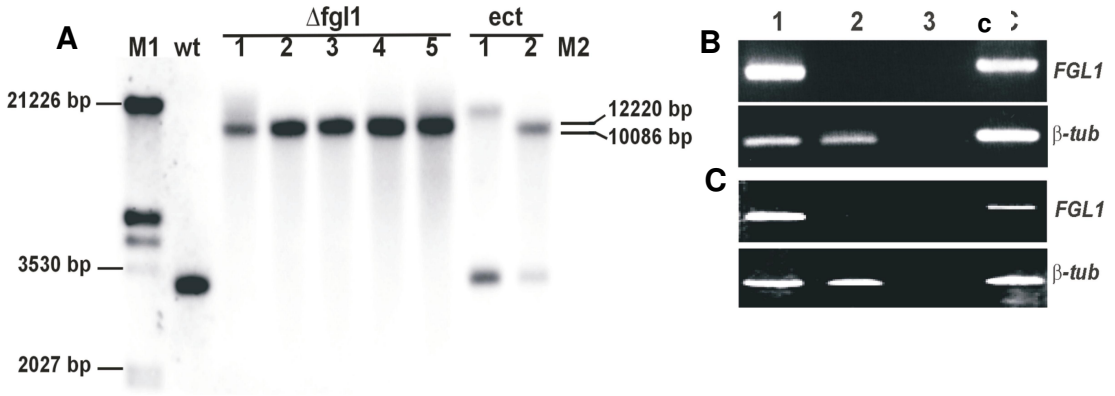

Figure 11. Analysis of *F. graminearum* wild-type and mutant strains via Southern blot and *FGL1* gene expression.

A. Genomic DNA of *F. graminearum* wild type (wt), *Δfgl1* strains (Δfgl1-1/-2/-3/-4/-5), and ectopic transformants (ect1/2) was restricted with *Kpn*I. Hybridization was performed with DIG-labeled internal fragment of *FGL1* gene. Fragment sizes were determined with Dig-labeled DNA Molecular Weight Marker III (Roche, Mannheim, Germany) (M1) and Lambda Mix Marker, 19 (MBI-Fermentas, St. Leon-Rot, Germany) (M2). Relevant fragment sizes of Lambda Mix Marker, 19 derived from agarose gel photo-measuring. The detected shift of *Δfgl1* strains confirmed single homologous integration of disruption construct.

B. cDNA generated from isolated RNA of wheat germ oil induced *in vitro* cultures after 12 h.

C. cDNA generated from isolated RNA of wheat spikes 2 weeks post infection.

Cultures and spikes were inoculated with conidia of *F. graminearum* wild-type (1) and *Δfgl1* strain 3 (2). Water control and water inoculated wheat spikes, respectively, served as negative control (3). Genomic *F. graminearum* wild-type DNA (c) was used as positive control. PCR amplification was performed with *FGL1*-specific primers comprising complete *FGL1*-ORF(*FGL1*) and β-tubulin-specific primers (*β-tub*) as expression control.

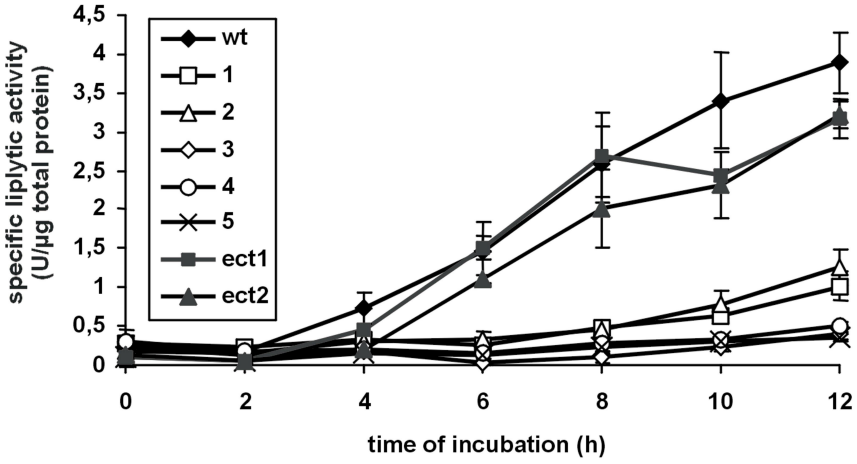

Figure 12. Extracellular lipolytic activity of *F. graminearum* wild type (wt), *Δfgl1* strains (1-5), and ectopic strains (ect1/2) after induction by wheat germ oil.

Cultures were incubated in water supplemented with 2 % wheat germ oil at 28°C and 150 rpm. During a time range of 12 h samples were taken every 2 h. Lipolytic activity was measured with pNPP lipase-assay. Error bars indicate confidence interval with probability of error of α = 0.05. Measurements were repeated twice with four replicates each.

III.6. Plant infection with *Δfgl1* strains

To determine if FGL1 is involved in pathogenicity, wheat spikes were infected with conidia from the five *Δfgl1* strains, the wild-type, and the two ectopic strains. Three weeks post inoculation, spikes infected with all five *Δfgl1* strains had drastically reduced symptoms compared to wild-type infected spikes. There were no significant differences among these strains (Table 2). Spikes inoculated with wild-type conidia were totally bleached except for the spikelets at the lower end of the spike. Similar results were obtained for the ectopic strains. However, the average percentage of infection of the ectopic strains was significantly reduced compared to the wild type (Table 2). In contrast to wild-type infection, only directly inoculated and adjacent spikelets were bleached during *Δfgl1* strain

infection (Figure 13). Apart from bleached spikelets, the remaining parts of the spike were not affected and did not differ in appearance compared to uninoculated spikes. This pattern of symptoms was similar to the ebelactone B-supplemented wild-type infection (Figure 10). To gain a more detailed picture of the infection pattern of the *Δfgl1* strains, kernels were removed from spikes three weeks post infection. The rachis of the wild-type infected spikes was completely bleached. Almost no symptoms of bleaching were detectable at the rachis of spikes infected with the *Δfgl1* strains. As a result, the rachis was comparable to one of uninfected spikes (Figure 14). Slight bleaching of the rachis of the spikes infected with the *Δfgl1* strains was only observed directly adjacent to the inoculated spikelets when spikelets grew close together (Figure 14).

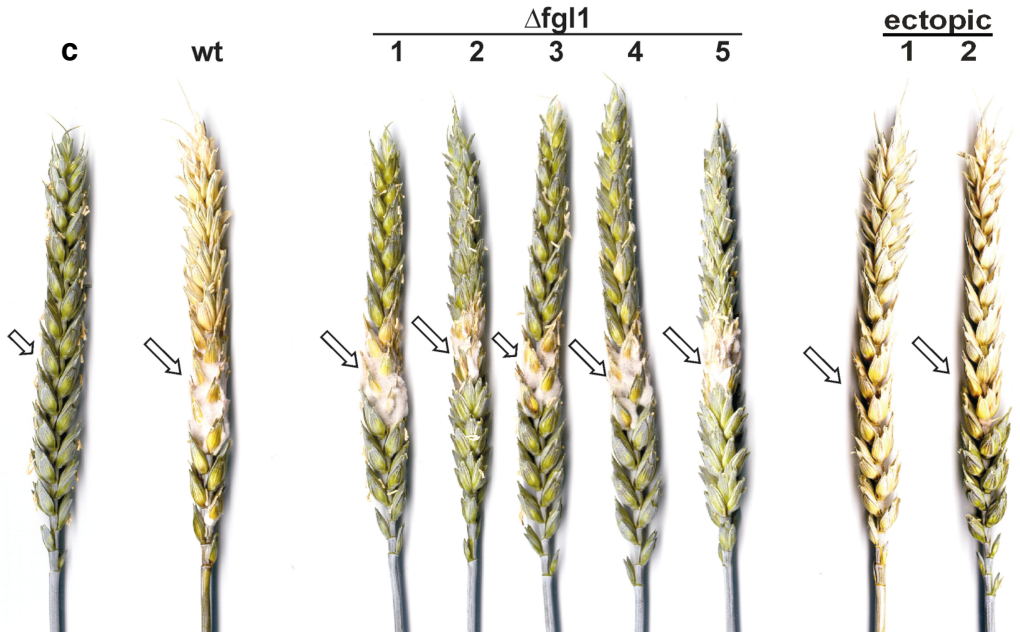

Figure 13.

Moreover, these results correlated to kernel quality. Kernels removed from bleached spikelets were completely shriveled and bleached or not even developed. Hence, wild-type infected spikes contained no unaffected kernels. Even kernels at the lower end of the spike had a shriveled surface and were reduced in size compared to kernels removed from uninfected spikes. In contrast, kernels of unbleached spikelets of spikes infected with the *Δfgl1* strains were not reduced in size and showed no signs of a shriveled surface. The quality of these kernels was comparable to that of uninfected spikes. They represented the majority of the harvested kernels of spikes infected with the *Δfgl1* strains. Reduced quality was limited to kernels harvested from inoculated spikelets and adjacent spikelets, which had symptoms similar to those of wild-type infected kernels (Figure 14).

←

Figure 13. Infection of wheat spikes (cv. Nandu) with *F. graminearum* wild-type, *Δfgl1* strains, and ectopic strains.

Two central spikelets were each inoculated with 10 µl of water (control, c), 200 wild-type conidia (wt), 200 conidia of each *Δfgl1* strain (Δfgl1-1/-2/-3/-4/-5), and 200 conidia of ectopic strains (ectopic 1/2). Arrows indicate inoculation site. Figure shows spikes 3 weeks post infection. Pathogenicity tests were repeated fifteen-times for every strain.

Figure 14. Spike stem appearance and kernel quality after infection of wheat spikes (cv. Nandu) with *F. graminearum* wild-type and *Δfgl1* strain 3.

Inoculation of two central spikelets each performed with 10 µl of water as control, 200 wild-type conidia, and 200 conidia of *Δfgl1* strain 3 (Δfgl1-3). Kernels represent the original position at the spike before harvesting and the yield of one spike 3 weeks post infection. Arrows indicate inoculation site. Parallel samples were obtained from replicates of the same attempt. Pathogenicity tests were repeated fifteen times for every strain.

Longitudinal sections of inoculated wheat spikelets and adjacent stem regions showed the extent of bleached and necrotic tissue (Figure 15). Both the inoculated and the adjacent spikelet of the wild-type infected spike were completely bleached and necrotic. The same symptoms were observed for the rachis. Bleached and necrotic tissue of spikes infected with *Δfgl1* strains was limited to the directly inoculated spikelet and adjacent parts of the stem. Additionally, a barrier-like zone of firm dark tissue was formed at the transition

zone of the rachilla and the rachis. The upper adjacent spikelet and rachis region were comparable to those of uninfected spikes (Figure 15).

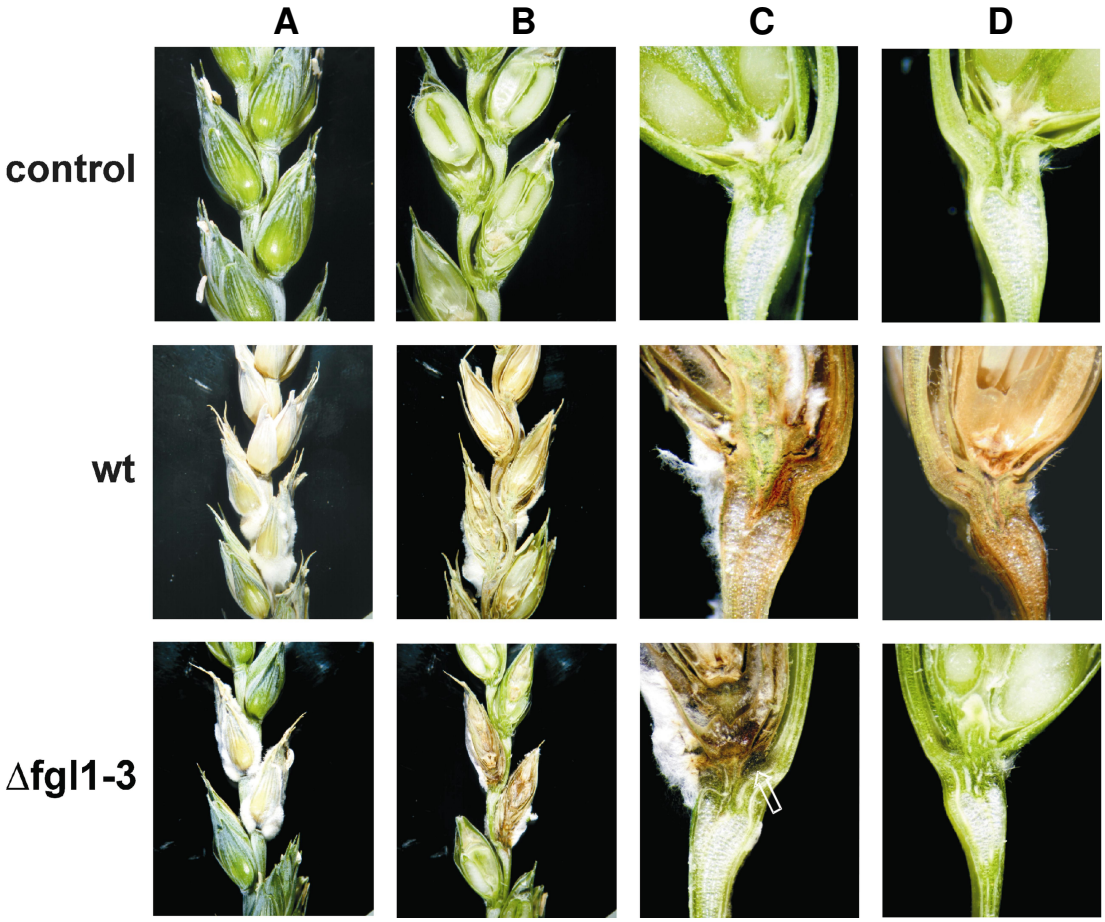

Figure 15. External view and longitudinal section of wheat spikelets (cv. Nandu) and adjacent rachis region of *F. graminearum* wild-type and *Δfgl1* strain 3 infection.

A. External view of wheat spikes comprising inoculated and adjacent spikelets.

B. Longitudinal section of same spike segment as shown in column A.

C. 3-times magnified view of the section as shown in B, comprising transition zone of rachilla and rachis of inoculated spikelets and adjacent rachis segment.

D. Analogous to C, comprising the spikelet next to inoculated spikelet.

Uninfected wheat spikes (control), *F. graminearum* wild-type infected spikelets (wt), and *Δfgl1* strain 3 infected spikelets (Δfgl1-3) were compared 3 weeks post infection. Arrow indicates formation of a barrier at transition zone of rachilla and rachis of the spikelet infected with strain Δfgl1-3.

Δfgl1 strains had reduced virulence on maize as well as wheat. Wild-type and ectopic strains caused completely rotten cobs. In contrast, cobs infected by *Δfgl1* strains showed only minor symptoms; there was normal kernel development on uninfected cob parts (Figure 16).

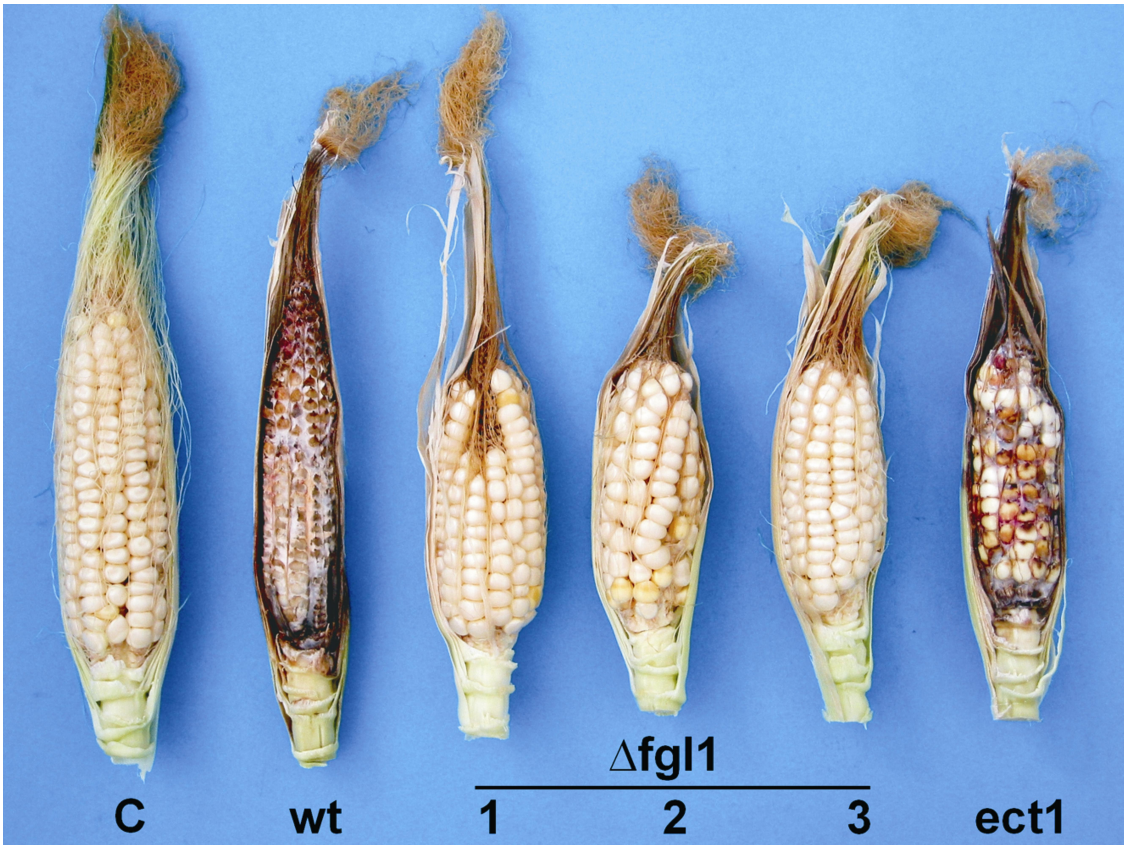

Figure 16. Infection of maize ears with *F. graminearum* wild-type, Δfgl1 strains 1, 2, and 3, and ectopic strain ect1.

Inoculation of ears was performed by injecting 4 ml of conidial suspension (8 x 10^5 conidia x ml^{-1}) of wild-type (wt), *Δfgl1* strains 1, 2, and 3 (Δfgl1-1/-2/-3), and ectopic strain (ect1) into the silk channel. As a control (c), 4 ml of water were injected. Figure shows cobs 5 weeks post infection Pathogenicity tests were repeated ten-times for each strain.

Disease severity on cobs, estimated visually by the rating method of Reid *et al.* (1995), was greatly reduced on maize inoculated with *Δfgl1* strains (a rating of 3 indicating 4 – 10 % infection), whereas wild-type and ectopic strains had ratings of almost 7 (76 – 100 % infection) (Table 2). No significant differences among the three *Δfgl1* strains were observed.

Table 2. Virulence of *F. graminearum* strains to wheat (cv. Nandu) and maize.

Treatment[a]	Wheat		Maize	
	Percentage of infection[b]		Rating[c]	
	Mean	Conf. Int.[d]	Mean	Conf. Int.[d]
Water control	0.0	-	1.0	-
Wild-type	94.1	4.8	6.7	0.3
Δfgl1-1[f]	12.8	2.7[e]	3.2	0.7[e]
Δfgl1-2[f]	12.6	1.7[e]	2.5	0.7[e]
Δfgl1-3[f]	12.3	3.4[e]	3.2	0.9[e]
Δfgl1-4[f]	12.5	2.7[e]	n.t.[h]	-
Δfgl1-5[f]	13.0	3.3[e]	n.t.[h]	-
ect1[g]	62.0	19.3	6.8	0.3
ect2[g]	60.9	15.1	n.t.[h]	-

[a]Repeat experiments gave similar results.

[b]Infection referred to partially or completely bleached spikelets observed 3 weeks post infection. Spikelets showing minor symptoms (tiny yellow or brown spots) were not counted. Results are the average of 15 inoculated wheat heads (14-22 spikelets per head) inoculated with 400 conidia.

[c]Disease severity estimated visually by the rating method of Reid *et al.* (1995) observed 5 weeks post infection.

Ratings ranged from 1.0 (0 % infection) to 7.0 (76 – 100 % infection). Results are the average of 10 maize ears inoculated with 3.2×10^5 conidia.

[d]Confidence interval with probability of error of $\alpha = 0.05$.

[e]Significantly different from wild-type and ectopic strains at $P < 0.05$.

[f]Homologous integration of disruption construct.

[g]Ectopic integration of disruption construct.

[h]Not tested.

III.7. Phylogenetic analysis of (1,3)-β-glucan synthases

A phylogenetic tree was generated by the alignment of sequences of putative (1,3)-β-glucan synthases, encoded by *GSL* genes, from *Triticum aestivum* (*TaGSL*), *Hordeum vulgare* (*HvGSL*), *Zea mays* (*ZmGSL*), *Oryza sativa* (*OsGSL*) and *Arabidopsis thaliana* (*AtGSL*) (Figure 17). All sequences were obtained from the cell wall database at Stanford University (http://cellwall.stanford.edu/).

Analysis of *TaGSL* sequences from this database revealed redundancy of these data. Even though 21 different *TaGSL* genes were specified in the database, only eight *TaGSL* genes could be identified as being to be definitely different and appropriate for the generation of phylogenetic tree and subsequent expression analysis. *TaGSL2* was composed of database data from *TaGSL2* and *4*, *TaGSL3* from *TaGSL3*, *7*, *16*, *17* and *20*, *TaGSL8* from *TaGSL8*, *11* and *18*, and *TaGSL12* from *TaGSL12* and *21*. *TaGSL10* and *19* showed no homology to other sequence data. Sequences for *TaGSL22* and *23* were constructed from singleton sequence data of the database. It was not possible to amplify fragments via PCR reaction using primer based on sequence data of *TaGSL1*. Further sequence data could not be identified as definitely independent *TaGSL* genes or were not suitable for expression analysis. Similar to *TaGSL* genes, the number of *GSL* genes, suitable for the alignment, was reduced for barley (8 out of 10) and maize (9 out of 17).

In general, full sequence is only known for a limited number of callose synthases. Therefore, the phylogenetic tree is based on the alignment of regions, which were found in all sequences. In a first step, known amino acid sequences were

aligned with the CLUSTL V method. Subsequently, amino acid sequences were restricted to the active domain and/or the C-terminal end, because these regions were present in all sequences. The final alignment was performed with the CLUSTL W method to generate the phylogenetic tree. As a result, TaGSL10, 22 and 23 form a group with low homology to other glucan synthases. Especially TaGSL19 reveals highest divergence amongst all other analyzed enzymes, resulting in the formation of single branch emerging from the tree's root. Apart from these wheat glucan synthases, only OsGSL11 from rice shows a low level of homology compared to other enzymes. In contrast to other rice synthases, OsGSL11 is not assembled in a subgroup with other enzymes. In general, further analyzed glucan synthases from wheat reveal high homology to synthases from barley and maize. Interestingly, glucan synthases from *A. thaliana* predominantly form their own subgroups (e.g. AtGSL3, 6, 9 and 12). Jacobs *et al.* (2003) have reported that the GSL genes *AtGSL1* and *5*, *AtGSL3* and *6* and *AtGSL7* and *11* are closely related. These homology are exactly reproduced by our alignment (Figure 17); thus proving the credibility of the phylogenetic tree.

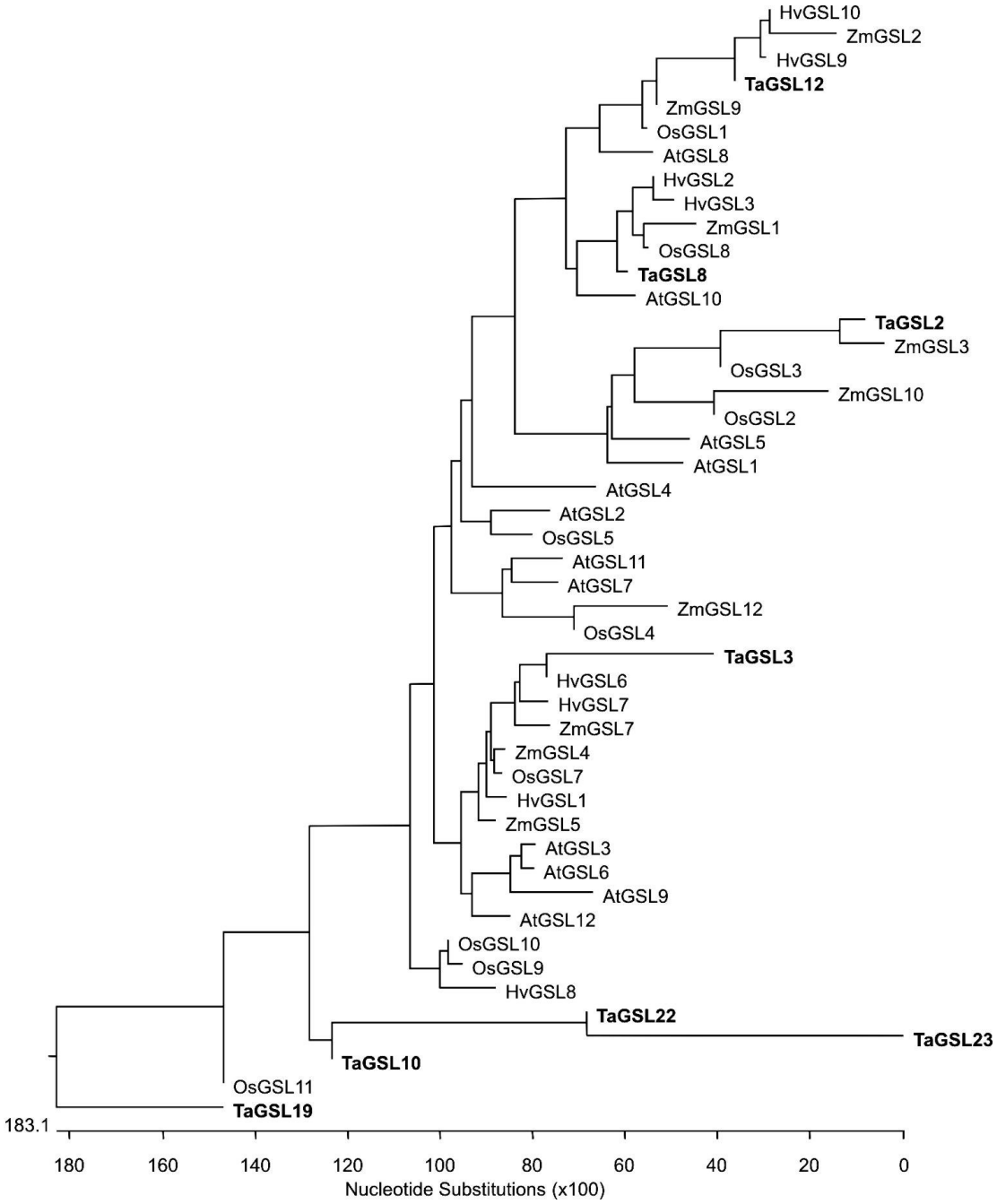

Figure 17. Phylogenetic tree of putative (1,3)-*β*-glucan synthases from *Triticum aestivum* (TaGSL), *Hordeum vulgare* (HvGSL), *Zea mays* (ZmGSL), *Oryza sativa* (OsGSL) and *Arabidopsis thaliana* (AtGSL).

Amino acid sequences were obtained from the cell wall database at Stanford University (http://cellwall.stanford.edu/). Alignments were performed at first with the CLUSTL V method. After limitation of sequences to active domain and/or the C-terminal end, the alignments were re-performed with the CLUSTL W method (Thompson *et al.*, 1994).

III.8. Organ specific expression analysis of *TaGSL* genes

cDNA used as template in quantitative real-time PCR (qPCR) reactions was generated from RNA from wheat spike, leaf blade and stem. To ensure that wheat plants were at the same developmental stage, samples were collected 7 days after anthesis, equivalent to Zadoks stages 7.5-7.9 (Zadoks *et al.*, 1974). Expression of ubiquitin (*TaUbiq*) was used as reference (Trevaskis *et al.*, 2003) in qPCR.

qPCR analysis revealed organ specific expression of *TaGSL* genes as well as high differences in expression levels of individual *TaGSL* genes within the same tissue, ranging from 2 x 10^{-5} to 40 mol *TaGSL* per mol *TaUbiq* (Figure 18). Regarding organ specificity, *TaGSL3*, *10* and *22* were predominantly expressed in one organ. Highest organ specificity was detected for *TaGSL3.* In the spike, *TaGSL3* was expressed at a level of 0.16 mol per mol *TaUbiq*, whereas expression was reduced nearly 90 % in the stem. Almost no *TaGSL3* expression was detectable in leaf blade tissue. *TaGSL10* revealed high specificity for the stem. The expression in the stem was over three-fold higher than in spike or leaf blade tissue.

In contrast to *TaGSL3* and *10*, *TaGSL22* was predominantly expressed in the leaf blade. Spike and stem tissue had expression reduced 40 % for this gene. *TaGSL12*, *19* and *23* showed nearly the same expression level in both leaf blade and stem, but a significantly lower expression in spike tissue. Only two out of eight analyzed *TaGSL* genes revealed no significant organ-specific expression, *TaGSL2* and *8*. While most expression levels (*TaGSL2*, *3*. *10*, *12*, *23*) ranged

from 0.02 to 0.2 mol *TaGSL* per mol *TaUbiq*, strong deviation at this level was determined for *TaGSL8* (40 mol *TaGSL8*/mol *TaUbiq*) and *TaGSL22* ($2x10^{-5}$ mol *TaGSL22*/mol *TaUbiq*). *TaGSL19* was expressed at a level of 1.5 to 3.5 mol per mol *TaUbiq*.

→

Figure 18. Expression of *TaGSL* genes in wheat spike, leaf blade and stem tissue (cv. Nandu).

RNA used for cDNA generation was isolated from tissue 7 d after anthesis. Expression of genes was analyzed in quantitative real-time PCR reactions. All cDNA samples were normalized against ubiquitin (*TaUbiq*) expression. All measurements were repeated twice with eight replicates each. Error bars indicate a confidence interval with a probability of error of $\alpha = 0.05$. Scale unit for all diagrams is mol *TaGSL* per mol *TaUbiq*.

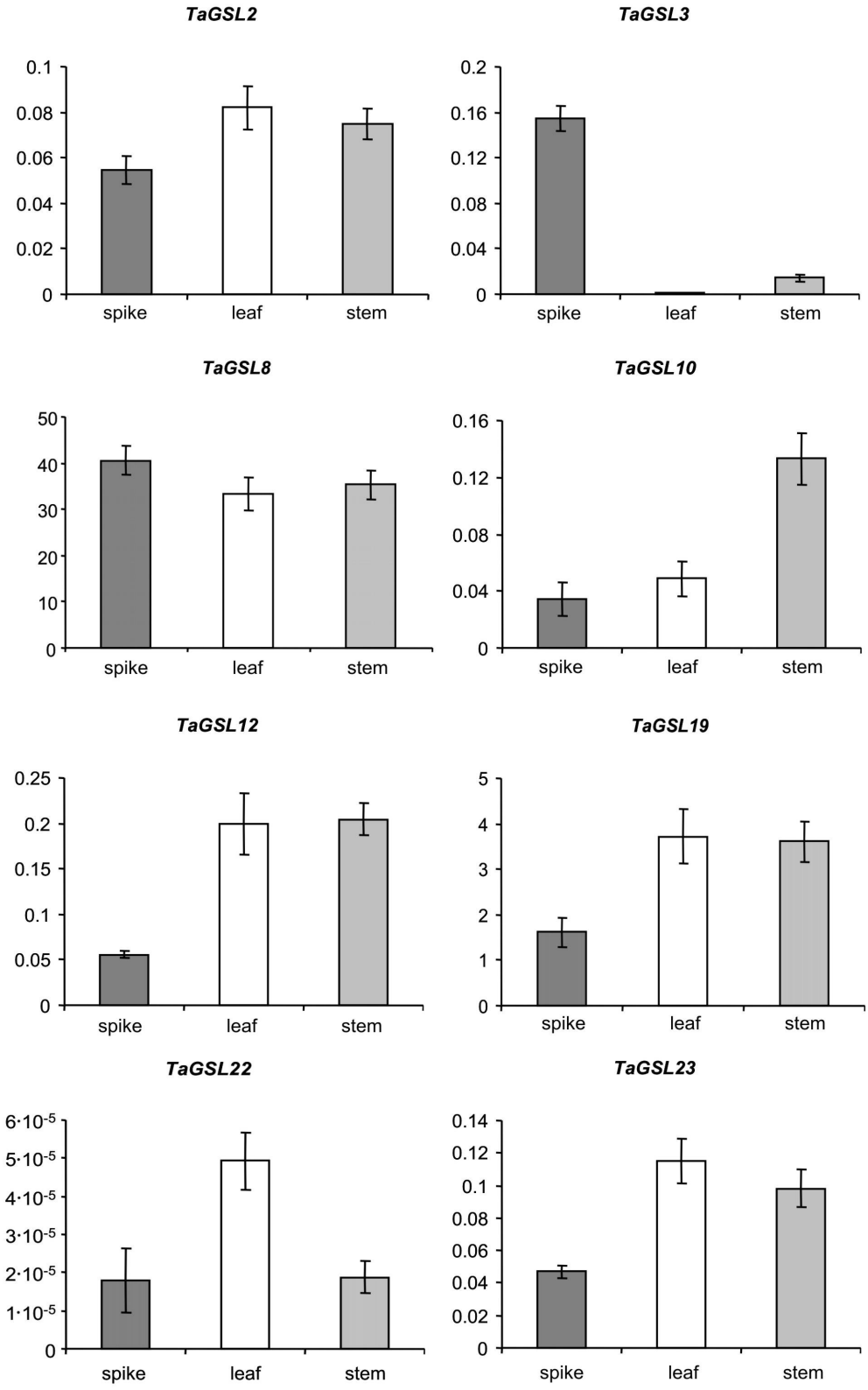
TaGSL2
0.1
0.08
0.06
0.04
0.02
0
spike
leaf
stem
TaGSL3
0.2
0.16
0.12
0.08
0.04
0
spike
leaf
stem
TaGSL8
50
40
30
20
10
0
spike
leaf
stem
TaGSL10
0.16
0.12
0.08
0.04
0
spike
leaf
stem
TaGSL12
0.25
0.2
0.15
0.1
0.05
0
spike
leaf
stem
TaGSL19
5
4
3
2
1
0
spike
leaf
stem
TaGSL22
6·10-5
5·10-5
4·10-5
3·10-5
2·10-5
1·10-5
0
spike
leaf
stem
TaGSL23
0.14
0.12
0.1
0.08
0.06
0.04
0.02
0
spike
leaf
stem

Figure 18.

III.9. Organ-specific callose concentration, callose synthase activity and callose deposition

(1,3)-β-glucan synthase activity of spike membranes was over four times higher than of leaf blade membranes and 2.5 times higher than of stem membranes (Figure 19 B). In general, enzyme activity correlated with the total amount of callose extracted from analyzed tissue. A more than three times higher amount was determined in spike tissue than in stem tissue, whereas total callose in leaf blade tissue was only reduced by 20 % compared to spike tissue (Figure 19 A). After staining with aniline blue, the sections of wheat tissue revealed different patterns of callose deposition. Whereas stem sections showed high callose deposition only in vascular bundles (Figure 19 H), high amounts of callose were deposited in vascular bundles as well as adaxial mesophyll and hypodermal sclerenchyma cells of leaf blade tissue (Figure 19 G). In general, callose was not detected in chlorenchyma. In contrast to stem and leaf blade, the amount of callose deposition in the spike depended on the position of the section. Intermediary rachis sections revealed only low amounts of callose. Similar to stem sections, callose deposition was restricted to vascular bundles (Figure 19 E). Very high amounts of callose were detected in the transition zone of the spike's rachis and rachilla (Figure 19 D and F). Depositions of callose were mainly found in vascular bundles close to the central cavity and adjacent sclerenchymatic cells. Longitudinal sections showed that strong callose depositions were restricted to the transition zone of the spike's rachis and rachilla where fibers of fluorescent callose were observed (Figure 19 F).

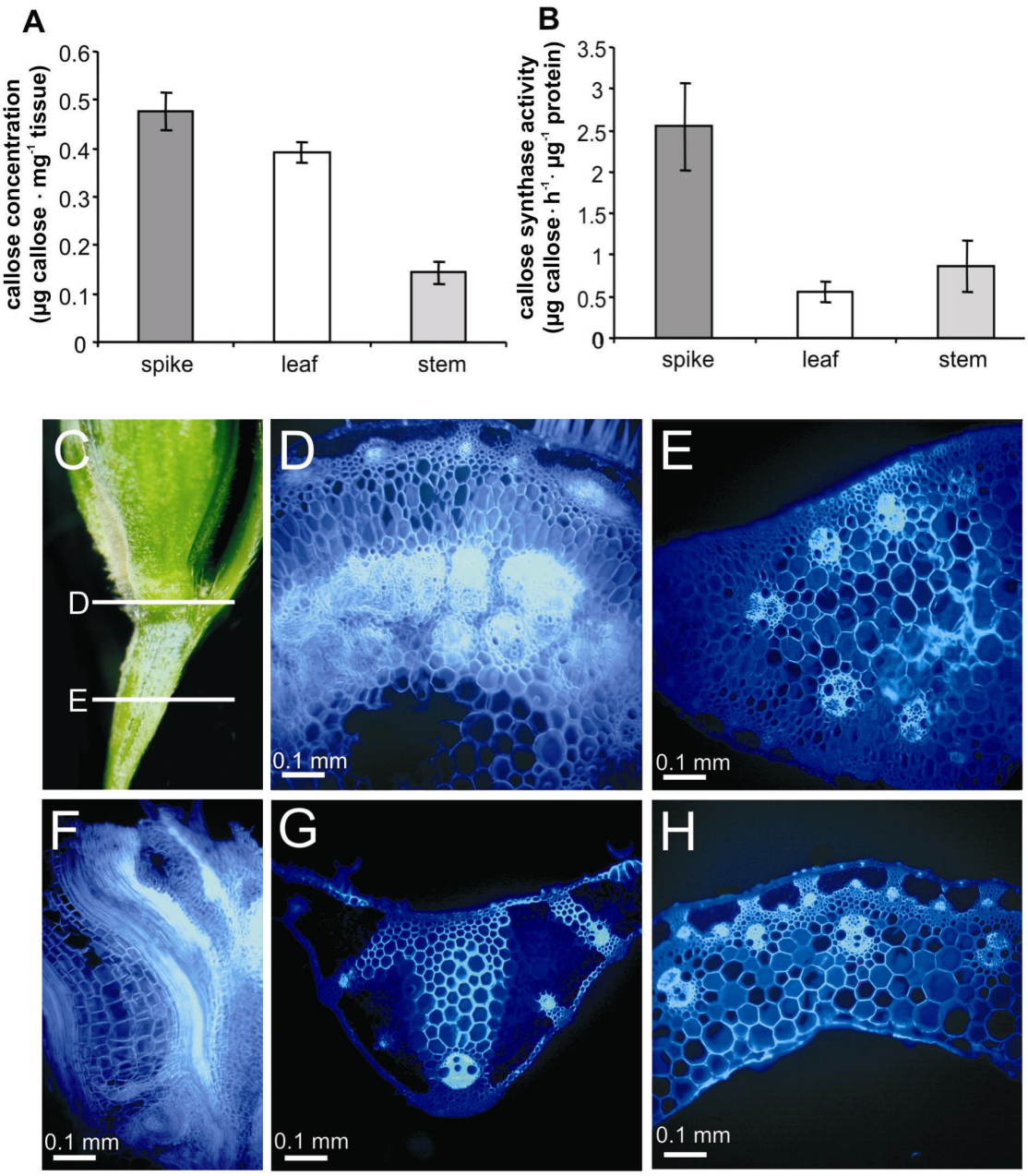
A
callose concentration (µg callose · mg-1 tissue)
0.6
0.5
0.4
0.3
0.2
0.1
0
spike
leaf
stem
B
callose synthase activity (µg callose · h-1 · µg-1 protein)
3.5
3
2.5
2
1.5
1
0.5
0
spike
leaf
stem
C
D
E
D
0.1 mm
E
0.1 mm
F
0.1 mm
G
0.1 mm
H
0.1 mm

Figure 19.

←

Figure 19. Determination of callose concentration and callose synthase activity in wheat tissue and detection of callose depositions in wheat tissue sections (cv. Nandu).

A, **B.** Spike-, leaf blade- and stem-tissue samples were collected from 6 independent wheat plants 7 d after anthesis.

A. Callose concentration of different tissues was determined after rinsing with ethanol and NaOH extraction.

B. (1,3)-*β*-glucan synthase activity of membranes isolated from spike, leaf blade and stem tissue was assayed using UDP-glucose as substrate.

All measurements were repeated twice with six replicates each. Error bars indicate the confidence interval with a probability of error of α = 0.05. Repeat experiments gave similar results.

C. Position of cross sections D and E at the wheat spike.

D-H. Sections of wheat tissue (7 d after anthesis) were stained with aniline blue to locate callose depositions by epifluorescent illumination. Three sections were made from the wheat spike: a cross (D) and a longitudinal (F) section of the transition zone of rachilla and rachis and a cross section of an intermediary rachis part (E). Two further cross sections were made from leaf blade (G) and stem (H). Selected pictures are representative for callose deposition 7 d after anthesis after examining at least 15 sections for each tissue region.

III.10. Callose deposition, concentration and synthase activity in wheat spikes during infection

Wheat spikes of the susceptible cultivar Nandu were inoculated with *F. graminearum* wild type, the lipase-deficient *F. graminearum* strain Δfgl1-2 and the barley-leaf pathogen *P. teres* to induce non-host specific reaction of wheat. Sections of the transition zone of rachilla and rachis of directly inoculated spikelets were stained with aniline blue to observe callose depositions. There were no visible differences between control and inoculated spikes 1 and 3 dpi (Figure 20 A). During the next stages of infection, which were monitored 7 and 14 dpi, changes in control spikes were not detected. Infection with *F. graminearum*

wild type resulted in increased necrotic plant tissue. Callose depositions were poorly detectable at 7 dpi, but not at 14 dpi. Necrotic plant tissue was also observed during infection with Δfgl1-2, but was limited to the directly inoculated spikelet and adjacent rachis region. Aniline blue staining resulted in detection of callose at all monitored time points of infection. The infection of wheat spikes with the non-host *P. teres* resulted in small areas of necrotic lemma tissue of directly inoculated florets (Figure 20 B). The sections of the transition zone did not show any indication of necrotic tissue. An increase in callose deposition at this region of the spike was detected at 7 and in particular at 14 dpi (Figure 20 A). Intense callose deposition was also visible at areas of necrotic tissue of the palea of inoculated florets (Figure 20 C). These observations corresponded to the callose concentration of tissue from directly inoculated spiklets and adjacent rachis tissue. Almost no change in callose concentration was measured for control spikes, whereas a slight decrease in callose concentration was observed during Δfgl1-2 infection. *F. graminearum* wild-type infection led to a constant decrease in callose concentration, resulting in the absence of callose 14 dpi. A significant increase in callose concentration was detectable only during *P. teres* infection. From 7 to 14 dpi, the callose concentration nearly doubled (Figure 20 D). The observed differences in callose concentration during infections also corresponded to the detected callose synthase activities of isolated membranes from the same tissue as previously used. Again, a constant decrease in callose synthase activity was measured during *F. graminearum* wild-type infection with only 20 % residual activity of the initial activity 7 and 14 dpi. In comparison to

control spikes, an induction of callose synthase activity was determined for both Δfgl1-2 and *P. teres* infection (Figure 20 E). Unlike callose synthase activity, the NADH oxidase activity of the isolated membranes did not differ between control and infected spikes (Figure 20 F).

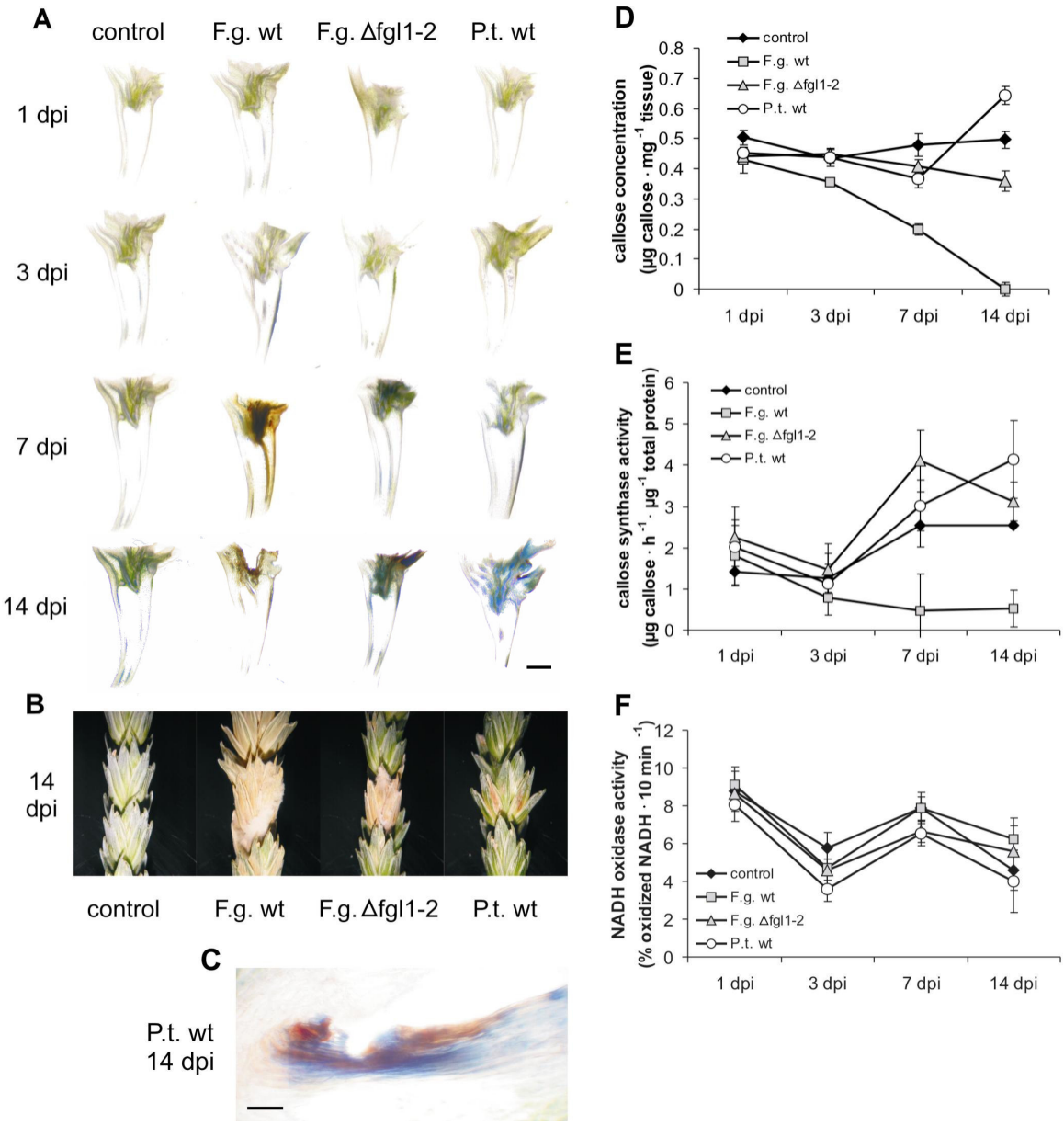

Figure 20.

←

Figure 20. Callose deposition, concentration and synthase activity in the wheat spike (cv. Nandu) after infection.

A. Sections from inoculated wheat spikes comprising the transition zone of rachilla and rachis of a directly inoculated spikelet 1, 3, 7 and 14 days post-inoculation (dpi) with *F. graminearum* wild type (F.g wt), a lipase-deficient mutant strain (F.g. Δfgl1-2) and *P. teres* wild type (P.t. wt). Uninoculated spikes served as control. Sections were stained with aniline blue to localize callose depositions (blue color) and examined with a stereo microscope. Selected pictures are representative for callose depositions for each infection type at each examined time point after monitoring at least 10 sections. Scale bar is equal to 1 mm.

B. External view on infected wheat spikes at the point of inoculation 14 dpi.

C. Microscopic examination of P.t. wt infected wheat palea at necrotic areas 14 dpi. Section was stained with aniline blue to localize callose depositions (blue color). Scale bar is equal to 10 µm.

D. Callose concentration in tissue from directly inoculated wheat spikelets and intermediary rachis region 1, 3, 7 and 14 dpi. Spikelets were inoculated with F.g wt, F.g. Δfgl1-2 and P.t. wt. Uninoculated spikes served as control. Callose was extracted with 1 N NaOH. Amount of callose was quantified after addition of aniline blue-containing buffer in a plate assay with a fluorescence plate reader.

E. (1,3)-*β*-glucan (callose) synthase activity of membranes isolated from the same tissue as indicated in (D). Activity was measured in a plate assay using UDP-glucose as substrate. Produced callose was quantified as described in (D).

F. NADH oxidase activity of same isolated membranes as used for callose synthase activity (E). Activity was measured in a plate assay. Changes in absorbance were quantified with a fluorescence plate reader.

All measurements (D-F) were repeated twice with eight replicates each. Error bars indicate a confidence interval with a probability of error of $\alpha = 0.05$.

III.11. Glucan synthase-like gene expression in wheat spikes during infection

The expression of eight glucan synthase-like (*TaGSL*) genes during infection of wheat was determined via quantitative real-time PCR in the same spike tissue as used for callose synthase activity. In general, a constant decrease in expression was detectable for all *TaGSL* genes, except *TaGSL22* revealing the lowest

expression level of all examined genes. Among the three infection approaches, only slight deviations were determined. A significantly higher expression was mainly detected in control spikes 3 dpi for *TaGSL2*, *3*, *8* and *19*. The expression of *TaGSL2* and *3* was significantly lower due to *F. graminearum* infection 7 dpi. A significant induction of *TaGSL* expression due to infection was only observed for *TaGSL10* during Δfgl1-2 infection from 3 to 7 dpi (Figure 21). For this gene, transcripts were not detectable at 14 dpi, except for *P. teres* infection, which still showed expression. Additionally, the expression level of the *TaGSL* genes not only varied during progression of infection and regular development respectively, but also in comparison to different genes at same monitored time point. For instance, the expression level ranged from 2x10-5 (*TaGSL2*) to 70) mol (*TaGSL8*) *TaGSL* transcripts per mol *TaUbiq* transcripts 1 dpi (Figure 21).

→

Figure 21. Expression analysis of glucan synthase-like genes (*TaGSL*) in wheat spikes (cv. Nandu).

RNA was isolated from directly inoculated spikelets and intermediary rachis region 1, 3, 7 and 14 days post inoculation (dpi) with *F. graminearum* wild type (F.g. wt), lipase-deficient *F. graminearum* strain Δfgl1-2 and *P. teres* wild type (P.t. wt). Uninoculated spikes served as control. Generated single-stranded cDNA was used as template in quantitative real-time PCR reactions. All cDNA samples were normalized against ubiquitin (*TaUbiq*) expression. All measurements were repeated twice with eight replicates each. Error bars indicate a confidence interval with a probability of error of $\alpha = 0.05$. Scale unit for all diagrams is mol *TaGSL* per mol *TaUbiq*.

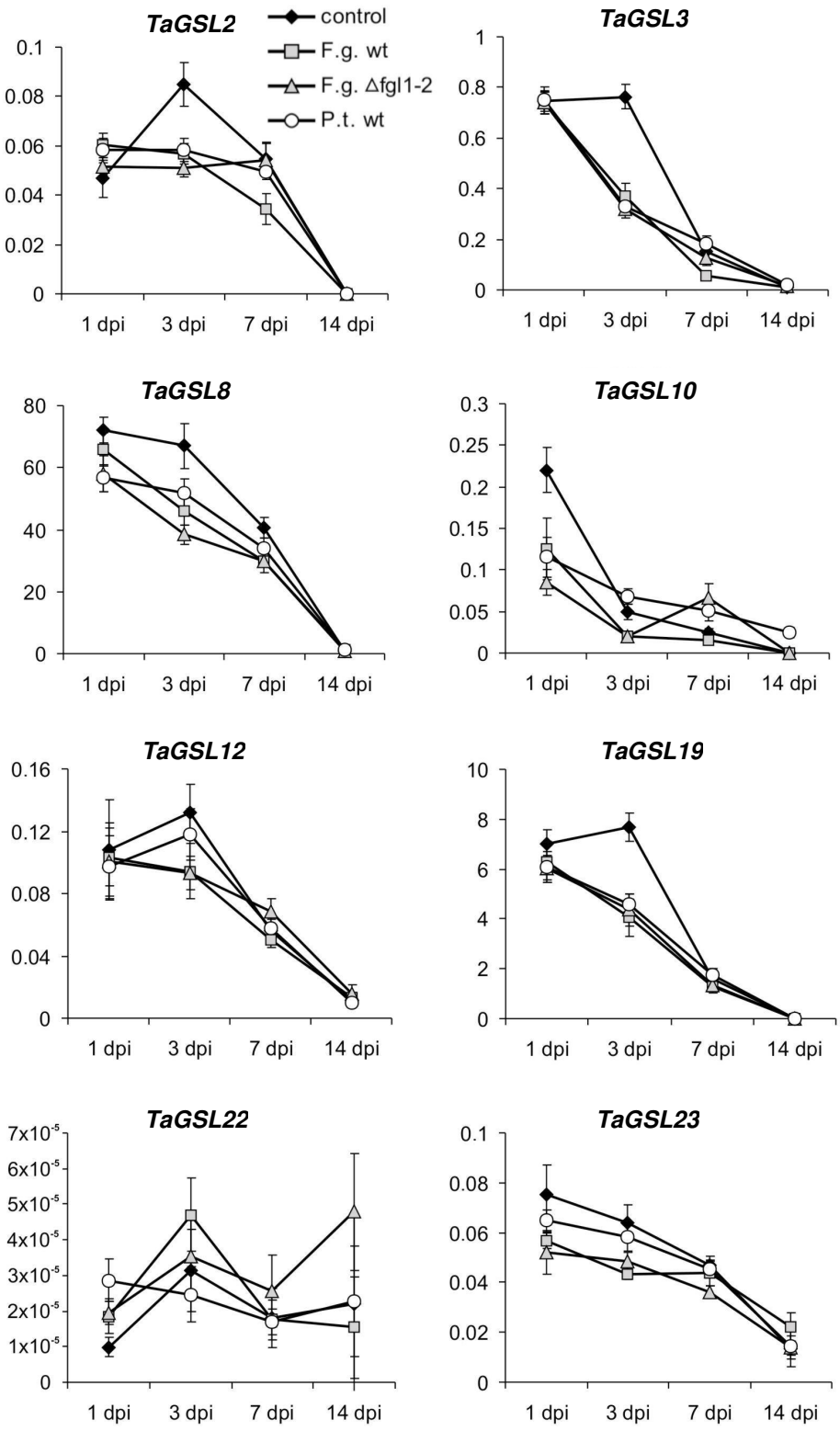
TaGSL2
control
F.g. wt
F.g. Δfgl1-2
P.t. wt
TaGSL3
TaGSL8
TaGSL10
TaGSL12
TaGSL19
TaGSL22
TaGSL23
1 dpi
3 dpi
7 dpi
14 dpi

Figure 21.

III.12. Differences in type II resistance against *F. graminearum* infection and in inhibition of callose synthase due to free fatty acid application of the wheat cultivars Nandu and Batis

To determine a possible involvement of callose synthase in type II resistance of wheat, two cultivars were chosen that greatly differed in their susceptibility to *F. graminearum* infection due to point inoculation of spikelets (Figure 22 A). Type II resistance refers to the spread of the pathogen within a host (Schroeder and Christensen, 1963). 21 dpi, the spike of the susceptible cultivar Nandu, was almost completely bleached, whereas only directly inoculated and adjacent spikelets of the more resistant cultivar Batis were bleached (Figure 22 B). These differences in type II resistance corresponded to the measured callose concentration and synthase activity of tissue from directly inoculated spikelets and adjacent rachis region 14 d after *F. graminearum* infection. In control spikes, callose concentration and synthase activity was almost equal in both cultivars. In contrast to this, callose was almost not detectable in tissue from cultivar Nandu, whereas callose remained in Batis tissue, but reduced 80 % in comparison to the control (Figure 22 C). Additionally, the residual callose synthase activity was also twice as high in Batis as in Nandu (Figure 22 D). To examine possible differences in susceptibility of callose synthase against free fatty acid (FFA) application, membranes were isolated from uninoculated wheat spikes of both cultivars at Zadoks stages 7.5-7.9 (Zadoks *et al.*, 1974). In general, the addition of ethanol to the membranes (as control for ethanol-dissolved FFA application) did not influence the callose synthase activity significantly. A slightly higher activity

(~10%) was detected for Batis than for Nandu (Figure 22 E). The addition of stearic acid (18:0) affected callose synthase activity in none of the cultivars at the applied concentrations ranging from 0.7 to 700 µM. An inhibitory effect of unsaturated FFA-application was detected for both cultivars. However, inhibition was observed in Nandu also at the lower FFA concentration of 0.7 and 7 µM, whereas activity in Batis was not significantly reduced at these concentrations (Figure 22 E). At a concentration of 17.5 µM of unsaturated FFA, the activity was only reduced 25 % for Batis, but almost 80 % for Nandu. Complete inhibition of callose synthase activity due to application of linoleic and linolenic acid (polyunsaturated FFA: PUFA) was observed at a concentration 35 µM for Nandu. At this concentration, a residual activity of almost 30 % was detected for Batis. Activity was completely inhibited at a PUFA concentration of 70 µM. The inhibitory effect of the monounsaturated oleic acid (18:1) was not as strong as the polyunsaturated FFA. At concentrations of complete activity inhibition due to PUFA application, residual callose synthase activity was still detectable in oleic acid-supplemented approaches.

A

Treatment[a]	Percentage of infection[b]	
	Mean	Conf. Int.[c]
Nandu control	0.0	-
Nandu F.g. wt	93.2	3.6
Batis control	0.0	-
Batis F.g. wt	23.2	3.1

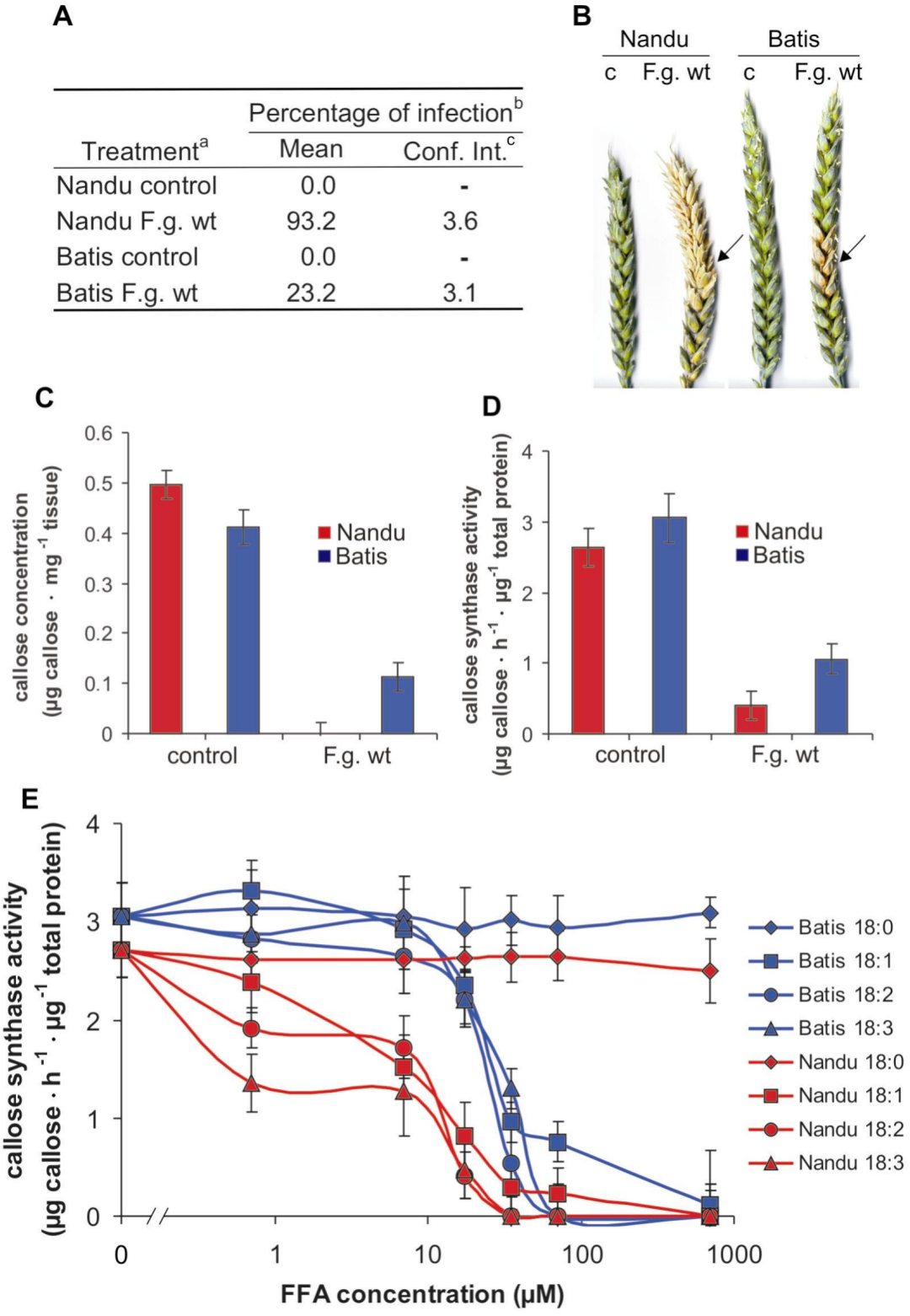

Figure 22.

←

Figure 22. Susceptibility against *F. graminearum* infection and callose synthase activity of the wheat cultivars Nandu and Batis after addition of free fatty acids (FFA).

A. Table indicating the susceptibility of the wheat cultivars Nandu and Batis against *F. graminearum* infection (F.g. wt). Repeat experiments gave similar results (a). Infection referred to partially or completely bleached spikelets observed 3 weeks post-infection. Spikelets showing minor symptoms (tiny yellow or brown spots) were not counted. Results are the average of 15 inoculated wheat heads (16-24 spikelets per head) inoculated with 400 conidia (b). Confidence interval with probability of error of $\alpha = 0.05$ (c).

B. Two central spikelets were each inoculated with 10 µl of water (c) and 200 *F. graminearum* wild-type conidia (F.g. wt). Arrows indicate inoculation site. Figure shows spikes 3 weeks post-infection.

C. Callose concentration in tissue from directly inoculated wheat spikelets and intermediary rachis region 14 dpi. Spikelets were inoculated with F.g wt. Uninoculated spikes served as control.

D. (1,3)-*β*-glucan (callose) synthase activity of membranes isolated from the same tissue as indicated in C.

E. (1,3)-*β*-glucan (callose) synthase activity of membranes isolated from untreated spikes of wheat cultivars Nandu and Batis 7 d after anthesis (Zadoks stages 7.5-7.9 (Zadoks *et al.*, 1974)). FFA dissolved in ethanol was added to the membranes reaching final concentrations of 0.7, 7, 17.5, 35, 70 and 700 µM in the reaction buffer. FFA: stearic acid (18:0), oleic acid (18:1), linoleic acid (18:2), linolenic acid (18:3).

C-E. Callose was quantified as indicated in Figure 1; all measurements were repeated twice with eight replicates each. Error bars indicate a confidence interval with a probability of error of $\alpha = 0.05$.

III.13. Differences in infection progress and restoration of virulence of a lipase-deficient *F. graminearum* mutant due to FFA application *in planta*

The results of the *in vitro* callose synthase activity assay showed the inhibitory effect of unsaturated FFA. To examine a similar effect *in planta*, FFA of a concentration of 3.2 mM were added to previously inoculated wheat spikelets. The generation of a GFP-tagged wild type-like (wt-GFP-1) and a lipase-deficient strain (Δfgl1-GFP-1) (Figure 23) made it possible to monitor differences in the

infection progress of the different strains with and without addition of FFA. The GFP-tagged strains wt-GFP-1 and Δfgl1-GFP-1 used were significantly different from *F. graminearum* wild type and untagged lipase-deficient strain Δfgl1-2 (Figure 12) respectively; neither in their lipolytic traits (Figure 23) in culture nor in virulence (Table 3). The addition of ethanol and ethanol-dissolved FFA to control spikes did not show any effect. Similarly, the wt-GFP-1 infection was also not affected. A significant difference was detected neither in percentage of infection nor in general rachis colonization and colonization severity (Table 3). In contrast to the wild type-like strain, the addition of unsaturated FFA partly restored the virulence of the lipase-deficient strain Δfgl1-GFP-1. Whereas inoculation without subsequent addition of FFA resulted in 20 % of infected spikelets, the addition of unsaturated FFA increased infection to 50 %. Bleached spikelets were mainly found above the point of inoculation showing the same pattern of symptoms as wild-type infected spikes (Figure 24 A). The addition of the saturated stearic acid did not increase infection significantly (Table 3). These results corresponded to the *in vitro* assay, in which callose synthase activity was strongly inhibited only by unsaturated FFA. However, a slight effect was shown for stearic acid resulting in an increased percentage of rachis colonization as compared to Δfgl1-GFP-1 infection without addition of FFA.

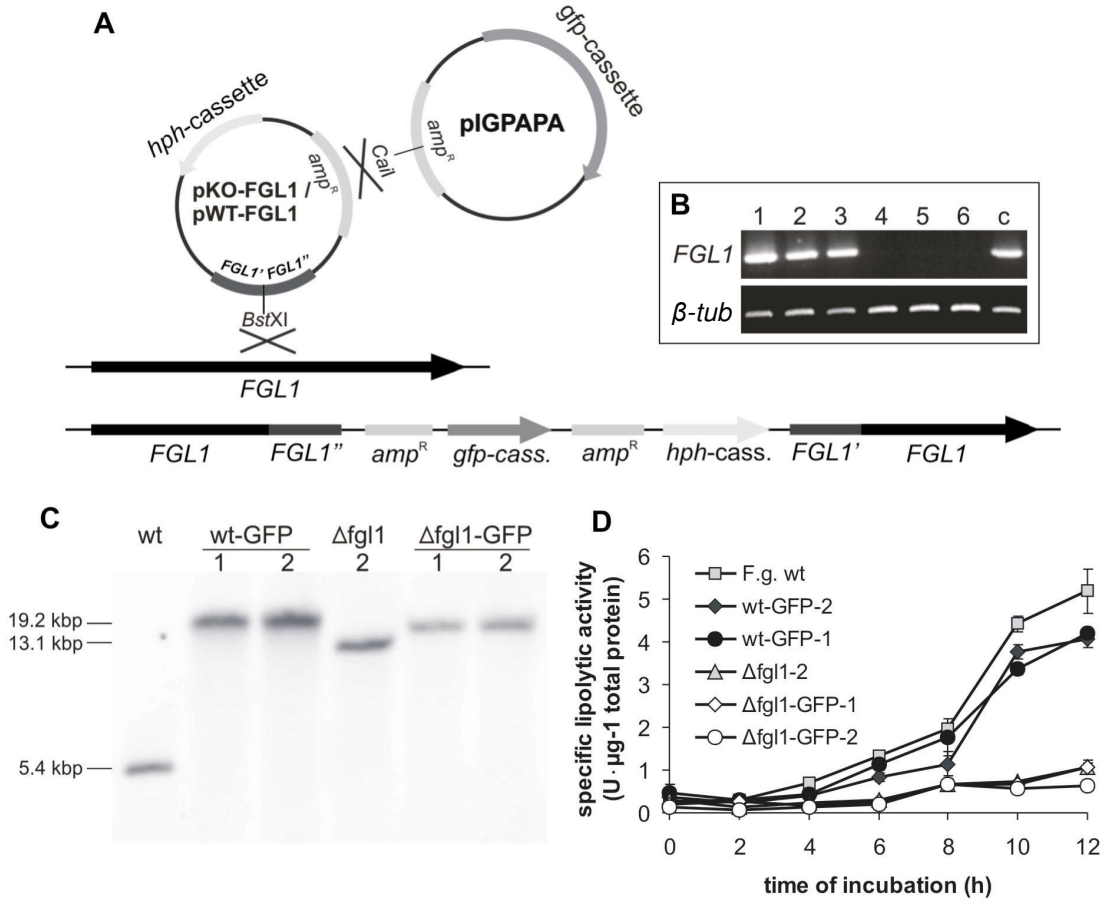

Figure 23. Schematic overview of possible cross-over events during transformation and characterization of resulting GFP-tagged *F. graminearum* strains.

A. For homologous integration of the constructs pKO-FGL1 and respectively pWT-FGL1 into the *FGL1* gene, a single cross-over event has to occur. An additional homologous integration of the second vector, which provides the green fluorescent protein (gfp)-cassette (pIGPAPA), into the first construct requires a second cross-over events. As a result, the *FGL1* gene is disrupted after integration of pKO-FGL1 since both fragments, *FGL1'* and *FGL1",* contain deletions. The integration of pWT-FGL1 results in a wild type-like genotype since only fragment *FGL1'* has a deletion. The resulting shift of the genomic locus can be detected by Southern blot analysis and the appropriate choice of restriction enzymes (see C).

B. cDNA generated from isolated RNA of mycelium from *F. graminearum* wild type (1), wt-GFP-1 and -2 (2 and 3), lipase-deficient strain Δfgl1-2 (4) and Δfgl1-GFP-1 and -2 (5 and 6). For induction of *FGL1* transcription, mycelium was incubated for 12 h at 28°C in H_20 supplemented with 2 % wheat germ oil. Genomic *F. graminearum* wild-type DNA was used as control (c). PCR amplification was performed with *FGL1*-specific primers and β-tubulin-specific primers (*β-tub*) as expression control.

←
Figure 23.

C. Genomic DNA of *F. graminearum* wild-type (wt), GFP-tagged wild type-like strains (wt-GFP-1/-2), lipase-deficient strain (Δfgl1-2) and GFP-tagged *Δfgl1*-strains (Δfgl1-GFP-1/-2) was restricted with *Pfl*23II. Hybridization was performed with a DIG-labeled internal fragment of the *FGL1* gene. The detected shift of GFP-tagged strains confirmed homologous integration of pKO-FGL1 and pWT-FGL1, respectively. Homologous integration of pIGPAPA into the first construct was confirmed by *gfp*-specific probing (data not shown).

D. Extracellular lipolytic activity of *F. graminearum* wild-type (wt), lipase-deficient strain Δfgl1-2 and GFP-tagged strains (wt-GFP-1/-2 and Δfgl1-GFP-1/-2) after induction by wheat germ oil. Cultures were incubated in water supplemented with 2 % wheat germ oil at 28°C and 150 rpm. During a time range of 12 h, samples were taken every 2 h. Lipolytic activity was measured with pNPP lipase-assay. Error bars indicate confidence interval with probability of error of $\alpha = 0.05$. Measurements were repeated twice with six replicates each.

Sections comprising the transition zone of rachilla and rachis of directly inoculated spikelets revealed the differences in infection progress of wt-GFP-1 and Δfgl1-GFP-1 with and without addition of unsaturated FFA. During wild-type infection, mycelium had already entered the transition zone 3 dpi and completely colonized the rachis adjacent to the inoculated spikelet 7 dpi. The spread of the mycelium continued in same strength, resulting in almost complete colonization of spike 14 dpi (Figure 24 B). In contrast to this, the lipase-deficient mutant was not able to spread through the rachis. 3 dpi, mycelium was only detected in the inoculated spikelet. The further spread of the mycelium was stopped at the transition zone. Therefore, only single hyphae were detectable in the rachis directly adjacent to the site of inoculation 7 and 14 dpi, without further growth to other parts of the spike (Figure 24 B). The effect of the addition of unsaturated FFA 3 dpi to Δfgl1-GFP-1 infected spikelets was clearly visible at 7 dpi. The

mycelium of the lipase-deficient mutant spread through the transition zone and colonized the adjacent rachis region. In the progress of infection, almost all parts of the spike above inoculation site were colonized and bleached. Spikelets below the site of inoculation were generally not infected, even though the rachis was mainly colonized at this part of the spike. Longitudinal sections from this region revealed that the mycelium was prevented from entering the spikelets (Figure 24 D). In general, the severity of rachis colonization due to Δfgl1-GFP-1 inoculation with addition of unsaturated FFA was significantly lower than of wt-GFP-1 infected spikes (Table 3).

Table 3. Differences in virulence of GFP-tagged *F. graminearum* strains to wheat (cv. Nandu) due to addition of free fatty acids (FFA).

Treatment[a]	Percentage of infection[b]		Percentage of rachis colonization[c]	Rating of rachis colonization severity[d]	
	Mean	Conf. Int.[e]		Mean	Conf. Int.[e]
EtOH control	0.0	-	-	-	-
18:0 control	0.0	-	-	-	-
18:1 control	0.0	-	-	-	-
18:2 control	0.0	-	-	-	-
18:3 control	0.0	-	-	-	-
wt-GFP-1	81.8	10.2[f]	100	2.7	0.3[f]
wt-GFP-1+ EtOH	88.2	11.2[f]	100	2.9	0.2[f]
wt-GFP-1 + 18:0	86.5	9.5[f]	100	2.8	0.3[f]
wt-GFP-1 + 18:1	84.9	10.0[f]	100	2.8	0.3[f]
wt-GFP-1 + 18:2	82.8	10.2[f]	100	2.9	0.2[f]
wt-GFP-1 + 18:3	81.5	10.2[f]	100	2.9	0.2[f]
Δfgl1-GFP-1	22.1	9.8[g]	45.0	0.7	0.3[g]
Δfgl1-GFP-1 + EtOH	20.5	7.6[g]	39.1	0.5	0.3[g]
Δfgl1-GFP-1 + 18:0	31.2	10.3[h]	60.0	1.1	0.5[i]
Δfgl1-GFP-1 + 18:1	51.2	12.8[k]	73.7	1.6	0.5[k]
Δfgl1-GFP-1 + 18:2	51.8	11.5[k]	90.0	1.9	0.4[k]
Δfgl1-GFP-1 + 18:3	49.6	13.8[k]	85.0	1.9	0.4[k]

←

Table 3.

Wheat spikelets were inoculated with the GFP-tagged wild type-like *F. graminearum* strain wt-GFP-1 and the lipase-deficient strain Δfgl1-GFP-1. A part of infected spikes was treated with FFA. 4 µl of ethanol-dissolved FFA (concentration: 3.2 mM) and pure ethanol as control (EtOH) were added 3 dpi to each of the previously inoculated spikelets; FFA: stearic acid (18:0), oleic acid (18:1), linoleic acid (18:2), linolenic acid (18:3).

[a]Repeat experiments gave similar results.

[b]Infection referred to partially or completely bleached spikelets observed 3 weeks post-infection. Spikelets showing minor symptoms (tiny yellow or brown spots) were not counted. Results are the average of 10 (control and wild type-GFP) and 20 (Δfgl1-GFP) wheat heads (16-22 spikelets per head), respectively, inoculated with 400 conidia.

[c]Percentage of all inoculations, in which GFP-tagged *F. graminearum* mycelium was detectable in rachis tissue located between two inoculated spikelets.

[d]Colonization severity estimated visually by rating the green fluorescence of GFP-tagged *F. graminearum* mycelium in rachis tissue located between two inoculated spikelets 3 weeks post-infection (see Figure 20E). Ratings ranged from 0 (no green fluorescence) to 3 (complete green fluorescence in all tissue parts). Results are the average of 10 (wild type-GFP) and 20 (Δfgl1-GFP) wheat heads, respectively, inoculated with 400 conidia.

[e]Confidence interval with probability of error of $\alpha = 0.05$.

[f]Significantly different from Δfgl1-GFP strain with and without addition of FFA, no significant differences among approaches with or without addition of FFA at $P < 0.05$.

[g]Significantly different from Δfgl1-GFP strain with addition of unsaturated FFA, no significant differences between the approach with or without addition of ethanol at $P < 0.05$.

[h]Infection significantly different from Δfgl1-GFP strain with addition of unsaturated FFA, but not significantly different from Δfgl1-GFP without addition of FFA at $P < 0.05$.

[i]Rachis colonization severity significantly different from Δfgl1-GFP strain neither with addition of unsaturated FFA nor without addition of FFA at $P < 0.05$.

[k]Significantly different from wild type-GFP and Δfgl1-GFP without addition of FFA, no significant differences among approaches with addition of different unsaturated FFA at $P < 0.05$.

In contrast to the later stages of infection, no differences were observed between wild-type and Δfgl1 infection 1 dpi. Conidia predominantly germinated on pollen-covered stigma of the floret's pistil and hyphae grew in direction to the ovary (Figure 24 C).

→

Figure 24. Infection progress in wheat spikes (cv. Nandu) inoculated with GFP-tagged *F. graminearum* strains.

A. Two central spikelets were each inoculated with 10 µl of water (c) and 200 conidia of the GFP-tagged wild type-like *F. graminearum* strain wt-GFP-1 and the lipase-deficient strain Δfgl1-GFP-1. 4 µl of ethanol-dissolved FFA (concentration: 3.2 mM) and pure ethanol as control (EtOH) were added to each of previously inoculated spikelets 3 dpi (compare Table 1). Arrows indicate inoculation site. Pathogenicity tests were repeated ten-times for strain wt-GFP-1 and twenty-times for strain Δfgl1-GFP-1. Spikes are representative for severity of each infection type 21 dpi. F.g. wt-GFP-1-inoculated spike is representative for infection with and without addition of FFA (no differences, compare Table 1). FFA: stearic acid (18:0), oleic acid (18:1), linoleic acid (18:2), linolenic acid (18:3).

B. Sections comprising the transition zone of the rachilla and rachis of directly inoculated spikelets as described in (A) were examined with a stereo fluorescence microscope. Pictures are representative for the infection progress in spikelets inoculated with wt-GFP-1 (no differences with and without addition of FFA) and with Δfgl1-GFP-1 Changes in infection progress due to addition of unsaturated FFA to Δfgl1-GFP-1 infected spikelets are represented by the pictures of infection after addition of linolenic acid (18:3).

C. Isolated stigmas and pistil from floret 1 dpi. Hyphae grow from pollen on stigmas in direction to the ovary. No differences between the wild type-like strain wt-GFP-1 and the lipase-deficient strain were observed at this stage of infection. Scale bars are equal to 40 µm.

D. Rachis section below the site of inoculation with adjacent uninfected spikelet 21 dpi (compare A). Picture is representative for spikes inoculated with strain Δfgl1-GFP-1 and addition of unsaturated FFA 3 dpi.

E. Sections of colonized rachis tissue located between two inoculated spikelets 21 dpi. Pictures represent different degrees of colonization severity, which is estimated visually by rating green fluorescence of GFP-tagged mycelium (see Table 1).

(B, D, E) Scale bars are equal to 1 mm.

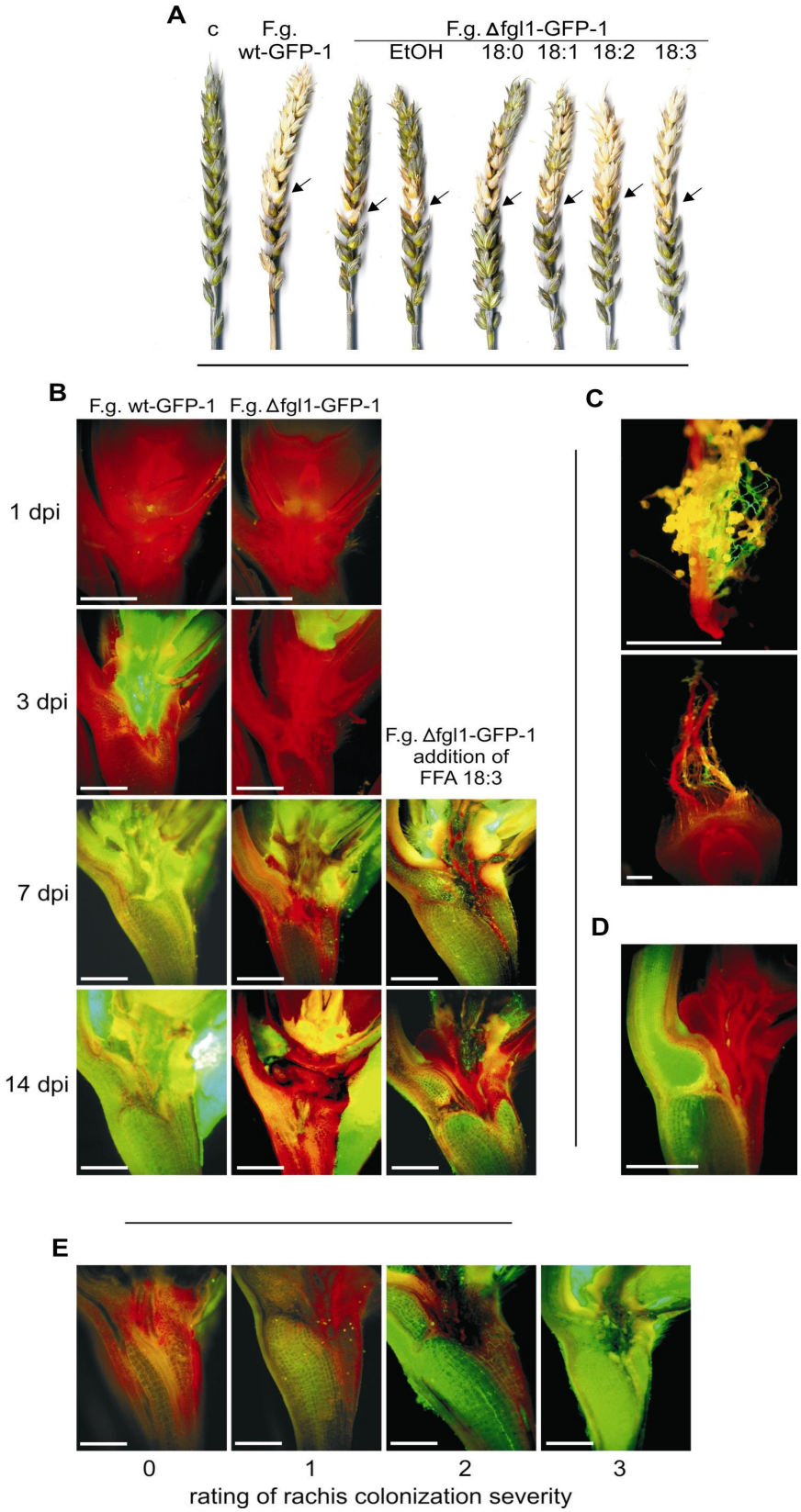
A
c
F.g. wt-GFP-1
F.g. Δfgl1-GFP-1
EtOH
18:0
18:1
18:2
18:3
B
F.g. wt-GFP-1
F.g. Δfgl1-GFP-1
1 dpi
3 dpi
7 dpi
14 dpi
F.g. Δfgl1-GFP-1 addition of FFA 18:3
C
D
E
0
1
2
3
rating of rachis colonization severity

Figure 24.

IV. Discussion

IV.1. Characterization of the secreted lipase FGL1

It was determined that the level of extracellular lipolytic activity depends heavily on the oil used for induction. Similar results were shown for the pathogenic fungi *Candida rugosa* and *Fusarium solani* (Lakshmi *et al*., 1999; Maia *et al*., 2001). Both fungi also revealed varying lipolytic activities depending on the oil used for induction. Hence, the composition of esterified fatty acids in oil could determine the ability to induce lipolytic activity in the fungus. Therefore, different oils should generally be tested to optimize induction of lipolytic activity. For *F. graminearum*, wheat germ oil was the best inducing oil (Figure 5). Nevertheless, further work will reveal whether a highly inducing oil also constitutes a preferred substrate for a secreted lipase.

The genome of the *F. graminearum* strain PH-1 (FGSC 9075, NRRL 31084) has been sequenced and published in 2003 by the Whitehead Institute, Center for Genome Research (Cambridge, USA). The sequence of the *FGL1* lipase gene described in this study differs in the sequence of nucleotides resulting in a different amino acid sequence at position 274 and at the C-terminal end. These differences may be due to the different *F. graminearum* strain used in this work. Even though all lipase sequences used for *in silico* comparisons belong to the *Rhizomucor* lipase family, only those lipases originating from fungi taxonomically close to *F. graminearum* (e.g., *F. heterosporum*) have high (66.2 %) similarity to *FGL1.* This supports reports of low conservation in this class of enzymes (Jaeger *et al*., 1994).

Results from *in vitro* expression analysis of *FGL1* indicated that the lipase gene is inducible by suitable substrates and is not expressed constitutively as *FGL1*-transcripts were only detected in a medium supplemented with wheat germ oil as sole carbon source (Figure 7). The repression of the *FGL1* gene in media supplemented with glucose can be explained by the metabolic process known as catabolite or glucose repression, which is described for plant pathogenic fungi (Tudzynski *et al*., 2000; Gomez-Gomez *et al*., 2002). In addition, the absence of any carbon source in the medium prevented the expression of *FGL1* (Figure 7). To activate transcription of *FGL1*, the presence of an appropriate substrate is needed. The release of hydrolysis products, diacylglycerol or FFA, could result in signal transduction inside the cell. This has been reported for lipases (Shimada *et al*., 1992) and other inducible genes (Kolattukudy *et al*., 1991; Schenk *et al*., 2003). Nevertheless, this raises the question of whether putative hydrolysis products are provided by FGL1 itself or other secreted hydrolyzing enzymes when the fungus encounters an appropriate substrate. The first case would require low level constitutive expression of *FGL1* that could not be detected. Involvement of other hydrolyzing enzymes in *FGL1* expression cannot be excluded, since the *F. graminearum Δfgl1* strains revealed remaining lipolytic activity of their supernatants (Figure 12).

IV.2. Importance of the secreted lipase FGL1 to virulence

Due to heterologous gene expression in *P. pastoris*, it was possible to establish the functional identity of the *FGL1* gene and to determine the inhibitory effect of

ebelactone B on FGL1 (Figure 9). Inhibition of lipases by ebelactone B has been reported by Umezawa *et al*. (1980) and Köller *et al*. (1990). Wheat infections with *F. graminearum* wild-type conidia supplemented with ebelactone B revealed a large reduction in virulence (Figure 10). Reduced virulence due to ebelactone B application has also been previously reported for the plant pathogenic fungi *Pyrenopeziza brassicae* (Davies *et al*., 2000), *Erysiphe graminis* (Francis *et al*., 1996), and *Rhizoctonia solani* (Chun *et al*., 1995). Since ebelactone B is described as a general serine esterase inhibitor (Umezawa *et al*., 1980), the decision whether the detected phenotype resulted from inhibition of the single enzyme FGL1 or from inhibition of a combination of hydrolytic enzymes secreted by *F. graminearum* during infection could only be solved by gene deletion experiments.

Wheat infections using *Δfgl1* strains gave the same result as when ebelactone B was applied (compare Figure 10 and 13). Hence, the impact of ebelactone B on plant infection by *F. graminearum* can be explained by its inhibition of secreted lipase FGL1. In contrast to data from Comménil *et al*. (1995, 1998, 1999) and Berto *et al*. (1999), indicating a putative role of lipases during early stages of host-pathogen interactions, the secreted lipase FGL1 from *F. graminearum* seems to be essential in later stages of invasive growth. The fungus spreads by systemic growth through the rachis from one spikelet to another (Kang and Buchenauer, 1999; Ribichich *et al*., 2000; Wanjiru *et al*., 2002) and colonizes parenchymatous and vascular tissue (Kang and Buchenauer, 1999). In contrast to the wild-type strain, the infections with the *Δfgl1* strains were restricted to the

inoculated spikelets. In some cases, infection of the spikelet adjacent to the inoculated spikelet without infection of the rachis was also observed (Figure 13). This can be explained by direct penetration of the surface of the bracts, especially at spikelets located close to each other. Similar observations have been reported by Wanjiru *et al*. (2002). The general importance of the secreted lipase was supported by infection of maize ears (Table 2). Ears infected by wild-type conidia revealed strong symptoms of *F. graminearum* ear rot (Figure 16), which is characterized by the growth of white to pinkish mold on silks, kernels, rachis, and husks (Sutton, 1982). In contrast, symptoms of ear rot on maize ears infected with *Δfgl1* strains were limited to small lesions on the rachis (Figure 16). Thus, involvement of the secreted lipase during infection is equally important for wheat and maize, the two most economically important hosts of *F. graminearum*.

To explain the reduced virulence of *Δfgl1* strains, FGL1 could be involved in activation and expression of other enzymes responsible for the fast growth of fungal hyphae. Activation could be initiated by the release of diacylglycerol or free fatty acids due to hydrolysis of an appropriate substrate. The function of diacylglycerol as a second messenger during infection was shown for the phytopathogenic fungus *Magnaporthe grisea,* where it stimulates appressorium formation on noninductive (hydrophilic) surfaces (Thines *et al*., 1997). In addition, it can also restore appressorium formation to a *Δpth11* mutant (DeZwaan *et al*., 1999). Moreover, Klose *et al.* (2004) hypothesize that lipid substrates of lipases may be one of the signals that maintain and promote the filamentous growth of the fungus in the host environment. The involvement of FGL1 even prior to

hyphae reaching the transition zone of spikelet and spike spindle can be deduced from expression analysis based on infected wheat spikes. Here, *FGL1* gene expression was already activated 24 h after inoculation (Figure 8); thus, at early stages of infection. However, further elucidation of the role of FGL1 as a virulence factor also depends on the determination of its substrate.

IV.3. General importance of extracellular lipases

The first indications that secreted lipases might serve as virulence factors in plant pathogenic fungi was shown for *Botrytis cinerea* (Comménil *et al*, 1995, 1999). Supplementation of *B. cinerea* conidia with anti-lipase polyclonal antiserum suppressed their ability to penetrate intact plant tissue (Comménil *et al*., 1998). Similar results were reported by Berto *et al*. (1999), who raised *B. cinerea* anti-lipase antibodies against a lipase secreted by spores of *Alternaria brassicicola*. Additionally, several studies on different plant pathogenic fungi revealed that the application of serine esterase inhibitors, such as ebelactones and other organophosphorus pesticides, could prevent infection of host plants (Maiti and Kolattukudy, 1979; Köller *et al*., 1982; Chun *et al*., 1995; Köller *et al*., 1995; Francis *et al*., 1996; Davies *et al*., 2000). It was assumed that the observed effect resulted from inhibition of cutinolytic activity. Hence, cutinases were proposed to be exclusively required for adherence to the plant cuticle, cuticular penetration, and generation of triggering signals. Contrary to the postulated function of this enzyme, disruption of cutinase genes in *N. haematococca* and other fungal pathogens did not affect their ability to adhere to plant surfaces or to penetrate

the host cuticle (Stahl and Schäfer, 1992; Sweigard *et al*., 1992; Rogers *et al*., 1994; Stahl *et al*., 1994; Crowhurst *et al*., 1997; van Kan *et al*., 1997). These results imply that cutinase inhibition is not entirely responsible for reduced virulence of plant pathogenic fungi. Two facts speak for a possible involvement of lipases in the infection process of these fungi. First, in studies with applied serine hydrolase inhibitors, the potential inhibition of lipases by the same compounds was not considered. Second, the present results clearly show that secreted lipases can be regarded as virulence factors of pathogenic fungi. The combination of these results and previously published results of lipase inhibition by antibodies would indicate that an involvement of secreted lipases in a broad array of pathogenic fungi could be postulated.

IV.4. Papilla-like barrier formation associated with *Δfgl1* infection

Dissection of *Δfgl1*-infected spikelets indicated the formation of a barrier at the transition zone between rachilla and rachis of the wheat spike (Figure 15), where fungal growth was almost stopped. Hence, this barrier seemed to be related to the defense reaction of the plant. In general, this would include mechanisms of cell wall modifications resulting in the rapid formation of papillae, which are local appositions of dense material between the plasmalemma and the cell wall. Moreover, cell wall thickening or deposition of amorphous material within the vascular bundles of wheat can slow the growth of *F. graminearum* (Ribichich *et al*., 2000). Histological studies on wheat indicate that the formation of these barriers is fast and localized, and that the reaction of infected tissue is probably

associated with the resistance to fungal infections in different wheat strains of altered susceptibility (Ribichich *et al*., 2000). Both cell wall strengthening and formation of papillae are not regarded as defense reactions that can completely stop the pathogen. Instead, they are thought to slow pathogen growth to gain time for the initiation of defense reactions that require gene activation and expression. As a result, the plant can initiate hypersensitive reactions, synthesis of phytoalexins and pathogenesis-related (PR) proteins (Lamb and Dixon, 1997). Since papillae are described to be associated with callose deposition (Mangin, 1895; Heitefuss, 1997), the question was raised whether callose synthesis would be involved in interactions of the pathosystem *T. aestivum – F. graminearum*. This field of investigation was interesting because the role of callose in defense reactions against fungal attack is still controversially discussed and a precise function has not been demonstrated unequivocally, even though it is one of the earliest observed reactions to pathogen penetration (deBary, 1863).

IV.5. Organ-specific *GSL* gene expression in wheat during normal growth

Prior to examining an active role of callose in fungal penetration in the investigated pathosystem, it was necessary to get a general idea of callose synthesis in wheat. Despite the great importance to agriculture and the basic role of callose in plant development, only little was known about the regulation of callose synthesis in wheat. The results of this work prove that *GSL* genes are differently expressed in organs of wheat. Thus, organ-specificity represents one aspect of the relatively high number of *GSL* genes in higher plants. Additionally,

the expression level is a further aspect used to discriminate between different *GSL* genes. In this work, wheat plants at the Zadoks stages 7.5-7.9 (Zadoks *et al*., 1974) were chosen for examination. These stages are normally reached 7 days after anthesis. The advantage of these Zadoks stages is that they are easily identified helping to ensure a consistent developmental stage of the wheat plants.

In wheat, *TaGSL3* showed a very high organ specificity of expression. At the developmental stage of the plant examined, it was almost exclusively expressed in the spike (Figure 18). Phylogenetic analysis of the encoded enzyme fragment revealed high homology to putative callose synthases in barley and maize (Figure 17). Therefore, it would be interesting to examine whether the callose synthase encoding genes, *HvGSL6* and *7* and *ZmGSL7*, are also specifically expressed in the spike and/or the ear. *TaGSL10* is another gene that was predominantly expressed in one organ: the stem. Interestingly, the encoded enzyme showed almost no homology to known amino acid sequences of *GSL* encoded callose synthases; neither from closely related plants, like barley, rice and maize, nor from *A. thaliana*. Because of the organ-specific expression of *TaGSL3* and *TaGSL10*, an involvement in specialized callose synthesis by these genes was hypothesized. *TaGSL3* might contribute to callose formation in pollen or pollen tubes; thus, it is almost exclusively expressed in the spike and not in the other organs. An exclusive expression in specific spike tissues was shown previously for *NaGSL1* from *Nicotiana alata* (Doblin *et al*., 2001). Dong *et al.* (2005) described a similar function for *AtGSL2* (*CalS5*) from *A. thaliana*. In

general, organ-specificity might be also linked with defense mechanisms, like papillary callose formation against organ-specific pathogenic attack. Nevertheless, subsequent transcription analyses have shown that neither *TaGSL3* nor *TaGSL10* are involved in defense mechanisms of the wheat spike after fungal infection. An induction of expression during fungal infection was not observed (Figure 21). *TaGSL22* transcripts were mainly detected in the leaf blade and in significantly reduced amounts in the other tested organs. Similar to TaGSL10, homology to known callose synthases from other plants was very limited. At the examined stage of plant development (Zadoks stages 7.5-7.9), an important involvement of *TaGSL22* in callose synthesis can be questioned since the expression level was dramatically lower than of all other *TaGSL* genes (Figure 18). It would therefore be interesting to determine whether the *TaGSL22* expression level increases at different developmental stages of the plant, providing that it retains its high organ specificity. In contrast to *TaGSL3*, *10* and *22*, *TaGSL2* and *8* were almost equally expressed in each of the examined organs. Combining the unspecific expression with the very high expression level of *TaGSL8*, it can be hypothesized that the encoded callose synthase might be involved in general callose synthesis processes, which do not depend on external induction and which are essential for development in all examined organs. These processes could include callose depositions at the cell plate, plasmodesmatal canals, and spiral thickenings in tracheids (Stone and Clarke, 1992). However, TaGSL8 showed homology to the extensively characterized callose synthase HvGSL2 in barley. Here, the nomenclature as indicated at

http://cellwall.stanford.edu/ was chosen. This sequence is identical to HvGSL1 published by Li *et al.* (2003). Unlike *TaGSL8*, *HvGSL2* was differently expressed in leaf blade, stem and floret tissue. Therefore, a putative connection between sequence homology and organ-specific expression has to be questioned. However, it has to be considered that the developmental stage of the barley plant cannot be directly compared to the stage of the wheat plants that were examined. Additionally, the present results reveal that even within a plant species it is not possible to correlate organ-specific expression profiles with high homology. Although *TaGSL12*, *19* and *23* showed an almost identical expression pattern and a similar expression level (especially *TaGSL12* and *23*, Figure 2), they are phylogenetically distantly related (Figure17). Hence, predicting a putative function of TaGSL2 due to homology to AtGSL5 (Figure 17), (one of the best characterized callose synthases; Jacobs *et al.*, 2003; Nishimura *et al.*, 2003), might be deceptive. Nevertheless, only detailed organ-specific expression analysis of *GSL* genes in closely related plants like wheat and barley could elucidate any correlation of expression profile and sequence homology.

IV.6. Organ-specific callose synthesis in wheat during normal growth

Another interesting aspect of our results is the different callose synthase activity of the examined organs. Highest activity was detected in spike tissue whereas activity was reduced almost 70 % in leaf blade and stem tissue (Figure 19 B). Considering *TaGSL* gene expression, TaGSL3 might be responsible for the higher enzyme activity of the spike. *TaGSL3* was almost exclusively expressed in

spike tissue (Figure 17). In contrast to a putative involvement of TaGSL3, the contribution of TaGSL10 to callose synthase activity in stem tissue seems to be low. Even though *TaGSL10* was found to be predominantly expressed in stem tissues, callose synthase activity was not significantly increased as compared to leaf blade tissue (Figure 19 B). Nevertheless, a putative involvement of still unknown callose synthases encoded by *TaGSL* genes in wheat cannot be excluded. However, predicting a high number of further *TaGSL* genes due to comparison with identified *GSL* genes from related plants like barley, rice and maize is not convincing. Despite the high number of putative *GSL* gene fragments (http://cellwall.stanford.edu/), the number of significantly different *GSL* genes for barley was reduced from 10 to 8, for maize from 17 to 9 and additionally, for wheat from 21 to 8. This was necessary since redundant and ambiguous sequence data was found in the database. In addition, it was not possible to amplify any unknown *TaGSL* genes from either full-length cDNA, which represented different developmental stages and biotic stress, or from genomic DNA. Thus, expression of further *TaGSL* genes might be low or induced only during specific developmental stages, including response to environmental conditions. In general, the data suggest that callose synthesis is highly regulated by a combination of *GSL* genes. There is a number of genes that might be involved in general developmental processes for the whole plant. The hypothesis is that *GSL* genes revealing a relatively high and non-specific expression contribute to these processes. Additionally, specifically expressed *GSL* genes

regulate the complex callose synthesis in each organ, which are induced during differential developmental stages or in respond to environmental conditions.

IV.7. Organ-specific callose deposition in wheat during normal growth

In contrast to spike and stem tissue, showing a correlation of callose synthase activity and callose concentration, a relatively low enzyme activity but high callose concentration was detected in the leaf blade (compare Figure 19 A and B). Therefore, synthesis and subsequent deposition of callose might occur during early developmental stages of the leaf blade. Generally, the aniline blue staining of tissue sections revealed callose depositions mainly at vascular bundles (Stone and Clarke, 1992). In leaf blade tissue, callose depositions were also detected in adaxial mesophyll and hypodermal sclerenchyma cells. This contributes to the higher total amount of callose in leaf blade tissue compared to stem tissue. Interestingly, the callose concentration of the spike did not increase as strongly as compared to the leaf blade (Figure 19 A); even though massive callose depositions were located in the spike (Figure 19D and E). However, these depositions were restricted to the transition zone of the rachilla and rachis. Intermediary rachis sections showed callose deposition only at vascular bundles (Figure 19 F); therefore reducing the total callose concentration of spike tissue. The heterogeneous pattern of callose deposition in the spike, which is contrary to the relatively homogeneous ones in the leaf blade and the stem, suggests a higher complexity of callose synthase regulation than in other organs.

This experimental combination of gene expression, enzyme activity and product determination as well as product localization facilitates a comprehensive overview of organ-specific callose regulation for the first time in the wheat plant. Nevertheless, to elucidate callose synthesis and regulation in detail, it is essential to downregulate and/or overexpress specific *GSL* genes. This has been done in *A. thaliana* by using the method of RNA silencing (Jacobs *et al*., 2003), which constitutes an appropriate tool for many plants in general (Kooter, *et al*., 1999; Matzke *et al*., 2001; Baulcombe, 2004; Wang and Metzlaff, 2005).

IV.8. Suppression of wheat callose synthesis during infection

Following organ-specific callose synthesis regulation at normal growth stage, callose concentration, callose synthase activity and *GSL* gene expression during wheat spike infection was compared. Wheat spikes were inoculated with *F. graminearum* wild type and a lipase-deficient mutant (Δfgl1-2). Whereas wild-type infection resulted in complete Fusarium head blight (FHB) of the susceptible wheat cultivar Nandu, a strong type II resistance (Schroeder and Christensen, 1963) was established after infection with Δfgl1-2. Type II resistance refers to the spread of the pathogen within a host. This infection was accompanied by papilla-like barrier formation, as described previously. To induce non-host specific defense reactions, wheat spikes were additionally inoculated with the barley-leaf pathogen *P. teres*. As a result, callose synthase activity correlated with progress and severity of infection. Induction of callose synthase activity was only detected during Δfgl1-2 and *P. teres* infection (Figure 20 E) and correlated with the

occurrence of readily visible infection symptoms on the wheat head (7 dpi with Δfgl1 and 14 dpi with *P. teres,* Figure 20 B). In contrast, a constant loss of callose synthase activity was detected during *F. graminearum* wild-type infection (Figure 20 E). The inhibition of callose synthase cannot be attributed to a general degradation of the plasma membrane since activity of the membrane-associated NADH oxidase was not effected (Figure 20 F). Furthermore, the expression of the *Tri5* gene was analyzed. This gene encodes a trichodiene synthase that is decisive for the synthesis of the mycotoxin deoxynivalenol (DON). DON was identified as the first virulence trait of *F. graminearum* required for successful infection of wheat (Proctor *et al*., 1995; Desjardins *et al*., 1996). A putative involvement of DON might be suggested from similar phenotypes of DON-nonproducing strains and the *Δfgl1* strain; both do not cause disease spread in wheat spikes (Bai *et al*., 2001; Figure 13 A). However, a constant induction of the *Tri5* gene was detected in the *Δfgl1* strain that was not observed in *F. graminearum* wild type during wheat head infection. As a result, the expression level of this lipase-deficient strain was five times higher than of wild type 14 dpi. The *Tri5* expression corresponded to amount of DON determined in *Δfgl1*-infected wheat heads that was twice as high as wild type-infected 14 dpi (unpublished data). Hence, the reduced virulence of *Δfgl1* strains is not provoked by a reduced DON production. This also indicates that DON does not contribute to inhibition of callose synthase activity caused by *F. graminearum* wild type. Moreover, these results contribute to early observations indicating that callosic papillae may also exclude toxic material (Smith, 1900; Hanchey and Wheeler,

1971; Skipp *et al*., 1974). This could explain that the relatively high amount of DON produced by the *Δfgl1* strains has no effect on virulence because the infection is associated with papillae formation.

IV.9. Putative regulation of callose synthesis during infection

The determination of the total amount of callose in spike tissue from the site of inoculation revealed a correspondence to the callose synthase activity (compare Figure 20 D and E), except for Δfgl1 infection. Even though an induction of callose synthase activity was detected, the total amount did not increase and was slighter lower than in control spikes. This suggest a putative involvement of (1,3)-*β*-glucanases secreted by the pathogen independently from lipase secretion. Secreted fungal glucanaes during infection might also explain the rapid degradation of callose during *F. graminearum* infection (Figure 20 D). The annotated *F. graminearum* genome at the MIPS database (Munich Information Center for Protein Sequences, http://mips.gsf.de/genre/proj/fusarium/) reveals the possible existence of at least four endo-(1,3)-*β*-glucanases with a high probability of secretion. An involvement of secreted glucanases in fungal pathogenicity was already shown for mycoparasitic fungi (Kim *et al*., 2002; Amey *et al*., 2003). Because callose synthase activity might be regulated by *GSL* gene expression (Donofrio and Delaney, 2001), the expression of eight previously analysed *GSL* genes during wheat head infection was quantified. Expression during *F. graminearum* wild-type infection did not strongly deviate from *Δfgl1* and *P. teres* infection. Additionally, highest expression levels were detected for all infection

types and control at early measured time points (Figure 21). These expression results support the idea that callose synthase activity is not regulated by gene expression but rather by subcellular control of preexisting enzymes as proposed by Jacobs *et al*. (2003). Plant cells commonly respond to fungal penetration (Blume *et al*., 2000; Grant *et al*., 2000) and wounding (Leon *et al*., 1998, 2001) with a rapid increase in cytoplasmatic free Ca^{2+} levels. Since membrane-associated callose synthases in plants require Ca^{2+} (Kauss *et al*., 1983) the pathogen-induced increase in Ca^{2+} concentrations constitutes a likely mechanism to explain the increase in callose activity after fungal infection in our experiments. However, neither the expression studies nor the suggested Ca^{2+}-dependent activation of synthase activity were suitable to explain callose synthase inhibition caused by *F. graminearum* wild-type infection.

IV.10. Suppression of wheat callose synthesis caused by the secretion of FGL1

Kauss and Jeblick (1986) showed the influence of free fatty acids (FFA) on callose synthase activity of *Glycine max*. Similar to their results, it was demonstrated here that the inhibition of wheat callose synthase activity can be caused by the addition of unsaturated free fatty acids, whereas a saturated free fatty acid failed to inhibit activity at tested concentrations (Figure 22 E). In general, inhibition of activity was observed at the same range of FFA concentration as reported by Kauss and Jeblick (1986). Since oleic, linoleic, and linolenic acid constitute the main amount of the total unsaturated fatty acid

composition in wheat (Davis *et al*., 1980; Barnes, 1982), they are most likely to be released after lipid hydrolysis caused by the secretion of the *F. graminearum* lipase FGL1. Therefore, they were chosen in these assays as well as stearic acid, the corresponding saturated fatty acid. Moreover, *in vitro* data correlated with *in planta* results. The addition of unsaturated FFA to previously inoculated wheat spikelets significantly increased infection of the lipase-deficient strain. In contrast to this, stearic acid did not affect infection (Table 3). Observations of the infection progress of the GFP-tagged lipase-deficient strain Δfgl1-GFP-1 revealed the impact of the added unsaturated FFA. Unlike fungal growth without addition of FFA, Δfgl1-GFP-1 could pass the transition zone of rachilla and rachis and colonize the rachis and spikelets above the site of inoculation (Figure 24 A and B), but was still restricted from colonizing spikelets below the inoculation site (Figure 24 D). Combining callose synthase activity during *F. graminearum* wild-type and Δfgl1 infection with the inhibitory effect of unsaturated FFA to callose synthases, it can be concluded that: 1.) *F. graminearum* requires the secreted lipase FGL1 to release FFA for inhibition of plant defense, resulting in successful infection of the wheat head, and 2.) callose synthases and callose production play an active role in type II resistance of wheat. On this regard, Ribichich *et al*., (2000) also observed higher callose deposition in the rachis of the type II resistant wheat cultivar Sumai 3 than in a susceptible cultivar after *F. graminearum* infection. The present conclusions are supported and extended by additional results. Firstly, the growth of *F. graminearum* conidia after germination was directed to the ovary of the floret (Figure 24 C), similar to the

growth of *Fusarium culmorum* in inoculated wheat spikes (Kang and Buchenauer, 2000). The pistil is enriched in nutrients and in lipids. Furthermore, it is adjacent to the transition zone of rachilla and rachis, where a strong papillae-like barrier formation was observed during infection with *Δfgl1* strains. Hence, the combination of lipids and the position of the pistil's ovary suggests a key function in the inhibition of callose synthases and successful fungal establishment due to an initial lipid hydrolysis. Secondly, callose synthase extracted from the wheat cultivar Batis revealed a significantly higher resistance to unsaturated FFA than the cultivar Nandu did (Figure 22 E). In combination with the previously discussed involvement of callose synthase activity and FFA for the initiation of plant resistance, the lower susceptibility to FFA can explain the higher callose synthase activity of Batis 14 dpi (Figure 22 D). As a result, callose was still present in Batis at this stage of infection whereas it was absent in Nandu (Figure 22 C). Therefore, it can be concluded that the increased type II resistance of the wheat cultivar Batis to *F. graminearum* wild-type infection (Figure 22A and B) is directly associated with the susceptibility of callose synthases to unsaturated free fatty acids.

IV.11. Model of type II resistance to fungal infection in wheat

The results are summarized in a proposed model that can explain the correlation of callose synthase activity, amount of produces callose and type II resistance (Figure 25). It would be appropriate to explain observations that callosic papillae correlate with penetration failure (Figure 25 B and C), but not with successful

fungal establishment (Figure 25 A). The model also refers to increased callose formation that is more common in incompatible systems, for example involving *Phytophthora cinnamomi* (Cahill *et al*., 1989) or the wheat-*P. teres* system used here. Especially in incompatible systems, the pathogen might not be able to hydrolyze the lipids of the non-host or could not spread to lipid-rich tissue resulting in a non-release of FFA and strong callose formation (Figure 25 C). However, the model cannot explain the occurrence of callosic papillae without impeding fungal penetration (Rodriguez-Galvez and Mendgen, 1995) or a decreased fungal virulence in the absence of callosic papillae (Jacobs *et al*., 2003; Nishimura *et al*. 2003). This indicates that each pathosystem might have evolved specific interactions in terms of an active role of callose. Nevertheless, this proposed model might be generally applicable to closely related species, like grasses and cereals. Indication was given by chemical treatment of barley (Bayles *et al*., 1990) and reed canarygrass (Vance and Sherwood, 1976), which resulted in reduced papillae formation and increased susceptibility to fungal penetration. Additionally, the proportion of hyphae encased by papillae that fail to develop further is low in legumes (5–15 %), but high in grasses (70–100 %) (Politis, 1976; Sherwood and Vance, 1980). Therefore, the model should be seen as a first step into understanding the active role of callose in fungal penetration, especially in wheat and potentially in related species.

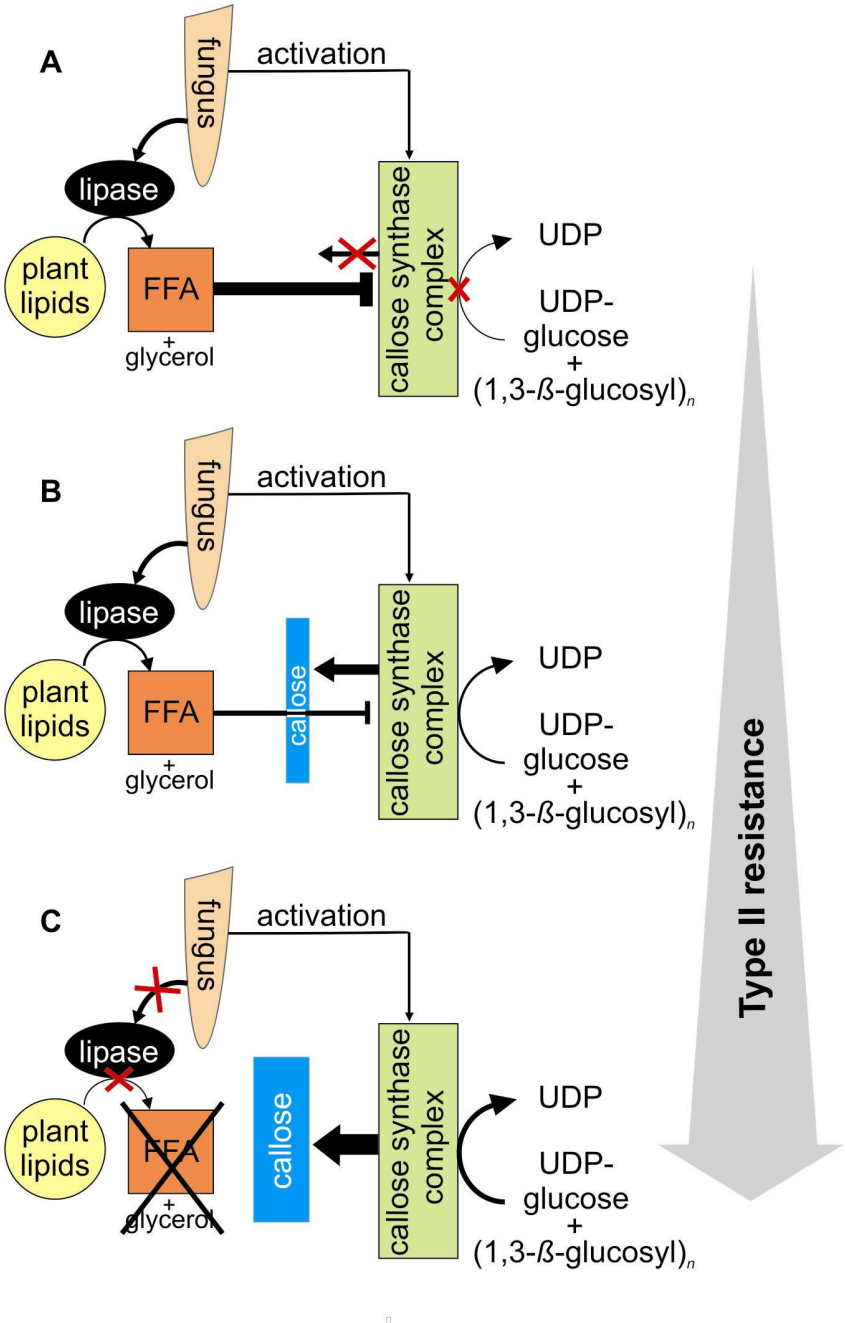

Figure 25. Model of type II resistance to fungal infection in wheat.

A. Susceptible wheat cultivar with callose synthases strongly inhibited by released free fatty acids (FFA). Callose production is suppressed.

B. Resistent cultivar with callose synthases weakly inhibited by FFA. Callose is produced as a response to fungal penetrstion.

C. Non-host / lipase-deficient pathogen infection without release of FFA and therefore no inhibition of callose synthases. Callose production is highly induced.

V. Summary

Fusarium graminearum is the causal agent of the Fusarium head blight (FHB) and a destructive pathogen of cereals accounting for extreme grain yield losses especially on wheat and maize. Like other fungal pathogens, *F. graminearum* secretes various extracellular enzymes, which are hypothesized to be involved in host infection. Extracellular lipolytic activity of *F. graminearum* was strongly induced in culture by wheat germ oil; this made it possible to isolate, clone, and characterize a gene (*FGL1*) which codes for a secreted lipase. Expression analysis indicated that *FGL1* is induced by lipid-containing substrates and repressed by glucose. *In planta*, *FGL1* transcription was detected one day post infection of wheat spikes. The function of the *FGL1* gene product was verified by specifically demonstrating lipase activity after expression in a heterologous host. Ebelactone B, a known lipase inhibitor, repressed the lipolytic activity of the enzyme. Disease severity was strongly reduced when wild-type conidia were supplemented with ebelactone B. Transformation-mediated disruption of *FGL1* led to reduced extracellular lipolytic activity in culture and to reduced virulence to both wheat and maize. Wheat infection with *Δfgl1* strains was associated with a strong barrier formation in the spike, impeding the fungus from spreading further (type II resistance).

Callose ((1,3)-*β*-glucan) is a main component of papillae. These are barriers that are considered to delay pathogenic spreading. The class of glucan synthase-like (*GSL*) genes represents an appropriate target to analyze the regulation of callose synthesis. The expression of eight *GSL* genes (*TaGSL*) was analyzed as well as

callose synthase activity and total callose content in the stem, leaf blade and spike of wheat. Organ-specific expression of six *TaGSL* genes and strong differences in expression levels were detected by quantitative real-time PCR. Differences were also determined in callose synthase activity and the total amount of callose in the examined organs. Aniline blue staining in tissue sections localized callose depositions. These data suggests that callose synthesis is highly regulated by a combination of *GSL* genes, which are involved either in general or organ-specific developmental processes.

Therefore, the callose content, callose synthase activity and *GSL* gene expression were examined during fungal infection. Wheat spikes were inoculated with *F. graminearum* wild type, a *Δfgl1* strain, and *Pyrenophora teres* to induce non-host reactions. A strong inhibition of callose synthase activity was observed during *F. graminearum* wild-type infection. Contrarily, enzyme activation was induced during *Δfgl1* and *P. teres* infection. The addition of unsaturated free fatty acids (FFA) to spikelets three days post inoculation significantly increased the virulence of *Δfgl1*. Thus, the release of FFA due to fungal lipase activity is necessary for full infection the host plant. Differences in inhibition of callose synthase activity by FFA of both a susceptible and a resistant wheat cultivar contribute to type II resistance in wheat. Thus, a model for type II resistance to fungal infection in wheat has been proposed in this study.

VI. Zusammenfassung

Fusarium graminearum ist der Hauptverursacher von Ährenfusariosen und zeigt sein zerstörerisches Potential gegenüber Getreide durch hohe Ernteverluste, insbesondere bei Weizen und Mais. Wie auch andere pathogene Pilze sekretiert *F. graminearum* zahlreiche extrazelluläre Enzyme, von denen vermutet wird, an der Infektion der Wirtspflanze beteiligt zu sein. Die extrazelluläre lipolytische Aktivität von *F. graminearum* wurde besonders stark durch Weizenkeimöl induziert. Dies ermöglichte die Isolierung, Klonierung und Charakterisierung eines Gens (*FGL1*), das eine sekretierte Lipase kodiert. Untersuchungen zeigten, dass die Expression von *FGL1* durch lipidhaltige Substrate induziert und durch Glukose reprimiert wird. *In planta* wurden *FGL1*-Transkripte bereits einen Tag nach der Infektion von Weizenähren nachgewiesen. Die Funktion des *FGL1*-Genproduktes wurde durch die spezifische Lipaseaktivtität nach der Expression in einem heterologen Wirt nachgewiesen. Neben einer Unterdrückung der lipolytischen Aktivität der Lipase wurde auch der Krankheitsgrad auf Weizenähren deutlich reduziert, wenn Wildtypkonidien zuvor mit dem bekannten Lipaseinhibitor Ebelacton B versetzt wurden. Als Folge einer transformationsvermittelten Disruption des *FGL1*-Gens wurden eine verminderte extrazelluläre lipolytische Aktivität in Kulturüberständen und eine reduzierte Virulenz gegenüber Weizen und Mais festgestellt. Die Infektion von Weizen mit *Δfgl1*-Stämmen war mit der Bildung von Barrieren in der Ähre begleitet, die eine weitere Ausbreitung des Pilzes (Typ II-Resistenz) verhinderten.

Callose ((1,3)-*β*-Glukan) ist die Hauptkomponente von Papillen, die als Barrieren angesehen werden, um eine Ausbreitung des Pathogens zu verzögern. Für die Analyse der Callosesynthese-Regulation eignet sich die Gruppe der Glukansynthase-ähnlichen (glucan synthase-like, *GSL*) Gene. Hierzu wurde die Expression von acht *GSL*-Genen (*TaGSL*) sowie die Callosesynthase-Aktivität und die Gesamt-Callosemenge im Stamm, der Blattscheide und der Ähre von Weizen untersucht. Mit Hilfe der quantitativen *real-time* PCR wurden sowohl eine organspezifische Expression von sechs *TaGSL*-Genen als auch starke Unterschiede im Expressionsniveau nachgewiesen. Zudem unterschieden sich die Callosesynthase-Aktivität und Gesamt-Callosemenge in den untersuchten Organen. Das Färben von Gewebeschnitten ermöglichte das Lokalisieren von Calloseanlagerungen. Diese Ergebnisse lassen darauf schließen, dass die Callosesynthese durch die Kombination der verschiedenen *GSL*-Gene, die entweder an generellen oder organspezifischen Entwicklungsprozessen beteiligt sind, ein hochgradig regulierter Prozess ist.

Nachfolgend wurde die *GSL*-Genexpression, Callosesynthase-Aktivität und Gesamt-Callosemenge während der Pilzinfektion analysiert. Dazu wurden Weizenähren mit *F. graminearum* Wildtyp, einem *Δfgl1*-Stamm und *Pyrenophora teres*, zum Hervorrufen von Nicht-Wirtsreaktionen, inokuliert. Eine starke Inhibierung der Callosesynthase-Aktivität wurde während der *F. graminearum* Wildtyp-Infektion beobachtet. Im Gegensatz dazu wurde die Enzymaktivität während der *Δfgl1*- und *P. teres*-Infektion induziert. Die Zugabe von ungesättigten freien Fettsäuren (FFS) zu Ährchen drei Tage nach der Inokulation

führte zu einem Anstieg der Virulenz des *Δfgl1*-Stammes. Daraus ergibt sich, dass das Freisetzen von FFS durch die Lipaseaktivität des Pilzes für eine volle Infektion der Wirtspflanze notwendig ist. Die unterschiedlich starke Inhibierung der Callosesynthase-Aktivität durch FFS in einem anfälligen und einem resistenten Weizenkultivar tragen zur Ausprägung der Typ II-Resistenz in Weizen bei. Ein Model zur Typ II-Resistenz gegenüber einer pilzlichen Infektion in Weizen fasst die erhaltenen Ergebnisse zusammen.

VII. References

Aist, J.R. (1976). Papillae and Related Wound Plugs of Plant Cells. In Annual Review of Phytopathology, K.F. Baker, G.A. Zentmyer, and E.B. Cowling, eds. (Palo Alto, CA: Annual Reviews Inc.), pp.145-163.

Aist, J.R., and Williams, P.H. (1971). The cytology and kinetics of cabbage root hair penetration by *Plasmodiophora brassicae*. Can. J. Bot. *49*, 2023-2034.

Amey, R.C., Mills, P.R., Bailey, A., and Foster, G.D. (2003). Investigating the role of a *Verticillium fungicola* beta-1,6-glucanase during infection of *Agaricus bisporus* using targeted gene disruption. Fungal Genet. Biol. *39*, 264-275.

Aspinall, G.O., and Kessler, G. (1957). The structure of callose from the grape vine. (London: Chem. Ind.), p. 1296.

Bai, G.-H., Desjardins, A.E., and Plattner, R. D. (2001). Deoxynivalenol-nonproducing *Fusarium graminearum* causes initial infection, but does not cause disease spread in wheat spikes. Mycopathologia *153*, 91–98.

Banks, G.R., and Taylor, S.Y. (1988). Cloning of the *PYR3* gene of *Ustilago maydis* and its use in DNA transformation. Mol. Cell. Biol. *8*, 5417-5424.

Barnes, P.J. (1982). Lipid composition of wheat germ and wheat germ oil. Fette. Seifen. Anstrichm. *84*, 256 – 269.

Baulcombe, D. (2004). RNA silencing in plants. Nature *431*, 356-363.

Bayles, C.J., Ghemawat, M.S., and Aist, J.R. (1990). Inhibition by 2-deoxy-D-glucose of callose formation, papilla deposition, and resistance to powdery mildew in *ml-o* barley mutant. Physiol. Mol. Plant Pathol. *36*, 63-72.

Berto, P., Commenil, P., Belingheri, L., and Dehorter, B. (1999). Occurrence of a lipase in spores of *Alternaria brassicicola* with a crucial role in the infection of cauliflower leaves. FEMS Microbiol. Lett. *180*, 183-189.

Blume, B., Nuernberger, T., Nass, N., and Schell, D. (2000). Receptor-mediated increase in cytoplasmic free calcium required for activation of pathogen defense in parsley. Plant Cell *12*, 1425-1440.

Borgström, B., and Brockman, H.L. (1984). Lipases. (Amsterdam: Elsevier).

Braune, W., Leman, A., and Taubert, H. (1983). Pflanzenanatomisches Praktikum I. (Jena: Gustav Fischer), p. 241.

Brown, I., Trethowan, J., Kerry, M., Mansfield, J., and Bolwell, G.P. (1998). Localization of components of the oxidative cross-linking of glycoproteins and of callose synthesis in papillae formed during the interaction between non-pathogenic strains of *Xanthomonas campestris* and French bean mesophyll cells. Plant J. *15*, 333-343.

Bulone, V., Fincher, G.B., and Stone, B.A. (1995). *In vitro* synthesis of a microfibrillar (1→3)-*β*-glucan by a ryegrass (*Lolium multiflorum*) endosperm (1→3)-*β*-glucan synthase enriched by product entrapment. Plant J. *8*, 213-225.

Cabib, E., Roh, D.-H., Schmidt, M., Crotti, L.B., and Verma, A. (2001). The yeast cell wall and septum as paradigms of cell growth and morphogenesis. J. Biol. Chem. *276*, 19679-19682.

Cahill, D., Legge, N., Grant, B., and Weste, G. (1989). Cellular and histological changes induced by *Phytophthora cinnamomi* in a group of plant species ranging from fully susceptible to fully resistant. Phytopathol. *79*, 417-424.

Chueh, P.J., Morré, D.M., Penel, C., DeHahn, T., and Morré, D.J. (1997). The hormone-responsive NADH oxidase of the plant plasma membrane has properties of a NADH:protein disulfide reductase. J. Biol. Chem. *272*, 11221-11227.

Chun, H.-K., Ko, H.-R., Moon, H.-S., and Kho, Y.-H. (1995). Preventive effect of ebelactone B, an esterase inhibitor on rice sheath blight caused by *Rizoctonia solani*. J. Microbiol. Biotechnol. *5*, 335-340.

Comménil, P., Belingheri, L., Bauw, G., and Dehorter, B. (1999). Molecular characterization of a lipase induced in *Botrytis cinerea* by components of grape berry cuticle. Physiol. Mol. Plant Pathol. *55*, 37-43.

Comménil, P., Belingheri. L., and Dehorter, B. (1998). Antilipase antibodies prevent infection of tomato leaves by *Botrytis cinerea*. Physiol. Mol. Plant Pathol. *52*, 1-14.

Comménil, P., Belingheri, L., Sanochelle, M., and Dehorter, B. (1995). Purification and properties of an extracellular lipase from the fungus *Botrytis cinerea*. Lipids *30*, 351-356.

Crowhurst, R.N., Binnie, S.J., Bowen, J.K., Hawthorne, B.T., Plummer, K.M., Rees-George, J., Rikkernik, E.H., and Templeton, M.D. (1997). Effect of disruption of a cutinase gene (*cutA*) on virulence and tissue specificity of *Fusarium solani* f. sp. *cucurbitae* race 2 towards *Cucurbita maxima* and *C. moschata*. Mol. Plant-Microbe Interact. *10*, 355-368.

Cui, X., Heungsop, S., Song, C., Laosinchai, W., Amano, Y., and Brown, R.M. Jr. (2001). A putative plant homolog of the yeast α-(1→3)-D-glucan subunit *FKS1* from cotton (*Gossypium hirsutum* L.) fibers. Planta *213*, 223-230.

D'Mello, J.P.F., and MacDonald, A.M.C. (1997). Mycotoxins. Animal Feed Sci. Technol. *69*, 155–166.

Davies, K.A., De Corono, I., Foster, S.J., Li D., Johnstone, K., and Visser, J. (2000). Evidence for a role of cutinase in pathogenicity of *Pyrenopeziza brassicae* on brassicas. Physiol. Mol. Plant Pathol. *57*, 63-75.

Davis, K.R., Litteneker, N., LeTourneau, D., and McGinnis, J. (1980). Evaluation of the nutrient composition of wheat. I. Lipid constituents. Cereal Chem. *57*, 178–184.

deBary, A. (1863). Recherches sur le développement de quelques champignons parasites. Ann. Sci. Nat. Bot. Biol. Veg. *20*, 5-148.

Delmer, D.P., Solomon, M., and Read, S.M. (1991). Direct photolabeling with [^{32}P]UDP-glucose for identification of a subunit of cotton fiber callose synthase. Plant Physiol. *95*, 556-563.

Desjardins, A.E., Proctor, H.R., Bairoch, A., McCormick, S.P., Shaner, G., Buechley, G., and Hohne, T.M. (1996). Reduced virulence of trichothecene nonproducing mutants of *Giberella zeae* in wheat field tests. Mol. Plant-Microbe Interact. *9*, 775-781.

DeZwaan, T.M., Carroll, A.M., Valent, B., and Sweigard, J.A. (1999). *Magnaporthe grisea* Pth11p is a novel plasma membrane protein that mediates appressorium differentiation in response to inductive surface cues. Plant Cell *11*, 2013-2030.

Dhugga, K.S., and Ray, P.M. (1994). Purification of (1→3)-*β*-D-glucan synthase activity from pea tissue – two polypeptides of 55 kD and 70 kD copurify with enzyme activity. Eur. J. Biochem. *220*, 943-953.

Dijkgraaf, G.J., Abe, M., Ohya, Y., and Bussey, H. (2002). Mutations in Fks1p affect te cell wall content of β-1,3- and β-1,6-glucan in *Saccharomyces cerevisiae*. Yeast *19*, 671-690.

Doblin, M.S., De Melis, L., Newbigin, E., Bacic, A., and Read, S.M. (2001). Pollen tubes of *Nicotiana alata* express two genes from different β-glucan synthase families. Plant Physiol. *125*, 2040-2052.

Dong, X., Hong, Z., Sivaramakrishnan, M., Mahfouz, M., and Verma, D.P. (2005). Callose synthase (CalS5) is required for exine formation during microgametogenesis and for pollen viability in Arabidopsis. Plant J. *42*, 315-328.

Donofrio, N.M., and Delaney, T.P. (2001). Abnormal callose response phenotype and hypersusceptibility to *Peronospora parasitica* in defence-comprised

Arabidopsis nim 1-1 and salicylate hydroxylase-expressing plants. Mol. Plant-Microbe Interact. *14*, 439-450.

Douglas, C.M., Foor, F., Marrinan, J.A., Morin, N., Nielsen, J.B., Dahl, A.M., Mazur, P., Baginsky, W., Li, W., El-Sherbeini, M., Clemas, J.A., Mandala, S.M., Frommer, B.R., and Kurtz, M.B. (1994). The *Saccharomyces cerevisiae FKS1* (*ETG1*) gene encodes an integral membrane protein which is a subunit of (1→3)-β-D-glucan synthase. Proc. Natl. Acad. Sci. USA *91*, 12907-12911.

Dubin, H.J., Gilchrist, L., Reeves, L., and McNab, A. (1997). Fusarium head scab: Global status and prospects. CIMMYT, DF, Mexiko.

Enns, L.C., Kanaoka, M.M., Torii, K.U., Comai, L., Okada, K., and Cleland, R.E. (2005). Two callose synthases, GSL1 and GSL5, play an essential and redundant role in plant and pollen development and in fertility. Plant Mol. Biol. *58*, 333-349.

Francis, S.A., Dewey, F.M., and Gurr, S.J. (1996). The role of cutinase in germling development and infection by *Erysiphe graminis* f.sp. *hordei*. Physiol. Mol. Plant Pathol. *49*, 201-211.

Frost, D.J., Read, S.M., Drake, R.R., Haley, B.E., and Wasserman, B.P. (1990). Identification of the UDP-glucose-binding polypeptide of callose synthase from *Beta vulgaris* L. by photoaffinity labeling with 5-azido-UDP-glucose. J. Biol. Chem. *265*, 2162-2167.

Gibeaut, D.M., and Carpita, N.C. (1994). Biosynthesis of plant cell wall polysaccharides. FASEB J. *8*, 904-915.

Gomez-Gomez, E., Ruiz-Roldan, M.C., Di Pietro, A., Roncero, M.I., and Hera, C. (2002). Role in pathogenesis of two endo-beta-1,4-xylanase genes from the vascular wilt fungus *Fusarium oxysporum*. Fungal Genet. Biol. *35*, 213-222.

Grant, M.R., Brown, I., Adams, S., Knight, M., Ainslie, A., and Mansfield, J.W. (2000). The *RPM1* plant disease resistance gene facilitates a rapid and

sustained increase in cytosolic calcium that is necessary for the oxidative burst and hypersensitive cell death. Plant J. *23*, 441-450.

Green, C.E., and Philips, R.L. (1975). Plant regeneration from tissue cultures of maize. Crop. Sci. *15*, 417-421.

Hanchey, P., and Wheeler, H. (1971). Pathological changes in ultrastructure: tobacco roots infected with *Phytophthora parasitica* var. *nicotianae*. Phytopathol. *61*, 33-39.

Heitefuss, R. (1997). Cell wall modifications in relation to resistance. In Resistance of crop plant against fungi, H., Hartleb, R., Heitefuss, and H.H., Hoppe, eds. (Jena, Stuttgart, Lübeck: Gustav Fischer Verlag).

Him, J.L.K., Pelosi, L., Chanzy, H., Putaux, J.L., and Bulone, V. (2001). Biosynthesis of (1→3)-*β*-D-glucan (callose) by detergent extracts of a microsomal fraction from *Arabidopsis thaliana*. Eur. J. Biochem. *268*, 4628-4638.

Hong, Z., Delauney, A.J., and Verma, D.P.S. (2001). A cell plate-specific callose synthase and its interaction with phragmoplastin. Plant Cell *13*, 755-768.

Horwitz, B. A., Sharon, A., Lu, S.-W., Ritter, V., Sandrock, T. M., Yoder, O. C., and Turgeon, B. G. (1999). A G protein alpha subunit from *Cochliobolus heterostrophus* involved in mating and appressorium formation. Fungal. Genet. Biol. *26*, 19-32.

Ishii, K. (1983). Chemistry of trichothecenes. In Trichothecenes, chemical, biological and toxicological aspects. Developments in Food Science 4, Y., Ueno, ed. (Amsterdam: Elsevier), pp. 7-19.

Itoh, Y., and Scott, B. (1997). Effect of de-phosphorylation of linearized pAN7-1 and of addition of restriction enzyme on plasmid integration in *Penicillium paxilli*. Curr. Genet. *32*, 147-151.

Jacobs, A.K., Lipka, V., Burton, R.A., Panstruga, R., Strizhov, N., Schulze-Lefert, P., and Fincher, G.B. (2003). An *Arabidopsis* callose synthase, GSL5, is required for wound and papillary callose formation. Plant Cell *15*, 2503-2513.

Jaeger, K.-E., and Reetz, M.T. (1998). Microbial lipases form versatile tools for biotechnology. Trends Biotechnol. *16*, 396-403.

Jaeger, K.-E., Ransac, S., Dijkstra, B.W., Colson, C., van Heuvel, M., and Misset, O. (1994). Bacterial lipases. FEMS Microbiol. Rev. *15*, 29-63.

Jenczmionka, N.J., Maier F.J., Lösch A.P., and Schäfer, W. (2003). Mating, conidiation and pathogenicity of *Fusarium graminearum*, the main causal agent of the head-blight disease of wheat, are regulated by the MAP kinase gpmk1. Curr. Genet. *43*, 87-95.

Kamat, U., Garg, R., and Sharma, C.B. (1992). Purification to homogeneity and characterization of 1,3-β-glucan (callose) synthase from germinating *Arachis hypogaea* cotyledons. Arch. Biochem. Biophys. *298*, 731-739.

Kang, Z., and Buchenauer, H. (2000). Cytology and ultrastructure of the infection of wheat spikes by *Fusarium culmorum*. Mycol. Res. *104*, 1083-1093.

Kang, Z., and Buchenauer, H. (1999). Immunocytochemical localization of *Fusarium* toxins in infected wheat spikes by *Fusarium culmorum*. Physiol. Mol. Plant Pathol. *55*, 275-288.

Kauss, H. (1996). Callose synthesis. In Membranes: Specialized Functions in Plants, M. Smallwood, J.P. Knox, and D.J. Bowles, eds., (Guildford, UK: Bios Scientific Publishers), pp. 77-92.

Kauss, H., and Jeblick, W. (1986). Influence of free fatty acids, lysophosphatidylcholine, platelet-activating factor, acylcarnitine, and Echinocandin B on 1,3-*β*-D-glucan synthase and callose synthesis. Plant Physiol. *80*, 7-13.

Kauss, H., Köhle, H., and Jeblick, W. (1983). Proteolytic activation and stimulation by Ca^{2+} of glucan synthase from soybean cells. FEBS Lett. *158*, 84-88.

Kim, D.J., Baek, J.M., Uribe, P., Kenerley, C.M., and Cook, D.R. (2002). Cloning and characterization of multiple glycosyl hydrolase genes from *Trichoderma virens*. Curr. Genet. *40*, 374-384.

Klose, J., Moniz de Sá, M., and Kronstad, J.W. (2004). Lipid-induced filamentous growth in *Ustilago maydis*. Mol. Microbiol. *52*, 8236-835.

Köhle, H., Jeblick, W., Poten, F., Blaschek, W., and Kauss, H. (1985). Chitosan-elicited callose synthesis in soybean cells as a Ca^{2+}-dependent process. Plant Physiol. *77*, 544-551.

Kolattukudy, P.E., Podila, G.K., Sherf, B.A., Bajar, M.A., and Mohan, R. (1991). Mutual triggering of gene expression in plant-fungus interactions. In Advances in Molecular Genetics of Plant-Microbe Interaction vol. 1, H., Hennecke, and D.P.S., Verma, eds. (Dordrecht: Kluweer Academic Publishers), pp. 242-249.

Köller, W., Yao, C., Trial, F., and Parker, D.M. (1995). Role of cutinase in the invasion of plants. Can. J. Bot. *73*, 1109-1118.

Köller, W., Trail, F., and Parker, D.M. (1990). Ebelactones inhibit cutinases produced by fungal plant pathogens. J. Antibiot. (Tokyo) *43*, 734-735.

Köller, W., Allan, C.R., and Kolattukudy, P.E. (1982). Protection of *Pisum sativum* from *Fusarium solani* f.sp. *pisi* by inhibition of cutinase with organophosphorus pesticides. Phytopathol. *72*, 1425-1430.

Kooter, J.M., Matzke, M.A., and Meyer, P. (1999). Listening to the silent genes: Transgene silencing, gene regulation and pathogen control. Trends Plant Sci. *4*, 340-347.

Kudlicka, K., and Brown, R.M. (1997). Cellulose and callose biosynthesis in higher plants 1. Solubilization and separation of (1→3)- and (1→4)-*β*-D-glucan synthase activities from mung bean. Plant Physiol. *115*, 643-656.

Kudlicka, K., Brown, R.M., Li, L.K., Lee, J.H., Shin, H., and Kuga, S. (1995). Beta-D-glucan synthesis in the cotton fiber. 4. *In vitro* assembly of the cellulose I anamorph. Plant Physiol. *107*, 111-123.

Lakshmi, B.S., Kangueane, P., Abraham, B., and Pennathur, G. (1999). Effect of vegetable oils in the secretion of lipase from *Candida rugosa* (DSM 2031). Lett. Appl. Microbiol. *29*, 66-70.

Lamb, C., and Dixon, R.A. (1997). The oxidative burst in plant disease resistance. Ann. Rev. Plant Physiol. Plant Mol. Biol. *48*, 251-275.

Leon, J., Rojo, E., and Sanchez, S.J.J. (2001). Wound signalling in plants. J. Exp. Bot. *52*, 1-9.

Leon, J., Rojo, E., Titarenko, E., and Sanchez, S.J.J. (1998). Jasmonic acid-dependent and –independent wound signal transduction pathways are differentially regulated by Ca^{2+} /calmodulin in *Arabidopsis thaliana*. Mol. Gen. Genet. *258*, 412-419.

Li, J., Burton, R.A., Harvey, A.J., Hrmova, M., Wardak, A.Z., Stone, B.A., and Fincher, G.B. (2003). Biochemical evidence linking a putative callose synthase gene with (1→3)-*β*-D-glucan biosynthesis in barley. Plant Mol. Biol. *53*, 213-225.

Li, L., and Brown, R.M., Jr. (1993). β-Glucan synthesis in the cotton fiber. II. Regulation and kinetic properties of β-glucan synthases. Plant Physiol. *101*, 1143-1148.

Maia, M.M.D., Heasley, A., Camargo de Morais, M.M., Melo, E.H.M., Morais Jr., M.A., Ledingham, W.M., and Lima Filho, J.L. (2001). Effect of culture conditions on lipase production by *Fusarium solani* in batch fermentation. Bioresource Tech. *76*, 23-27.

Maier, F.J., Malz, S., Lösch, A.P., Lacour, T., and Schäfer, W. (2005). Development of a highly efficient gene targeting system for *Fusarium graminearum* using the disruption of a polyketide synthase gene as a visible marker. FEMS Yeast Res. *5*, 653-62.

Maiti, I.B., and Kolattukudy, P.E. (1979). Prevention of fungal infection of plants by specific inhibition of cutinase. Science *205*, 507-508.

Mangin, L. (1895). Bull. Soc. Hist. Nat. Autun *8*, 55-108.

Marasas, W.F.O., Nelson, P.E., and Toussoun, T.A. (1984). Toxigenic *Fusarium* Species: Identity and Mycotoxicology. (University Park, PA: Pennsylvania State University Press).

Matzke, M.A., Matzke, A.J., Pruss, G.J., and Vance, V.B. (2001). RNA-based silencing strategies in plants. Curr. Opin. Genet. Dev. *11*, 221-227.

McCormack, B.A., Gregory, A.C.E., Kerry, M.E., Smith, C., and Bolwell, G.P. (1997). Purification of an elicitor-induced glucan synthase (callose synthase) from suspension cultures of French bean (*Phaseolus vulgaris* L.): purification and immunolocation of a probable M_r-65000 subunit of the enzyme. Planta *203*, 196-203.

McMullen, M., Jones, R.L., and Gallenberg, D. (1997). Scab of wheat and barley. A reemerging disease of devastating impact. Plant Dis. *81*, 1340-1348.

Meikle, P.J., Bonig, I., Hoogenraad, N.J., Clarke, A.E., and Stone, B.A. (1991). The location of (1→3)-*β*-glucans in the walls of pollen tubes of *Nicotiana alata* using a (1→3)-*β*-glucan specific monoclonal antibody. Planta *485*, 1-8.

Mercer, P.C., Wood, R.K.S., and Greenwood, A.D. (1974). Resistance to anthracnose of French bean. Physiol. Plant Pathol. *4*, 291-306.

Miedaner, T., Reinbrecht, C., and Schilling, A.G. (2000). Association among aggressiveness, fungal colonization, and mycotoxin production of 26 isolates of *Fusarium graminearum* in winter rye head blight. J. Plant Dis. Protect. *107*, 124-134.

Mims, C.W., Copes, W.E., and Richardson, E.A. (2000). Ultrastructure of the penetration and infection of pansy roots by *Thielaviopsis basicola*. Phytopathol. *90*, 843-850.

Mukherjee, K. D., and Hills, M.J. (1994). Lipases from Plants. In Lipases: their structure, biochemistry and application, P., Woolley, and S. B., Petersen, eds.(Cambridge: Cambridge University Press), pp. 49-75.

Nasser Eddine, A., Hannemann, F., and Schäfer, W. (2001). Cloning and expression analysis of *NhL1*, a gene encoding an extracellular lipase from the fungal pea pathogen *Nectria haematococca* MP VI (*Fusarium solani* f. sp. *pisi*) that is expressed *in planta*. Mol. Genet. Genomics *265*, 215-224.

Nganje, W.E., Johnson, D.D., Wilson, W.W., Leistritz, F.L., Bangsund, D.A., and Tiapo, N.M. (2001). Economic impacts of Fusarium Head Blight in wheat and barley: 1998-2000. In Agribusiness and Applied Economics Report 464. (North Dakota State University, Department of Agribusiness and Applied Economics, USA).

Nirenberg, H. (1981). A simplified method for identifying *Fusarium* spp. occuring on wheat. Can. J. Bot. *59*, 1599-1609.

Nishimura, M.T., Stein, M., Hou, B.-H., Vogel, J.P., Edwards, H., and Somerville, S.C. (2003). Loss of callose synthase results in salicylic acid-dependent disease resistance. Science *301*, 969-972.

Oeser, B., Heidrich, P.M., Muller, U., Tudzynski, P., and Tenberge, K.B. (2002). Polygalacturonase is a pathogenicity factor in the *Claviceps purpurea*/rye interaction. Fungal Genet. Biol. *36*, 176-186.

Østergaard, L., Petersen, M., Mattsson, O., and Mundy, J. (2002). An Arabidopsis callose synthase. Plant Mol. Biol. *49*, 559-566.

Politis, D. J. (1976). Ultrastructure of penetration by *Colletotrichum graminicola* of highly resistant oat leaves. Physiol. Plant Pathol. *8*,117-122.

Pricket, A.J., Macdonald, S., and Wildey, K.B. (2000). Survey of Mycotoxins in Stored Grain from the 1999 Harvest in the UK. (HGCA Project Report No 230. HGCA, London).

Pritsch, C., Vance, C.P., Bushnell, W.R., Somers, D.A., Hohn, T.M., and Muehlbauer, G.J. (2001). Systemic expression of defence response genes in wheat spikes as a response to *Fusarium graminearum* infection. Physiol. Mol. Plant Pathol. *58*, 1-12.

Proctor, R.H., Hohn, T.M., and McCormick, S.P. (1995). Reduced virulence of *Gibberella zeae* caused by disruption of a trichothecene toxin biosynthetic gene. Mol. Plant-Microbe Interact. *8*, 593-601.

Punt, P.J., Oliver, R.P., Dingemanse, M.A., Pouwels, P.H., and Van den Hondel, C.A.M.J.J. (1987). Transformation of *Aspergillus* based on the hygromycin B resistance marker from *Escherichia coli*. Gene *56*, 117-124.

Read, S.M., and Delmer, D.P. (1987). Inhibition of mung bean UDP-glucose:(1→3)-β-glucan synthase by UDP-pyridoxal: evidence for an active-site amino group. Plant Physiol. *85*, 1008-1015.

Reichard, U., Hung, C.-Y., Thomas, P.W., and Cole, G.T. (2000). Disruption of the gene which encodes a serodiagnostic antigen and chitinase of human fungal pathogen *Coccidioides immitis*. Infect. Immun. *68*, 5830-5838.

Reid, L.M., Hamilton, R.I., and Mather, D.E. (1995). Effect of macroconidial suspension volume and concentration on expression of resistance to *Fusarium graminearum* in maize. Plant Dis. *79*, 461-466.

Ribichich, K.F., Lopez, S.E., and Vegetti, A.C. (2000). Histopathological spikelet changes produced by *Fusarium graminearum* in susceptible and resistant wheat cultivars. Plant Dis. *84*, 794-802.

Richmond, T.A., and Somerville, C.R. (2000). The cellulose synthase superfamily. Plant Physiol. *124*, 495-498.

Rodriguez-Galvez, E., and Mendgen, K. (1995). Cell wall synthesis in cotton roots after infection with *Fusarium oxysporum*. The deposition of callose, arabinogalactans, xyloglucans, and pectic components into walls, wall appositions, cell plates and plasmodesmata. Planta *197*, 535-545.

Rogers, L.M., Flaishman, M.A., and Kolattukudy, P.E. (1994). Cutinase gene disruption in *Fusarium solani* f sp *pisi* decreases its virulence on pea. Plant Cell *6*, 935-45.

Royer, J.C., Moyer, D.L., Reiwitch, S.G., Madden, M.S., Bech Jensen, E., Brown, S.H., Yonker, C.C., Johnstone, J.A., Golightly, E.J., Yoder, W.T., and Shuster, J.R. (1995). *Fusarium graminearum* A 3/5 as a novel host for heterologous protein production. Biotechnol. *13*, 1479-1483.

Ryals, J.A., Neuenschwander, U.H., Willits, M.G., Molina, A., Steiner, H.Y., and Hunt, M.D. (1996). Systemic Acquired Resistance. Plant Cell *8*, 1809-1819.

Sargent., J.A., Tommerup, I.C., and Ingram, D.S. (1973). The penetration of a susceptible lettuce variety by the downy mildew fungus *Bremia lactucae* Regel. Physiol. Plant Pathol. *3*, 231-239.

Schenk, P.M., Kazan, K., Manners, J.M., Anderson, J.P., Simpson, R.S., Wilson, I.W., Somerville, S.C., and Maclean, D.J. (2003). Systemic gene expression in *Arabidopsis* during an incompatible interaction with *Alternaria brassicicola*. Plant Physiol. *132*, 999-1010.

Schlupmann, H., Bacic, A., and Read, S.M. (1993). A novel callose synthase from pollen tubes of *Nicotiana*. Planta *191*, 470-481.

Schmid, R.D., and Verger, R. (1998). Lipases: interfacial enzymes with attractive applications. Angew. Chem. Int. Ed. Engl. *37*, 1608-1633.

Schroeder, H.W., and Christensen, J.J. (1963). Factors affecting the resistance of wheat to scab caused by *Gibberella zeae*. Phytopathol. *53*, 831-838.

Scott-Craig, J.S., Panaccione, D.G., Cervone, F., and Walton, J.D. (1990). Endopolygalacturonase is not required for pathogenicity of *Cochliobolus carbonum* on maize. Plant Cell. *2*, 1191-1200.

Shedletzky, E., Unger, C., and Delmer, D.P. (1997). A microtiter-based fluorescence assay for (1,3)-*β*- glucan synthases. Analyt. Biochem. *249*, 88-93.

Sherwood, R.T., and Vance, C.P. (1980). Resistance to fungal penetration in gramineae. Phytopathology *70*, 273–279.

Sherwood, R.T., and Vance, C.P. (1976). Histochemistry of papillae formed in reed canarygrass leaves in response to noninfecting pathogenic fungi. Phytopathology *66*, 503-510.

Shieh, M.T., Brown, R.L., Whitehead, M.P., Cary, J.W., Cotty, P.J., Cleveland, T.E., and Dean, R.A. (1997). Molecular genetic evidence for the involvement of a specific polygalacturonase, P2c, in the invasion and spread of *Aspergillus flavus* in cotton bolls. Appl. Environ. Microbiol. *63*, 3548-52.

Shimada, Y., Sugihara, A., Nagao, T., and Tominaga, Y. (1992). Induction of *Geotrichum candidium* lipase by long-chain fatty acids. J. Ferment. Bioeng. *74*, 77-80.

Skipp, R.A., Harder, D.E., and Samborski, D.J. (1974). Electron microscopy studies on infection of resistant (Sr6 gene) and susceptible near-isogenic wheat lines by *Puccinia graminis* f. sp. *tritici*. Can. J. Bot. *52*, 2615-2220.

Smith, G. (1900). The haustoria of the Erysipheae. Bot. Gaz. *29*, 153-184.

Stahl, D.J., and Schäfer, W. (1992). Cutinase is not required for fungal pathogenicity on pea. Plant Cell *4*, 621-629.

Stahl, D.J., Theuerkauf, A., Heitefuss, R., and Schäfer, W. (1994). Cutinase of *Nectria haematococca* (*Fusarium solani* f. sp. *pisi*) is not required for fungal virulence or organ specificity on pea. Mol. Plant-Microbe Interact. *7*, 713-725

Stone, B.A., and Clarke, A.E. (1992). Chemistry and physiology of higher plant 1,3-*β*-glucans (callose). In Chemistry and Biology of (1,3)-*β*-Glucans, B.A. Stone, and A.E., Clarke, eds., (Bundoora, Australia: La Trobe University Press), pp. 365-429.

Sutton, J.C. (1982). Epidemiology of wheat head blight and maize ear rot caused by *Fusarium graminearum*. Can. J. Plant Pathol. *4*, 195-209.

Sweigard, J.A., Chumley, F.G., and Valent, B. (1992). Disruption of *Magnaporthe grisea* cutinase gene. Mol. Gen. Genet. *232*, 183-190

ten Have, A., Mulder, W., Visser, J., and van Kan, J.A. (1998). The endopolygalacturonase gene *Bcpg1* is required for full virulence of *Botrytis cinerea*. Mol. Plant-Microbe Interact. *11*, 1009-1016.

Thines, E., Eilbert, F., Sterner, O., and Anke, H. (1997). Signal transduction leading to appressorium formation in germinating conidia of *Magnaporthe grisea*: Effects of second messengers diacylglycerols, ceramides and sphingomyelin. FEMS Microbiol. Lett. *156*, 91-94

Thines, E., Weber, R.W., and Talbot, N.J. (2000). MAP kinase and protein kinase A-dependent mobilization of triacylglycerol and glycogen during appressorium turgor generation by *Magnaporthe grisea*. Plant Cell. *12*, 1703-1718.

Thompson, J.D., Higgins, D.G., and Gibson, T.J. (1994). CLUSTAL W: improving the sensitivity of progressive multiple sequence alignment through sequence weighting, position-specific gap penalties and weight matrix choice. Nucleic Acids Res. *22*, 4673-4680.

Trevaskis, B., Bagnall, D.J., Ellis, M.H., Peacock, W.J., and Dennis, E.S. (2003). MADS box genes control vernalization-induced flowering in cereals. Proc. Natl. Acad. Sci. USA *100*, 13099-13104.

Tudzynski, B., Liu, S., and Kelly, J.M. (2000). Carbon catabolite repression in plant pathogenic fungi: isolation and characterization of the *Gibberella fujikuroi* and *Botrytis cinerea creA* genes. FEMS Microbiol. Lett. *184*, 9-15.

Turner, A., Bacic, A., Harris, P.J., and Read, S.M. (1998). Membrane fractionation and enrichment of callose synthase from pollen tube of *Nicotiana alata* Link et Otto. Planta *205*, 380-388.

Umezawa, H., Aoyagi, T., Uotani, K., Hamada, M., Takeuchi, T., and Takahashi, S. (1980). Ebelactone, an inhibitor of esterase, produced by actinomycetes. J. Antibiot. (Tokyo) *33*, 1594-1596.

van Egmond, H.P. (1989). Mycotoxins in Dairy Products. (New York: Elsevier Science Pub. Co.).

van Kan, J.A., van't Klooster, J.W., Wagemakers, C.A., Dees, D.C., and van der Vlugt-Bergmans, C.J. (1997). Cutinase A of *Botrytis cinerea* is expressed, but not essential, during penetration of gerbera and tomato. Mol. Plant-Microbe Interact. *10*, 30-38.

Vance, C.P., and Sherwood, R.T. (1976). Cycloheximide treatments implicate papilla formation in resistance of reed canarygrass to fungi. Phytopathology *66*, 498-502.

Verma, D.P.S. and Hong, Z.L. (2001). Plant callose synthase complexes. Plant Mol. Biol. *47*, 693-701.

Wang, M.B., and Metzlaff, M. (2005). RNA silencing and antiviral defense in plants. Curr. Opin. Plant Biol. *8*, 216-22.

Wanjiru, W.M., Zhensheng, K., and Buchenauer, H. (2002). Importance of cell wall degrading enzymes produced by *Fusarium graminearum* during infection of wheat heads. Eur. J. Plant Pathol. *108*, 803-810.

Wasserman, B.P., Wu, A., and Harriman, R.W. (1992). Probing the molecular architecture of (1,3)-β-glucan (callose) synthase: polypeptide depletion studies. Biochem. Soc. Trans. *20*, 18-22.

Waterham, H.R., Digan, M.E., Koutz, P.J., Lair, S.V., and Cregg, J.M. (1997). Isolation of the *Pichia pastoris* glyceraldehyde-3-phosphate dehydrogenase gene and regulation and use of its promoter. Gene. *186*, 37-44.

Wegener, S., Ransom, R.F., and Walton, J.D. (1999). A unique eukaryotic beta-xylosidase gene from the phytopathogenic fungus *Cochliobolus carbonum*. Microbiol. *145*, 1089-1095.

Weiland, J.J., Steffenson, B.J., Cartwright, R.D., and Webster, R.K. (1999). Identification of molecular genetic markers in *Pyrenophora teres f.teres* associated with low virulence on 'Harbin' barley. Phytopathol. *89*, 179-181.

Winkler, U.K., and Stuckmann, M.J. (1979). Glycogen, hyaluronate, and some other polysaccharides greatly enhance the formation of exolipase by *Serratia marcescens*. J. Bacteriol. *138*, 663-670.

Wu, S.-C., Ham, K.-S., Darvill, A.G., and Albersheim, P. (1997). Deletion of two endo-b-1,4-xylanase genes reveals additional isoenzymes secreted by the rise blast fungus. Mol. Plant-Microbe Interact. *10*, 700-708.

Zadoks, J.C., Chang, T.T., and Konzak, D.F. (1974). A decimal code for the growth stages of cereals. Weed Res. *14*, 415-421.

Annotation

Parts of this study were published in the following journal:

Voigt, C.A., Schäfer, W., and Salomon, S. (2005). A secreted lipase of *Fusarium graminearum* is a virulence factor required for infection of cereals. Plant J. *42*, 364-375.

Anna Garleff Dipl. Psych. (UK) . Communication Consultant
Private Coach & Associate Lecturer
The Open University (UK),
U of Hamburg & U of Lüneburg
Poppenbütteler Bogen 70 . 22399 Hamburg.Germany
Tel : +49 40)60671993 / Mobile : +49 1732350615
email: AGarleff@bigfoot.com
intercultural communication competence : Analytic . Innovative . Motivating .

I hereby confirm that the level of English in this doctoral thesis is correct in every way, adhering to the highest level of academic standards.

Hamburg, the 15th of September, 2005

ANNA GARLEFF, PSYCH.
POPPENBÜTTELER BOGEN
70; 22399 HAMBURG, BRD
☎+49 40 60671993

Bank: Hamburger Sparkasse
BLZ: 200 505 50
Kto.Nr.: 1210/ 509384

Danksagung

An diese Stelle möchte ich mich bei Prof. Willi Schäfer darür bedanken, dass er mir nach meiner Diplomarbeit in seiner Arbeitsgruppe die Möglichkeit gegeben hat, in dem selben Arbeitsgebiet weiter zu forschen und zu promovieren.
Dabei möchte ich besonders hervorheben, dass Willi stets hilfsbereit war und nicht zuletzt durch seine zusätzlichen Anregungen, kombiniert mit den hervorragenden Arbeitsbedingungen, meiner wissenschaftliche Arbeit in dieser Form ermöglicht wurde.

Desweiteren gilt mein ganz besonderer Dank Sigi. Seine Hilfsbereitschaft, die sich nicht zuletzt in der regelmäßigen Rücksprache und Diskussion der Ergebnisse zeigte, hat stets dazu beigetragen, die Resultate richtig einzuordnen und sinnvoll fortzuführen. Dies hat sich wirklich ausgezahlt!

Das gleiche gilt natürlich auch für Frank, dessen Hilfs- und Einsatzbereitschaft ein Vorbild für viele von uns sein sollte. Danke, für die Betreunung der Pflanzen, ohne die ich die Vielzahl meiner Infektionstests nicht hätte durchführen können.

Bezüglich der Pflanzenbetreuung gilt mein ganz besonder Dank Angelika und Joe. Ohne eure Hilfe bei der Anzucht wäre es weitaus schwerer geworden. Auch Dank an Birgit, die stets ein gute Quelle war, um die ein oder andere Weizenpflanze zu ergattern.

Ein zusätzliches Dankeschön geht an all die anderen, auch ehemaligen Mitarbeiter der Arbeitsgruppe AMP III, die jetzt MPPG heisst (wirklich schwer, sich daran zu gewöhnen!). Dabei möchte ich besonders die Hilfsbereitschaft Cathrins erwähnen. Ich denke, ohne ihre und Birgits Durchführung der Bestellungen wäre so einiges ins Stocken geraten!

Und ein Dank an Anke. Die anregenden und aufschlussreichen Diskussionen mit ihr, führten oft genug dazu, die Experimente doch noch mal genauer zu durchdenken.

Darüber hinaus gilt mein Dank allen Diplomanden, die in meinem Themenbereich mitgearbeitet haben. Tijana, Sandra, Georg und Bianca, ihr habt alle tolle Arbeit geleistet! Ohne eure Hilfe hätte ich all die Experimente nicht bewältigen können.

Bei Prof. Horst Lörz möchte ich mich für die Übernahme des Zweigutachtens dieser Dissertation bedanken.

Anna Garleff danke ich für das abentliche Korrekturlesen und die Bestätigung, dass mein Englisch durchaus brauchbar ist.

In ganz besonderem Maße möchte ich mich auch bei meinen lieben Eltern, und allen Freunden und Bekannten bedanken. Die, wenn auch allzu oft nicht gerade üppige Freizeit, wäre ohne euch nur halb so schön gewesen.

Meine liebe Susanne, mein größter und herzlichster Dank geht an Dich!
Denn das Allerschönste, was während meiner Promotion passiert ist, sind nicht etwa die wissenschaftlichen Ergebnisse, sondern dass wir uns immer verstanden haben, uns immer noch über alle Maßen gut verstehen und lieben und dies auch in der Zukunft machen werden.
Unsere Hochzeit war deshalb auch das Schönste und Beste, was wir hätten tun können!
Trotzdem ich nicht immer sehr viel Zeit für Dich hatte, haben wir so viel Schönes zusammen erlebt. Und die Zukunft steht uns beiden noch offen.

Ich weiss, dass Du immer für mich da bist und ich immer für Dich!